Supporting Information

C(sp^2)–H Borylation of Heterocycles by Well-Defined Bis(silylene)pyridine Cobalt(III) Precatalysts: Pincer Modification, C(sp^2)–H Activation and Catalytically Relevant Intermediates

*Rebeca Arevalo, Tyler P. Pabst and Paul J. Chirik**

Department of Chemistry, Frick Laboratory
Princeton University, Princeton, NJ 08544, USA

pchirik@princeton.edu

Table of Contents

I. General Considerations

All air- and moisture-sensitive manipulations were carried out using vacuum line, Schlenk and cannula techniques or in an MBraun inert atmosphere (nitrogen) dry box unless otherwise noted. All glassware was stored in a pre-heated oven prior to use. The solvents used for air- and moisture-sensitive manipulations were dried and deoxygenated using literature procedures.[1] Deuterated solvents for NMR spectroscopy were distilled from sodium metal under an atmosphere of argon and stored over 4 Å molecular sieves. 2,6-lutidine, 2-methylfuran, benzofuran, mesitylene, 4-bromotoluene and *N*,*N*′-Di-tert-butylcarbodiimide were dried over CaH_2 degassed by three freeze-pump-thaw cycles, and distilled under vacuum prior to use. Cyclohexene was dried over lithium aluminum hydride and distilled prior to use. Carbon monoxide and hydrogen gases were passed through columns containing 4 Å molecular sieves before use. $NaHBEt_3$ (1.0 M toluene or 1.0 M in THF) was purchased from Aldrich. All other reagents were used as received. ^{Ph}SiNSi,[2] *p*-tolLi,[3] 4-D-2,6-lutidine,[4] 2,6-Diamine-*N*,*N*′-diethylpyridine[2,5] and DBPin[6] were prepared according to literature procedures. 2,6-Diamine-N,N′-diethylpyridine was distilled under vacuum prior to its use. ^{ptol}SiNSi was prepared in an analogous way to ^{Ph}SiNSi employing *p*-tolLi instead of PhLi.

^{1}H NMR spectra were recorded on either Varian Inova 400 or Bruker ADVANCE 500 spectrophotometers operating at 400.13 MHz, and 500.46 MHz, respectively. ^{13}C NMR spectra were recorded on a Varian Inova 400 spectrometer operating at 100.61 MHz. ^{29}Si and ^{11}B NMR spectra were recorded on a Varian Inova 400 spectrophotometer operating at 79.50 and 128.38 MHz respectively. ^{11}B NMR spectra were referenced to $BF_3(OEt_2)$ as an external standard. All ^{1}H and ^{13}C NMR chemical shifts are reported in ppm relative to $SiMe_4$ using the ^{1}H (chloroform-*d*: 7.26 ppm; benzene-d_6: 7.16 ppm) and ^{13}C (chloroform-*d*: 77.16 ppm; benzene-d_6: 128.06 ppm) chemical shifts of the solvent as a standard. ^{1}H NMR data are reported as follows: chemical shift, multiplicity (s = singlet, d = doublet, t = triplet, q = quartet, p = pentet, br = broad, m = multiplet, app = apparent, obsc = obscured), coupling constants (Hz), integration, assignment. ^{13}C NMR

data are reported as follows: chemical shift, number of protons attached to carbon (e.g. CH_2), assignment. QC stands for *quaternary carbon*. Infrared spectroscopy was conducted on a Thermo-Nicolet iS10 FT-IR spectrometer calibrated with a polystyrene standard.

GC analyses were performed using a Shimadzu GC-2010 gas chromatograph equipped with a Shimadzu AOC-20s autosampler and a Shimadzu SHRXI-5MS capillary column (15m x 250μm). The instrument was set to an injection volume of 1 μL, an inlet split ratio of 20:1, and inlet and detector temperatures of 250 °C and 275 °C, respectively. UHP-grade S3 helium was used as carrier gas with a flow rate of 1.82 mL/min. For mixtures containing products with relatively low molecular weight, the temperature program used was as follows: 60 °C, isothermal 1 min; 15 ºC/min to 250 °C, isothermal 2 min. GC yields of 2,6-lutidine, benzofuran and 2-methylfuran borylation reactions as well as for the kinetic analyses were determined by integration of the desired product peaks using mesitylene as an internal standard.

Elemental analyses were performed at Robinson Microlit Laboratories, Inc., in Ledgewood, NJ. Solid-state magnetic moments were determined using a Johnson Matthey Magnetic Susceptibility Balance that was calibrated with $HgCo(SCN)_4$. High-resolution mass spectra were obtained at Princeton University mass spectrometry facilities using an Agilent 6210 TOF LC/MS. Infrared spectroscopy was conducted on a Thermo-Nicolet iS10 FT-IR spectrometer calibrated with a polystyrene standard.

Single crystals suitable for X-ray diffraction were coated with polyisobutylene oil in a drybox, transferred to a nylon loop and then quickly transferred to the goniometer head of a Bruker SMART APEX DUO diffractometer equipped with a molybdenum X-ray tube (λ = 0.71073 Å) and a Cu X-ray tube (λ = 1.54178 Å). Preliminary data revealed the crystal system. The data collection strategy was optimized for completeness and redundancy using the Bruker COSMO software suite. The space group was identified, and the data were processed using the Bruker SAINT+ program and corrected for absorption using SADABS. The structures were solved using direct

methods (SHELXS) completed by subsequent Fourier synthesis and refined by full-matrix least-squares procedures.

II. Preparation of {(^{Ar}SiNSi)Co} Complexes and Stoichiometric Reactions

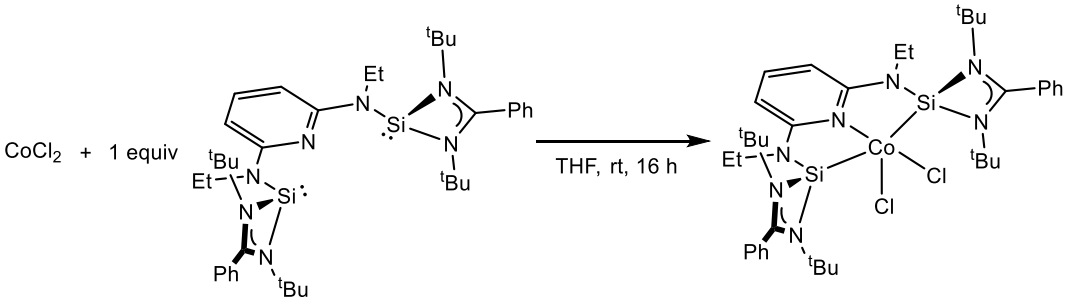

IIa. Preparation of [(^{Ph}SiNSi)CoCl$_2$]. [(^{Ph}SiNSi)CoCl$_2$] was prepared by the procedure described for [(^{Ph}SiNSi)CoBr$_2$][7] starting from CoCl$_2$ (0.075 g, 0.5776 mmol) and ^{Ph}SiNSi (0.395 mg, 0.5791 mmol) to yield 0.400 g (85% yield) of a dark red powder identified as [(^{Ph}SiNSi)CoCl$_2$].

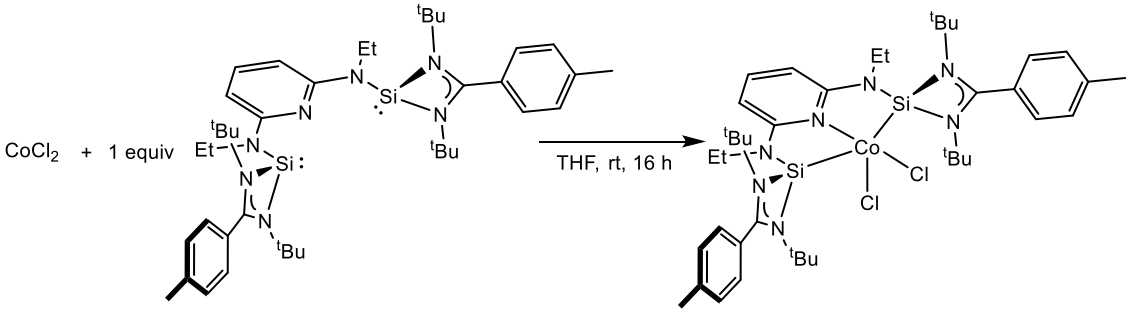

IIb. Preparation of [(^{ptol}SiNSi)CoCl$_2$]. [(^{ptol}SiNSi)CoCl$_2$] was prepared by the procedure described for [(^{Ph}SiNSi)CoCl$_2$] starting from CoCl$_2$ (0.075 g, 0.5776 mmol) and ^{ptol}SiNSi (0.395 mg, 0.5791 mmol) to yield 0.400 g (85% yield) of a dark red powder identified as [(^{ptol}SiNSi)CoCl$_2$]. Anal Calcd $C_{41}H_{63}Cl_2CoN_7Si_2$: C, 58.62; H, 7.56; N, 11.67. Found: C, 58.60; H, 7.76; N, 11.55.

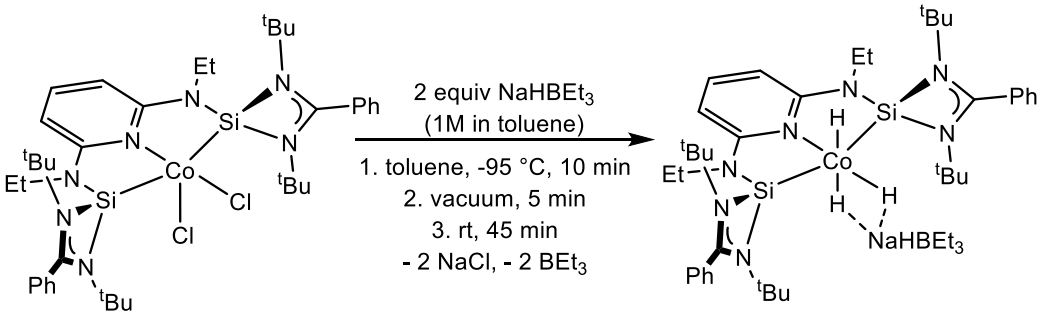

IIc. Preparation of [(^{Ph}SiNSi)CoH$_3$]·NaHBEt$_3$ (1-H$_3$·NaHBEt$_3$). NaHBEt$_3$ (0.30 mL of a 1.0 M solution in toluene, 0.3000 mmol) was added to a toluene (10 mL) solution of [(^{Ph}SiNSi)CoCl$_2$] (0.122 g, 0.1499 mmol) at -95°C in a 20 mL scintillation vial in a nitrogen filled glovebox. The resulting dark orange solution was let to reach room temperature, stirred for 10 minutes and vacuum was pulled for 5 minutes. The resulting solution was let to stir at room temperature for 45 minutes and filtered through Celite. Removal of the volatiles under vacuum and washing with pentane (2 x 3 mL) afforded a yellow powder in a 40% yield (0.052 g) that was identified as [(^{Ph}SiNSi)CoH$_3$]·NaHBEt$_3$**.** The reaction can be carried out in an analogous way with LiHBEt$_3$. The conditions employed for the synthesis (time, temperature, vacuum) have been optimized to minimize the formation of **3-H$_2$(H$_2$)** from reaction of the H$_2$ formed with the product **1-H$_3$·NaHBEt$_3$**. Anal Calcd for $C_{45}H_{78}BCoN_7NaSi_2$: C, 63.13; H, 8.15; N, 13.21. Found: C, 62.69; H, 8.40; N, 13.18. **^{1}H NMR (500 MHz, C$_6$D$_6$, 25 ºC):** δ 7.72 [d ($^3J_{HH}$ = 7.6), 2H, 2 CH Ph], 7.22 [t ($^3J_{HH}$ = 8.1), 1H, H4 py], 7.15 [m, 2H, 2 CH Ph obscured by residual C_6H_6], 7.02 [m, 4H, 4 CH Ph], 6.98 [m, 2H, 2 CH Ph], 5.97 [d ($^3J_{HH}$ = 8.1), 2H, H3 py], 3.34 [q ($^3J_{HH}$ = 7.0), 4H, CH_2-N], 1.59 [br, 9 H, 3 CH_3 NaHBEt$_3$], 1.30 [t ($^3J_{HH}$ = 7.0), 6H, CH_3], 1.27 [s, 36H, CH_3 *t*Bu], 0.99 [br, 6 H, 3 CH_2 NaHBEt$_3$], -17.00 [s, 3H, CoH_3]. **^{13}C{^{1}H} NMR (500 MHz, C$_6$D$_6$, 25 ºC):** δ 172.1 [N-C-N silylene], 165.3 [C2 and C6 py], 131.9 [C4 py], 130.9 [C_{ipso} Ph], 129.0 [CH Ph], 127.8 [CH Ph], 127.6 [CH Ph], 95.5 [C3 and C5 py], 54.9 [*C*$(CH_3)_3$], 38.4 [CH_2-N], 31.4 [C(*C*$H_3)_3$], 16.1 [br, CH_2-B (NaHBEt$_3$)], 14.7 [*C*H_3CH_2N], 13.2 [br, CH_3 (NaHBEt$_3$)]. **^{29}Si{^{1}H} NMR (400 MHz, C$_6$D$_6$, 25 ºC):** δ 67.7.

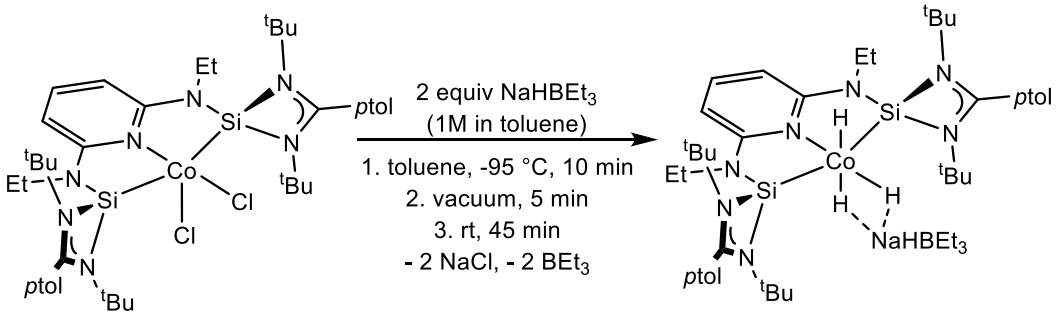

IId. Preparation of [(^{ptol}SiNSi)CoH$_3$]·NaHBEt$_3$ (2-H$_3$·NaHBEt$_3$). NaHBEt$_3$ (0.30 mL of a 1.0 M solution in toluene, 0.3000 mmol) was added to a toluene (10 mL) solution of [(^{ptol}SiNSi)CoCl$_2$] (0.122 g, 0.1499 mmol) at -95°C in a 20 mL scintillation vial in a nitrogen filled glovebox. The resulting dark orange solution was let to reach room temperature and stirred for 10 minutes and vacuum was pulled for 5 minutes. The resulting solution was let to stir at room temperature for 45 minutes and filtered through Celite. Removal of the volatiles under vacuum and washing with pentane (2 x 3 mL) afforded an orange-brown powder in a 43% yield (0.056 g) that was identified as [(^{ptol}SiNSi)CoH$_3$]·NaHBEt$_3$. Slow evaporation of a diethyl ether (10 mL) solution of **2-H$_3$·NaHBEt$_3$** at room temperature afforded yellow single-crystals suitable for X-ray diffraction. The reaction can be carried out in an analogous way with LiHBEt$_3$. The conditions employed for the synthesis (time, temperature, vacuum) have been optimized to minimize the formation of **4-H$_2$(H$_2$)** from reaction of the H$_2$ formed with the product **2-H$_3$·NaHBEt$_3$**.

^{1}H NMR (500 MHz, C$_6$D$_6$, 25 ºC): δ 7.68 [m, 2H, 2 CH Ph], 7.22 [m, 1H, H4 py obscured by residual C$_6$H$_6$], 7.00 [m, 4H, 4 CH Ph], 6.84 [d ($^3J_{HH}$ = 7.9), 2H, 2 CH Ph], 5.96 [d ($^3J_{HH}$ = 8.1), 2H, H3 py], 3.36 [q ($^3J_{HH}$ = 7.0), 4H, CH$_2$-N], 1.98 [s, 6H, 2 CH$_3$ *p*-tol], 1.59 [br, 9 H, 3 CH$_3$ NaHBEt$_3$], 1.32 [s, 36H, CH$_3$ *t*Bu], 1.28 [t ($^3J_{HH}$ = 7.0), 6H, CH$_3$ *Et*-N], 0.99 [br, 6 H, 3 CH$_2$ NaHBEt$_3$], -16.97 [s, 3H, CoH$_3$]. **^{13}C{^{1}H} NMR (500 MHz, C$_6$D$_6$, 25 ºC):** δ 172.5 [N-C-N silylene], 165.3 [C2 and C6 py], 140.2 [QC *C*-CH$_3$ *p*-tol], 130.8 [C$_{ipso}$ *p*-tol], 129.1 [C4 py], 128.9 [CH Ph], 95.5 [C3 and C5 py], 54.8 [*C*(CH$_3$)$_3$], 38.4 [CH$_3$CH$_2$-N], 31.4 [C(*C*H$_3$)$_3$], 20.7 [CH$_3$ *p*-tol], 16.1 [br, CH$_2$-B (NaHBEt$_3$)], 14.7 [*C*H$_3$CH$_2$N], 13.2 [br, CH$_3$ (NaHBEt$_3$)]. **^{29}Si{^{1}H} NMR (400 MHz, C$_6$D$_6$, 25 ºC):** δ 67.1.

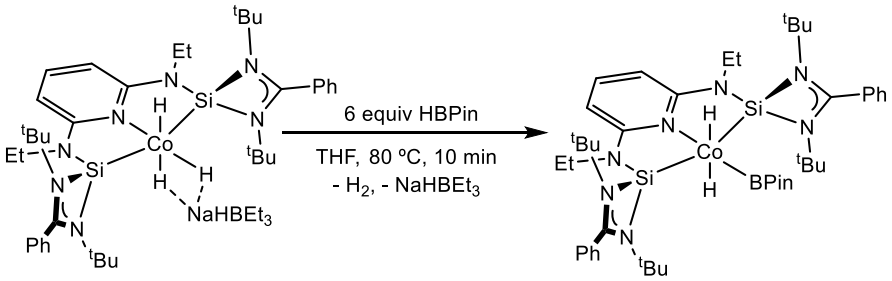

IIe. Preparation of [(^{Ph}SiNSi)CoH$_2$(BPin)] (1-(H)$_2$BPin). In a 20 mL scintillation vial in a nitrogen filled glovebox HBPin (210 µL, 1.4473 mmol) was added to a THF (10 mL) solution of **1-H$_3$·NaHBEt$_3$** (0.210 g, 0.2425 mmol) at 25°C. The resulting dark orange solution was heated up to 80 ºC for 10 minutes and, after cooling down, the solvent was removed under vacuum. The resulting brown residue was suspended in diethyl ether (10 mL) and collected in a fine frit to yield an orange powder that was dried under vacuum and identified as **1-(H)$_2$BPin**. Yield: 65% (0.137 g). The conditions employed for the synthesis (time, temperature) have been optimized to minimize the formation of [(^{Ph,H}SiNSi)CoH$_2$(HBPin)] (see below).

^{1}H NMR (500 MHz, C$_6$D$_6$, 25 ºC): δ 7.98 [d ($^3J_{HH}$ = 7.4), 2H, 2 CH$_o$ Ph], 7.33 [t ($^3J_{HH}$ = 8.0), 1H, H4 py], 7.13 [m, 4H, 4 CH Ph obscured by residual C_6H_6], 7.06 [m, 2H, 2 CH Ph], 7.00 [m, 2H, 2 CH Ph], 6.13 [d ($^3J_{HH}$ = 8.0), 2H, H3 py], 3.52 [q ($^3J_{HH}$ = 7.0), 4H, CH_2-N], 1.45 [s, 42H, CH_3 *t*Bu and C*H*$_3$CH$_2$-N], 1.42 [s, 12H, CH_3 BPin], -10.93 [s, 2H, CoH_2]. **^{13}C{^{1}H} NMR (500 MHz, C$_6$D$_6$, 25 ºC):** δ 170.1 [N-C-N silylene], 165.5 [C2 and C6 py], 134.0 [C$_{ipso}$ Ph], 132.7 [C4 py], 129.9, 129.4, 128.6, 127.5, 127.4 [CH Ph], 95.0 [C3 and C5 py], 79.3 [QC BPin], 54.6 [*C*(CH$_3$)$_3$], 38.7 [CH_2-N], 31.8 [C(*C*H$_3$)$_3$], 26.1 [CH_3 BPin], 15.5 [*C*H$_3$CH$_2$N]. **^{29}Si{^{1}H} NMR (400 MHz, C$_6$D$_6$, 25 ºC):** δ 67.3. **^{11}B{^{1}H} NMR (400 MHz, C$_6$D$_6$, 25 ºC):** δ 21.9.

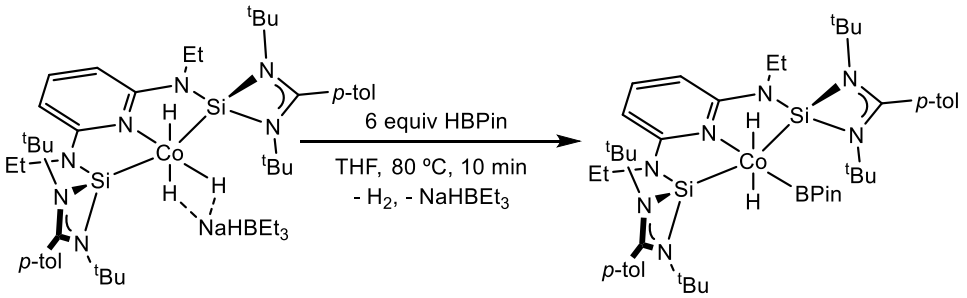

IIf. Preparation of [(^ptol^SiNSi)CoH$_2$(BPin)] (2-(H)$_2$BPin). Compound **2-(H)$_2$BPin** was prepared in an analogous way to **1-(H)$_2$BPin** starting from **2-H$_3$·NaHBEt$_3$** (0.233 g, 0.2610 mmol), HBPin (227 µL, 1.5644 mmol) and THF (10 mL) to yield 0.159 g of an orange powder identified as **2-(H)$_2$BPin** (68% yield). Slow evaporation of a diethyl ether (10 mL) solution of **2-(H)$_2$BPin** at room temperature afforded orange single-crystals suitable for X-ray diffraction. Anal Calcd for $C_{47}H_{77}BCoN_7O_2Si$: C, 62.86; H, 8.64; N, 10.92. Found: C, 62.43; H, 8.30; N, 10.67.

^{1}H NMR (500 MHz, C$_6$D$_6$, 25 ºC): δ 7.90 [dd ($^3J_{HH}$ = 7.8, $^4J_{HH}$ = 1.8), 2H, 2 CH$_o$ *p*-tol], 7.32 [t ($^3J_{HH}$ = 8.0), 1H, H4 py], 7.14 [dd ($^3J_{HH}$ = 8.6, $^4J_{HH}$ = 1.8), 2H, 2 CH *p*-tol obscured by residual C_6H_6], 6.97 [d ($^3J_{HH}$ = 7.8), 2H, 2 CH *p*-tol], 6.89 [d ($^3J_{HH}$ = 8.6), 2H, 2 CH *p*-tol], 6.12 [d ($^3J_{HH}$ = 8.0), 2H, H3 py], 3.55 [q ($^3J_{HH}$ = 7.0), 4H, CH_2-N], 2.06 [s, 6H, CH_3 *p*-tol], 1.49 [s, 42H, CH_3 *t*Bu and C*H*$_3$CH$_2$-N], 1.46 [s, 12H, CH_3 BPin], -10.91 [s, 2H, CoH_2]. **^{13}C{^{1}H} NMR (500 MHz, C$_6$D$_6$, 25 ºC):** δ 170.1 [N-C-N silylene], 165.2 [C2 and C6 py], 139.2 [QC *C*-CH$_3$ *p*-tol], 132.2 [C4 py], 130.8 [C$_{ipso}$ *p*-tol], 129.3, 128.2 [CH p-tol], 128.1 [2 CH *p*-tol], 94.5 [C3 and C5 py], 79.0 [QC BPin], 54.2 [*C*(CH$_3$)$_3$], 38.3 [CH_2-N], 31.5 [C(*C*H$_3$)$_3$], 25.7 [CH_3 BPin], 20.8 [CH_3 *p*-tol], 15.1 [*C*H$_3$CH$_2$N]. **^{29}Si{^{1}H} NMR (400 MHz, C$_6$D$_6$, 25 ºC):** *δ* 66.7.

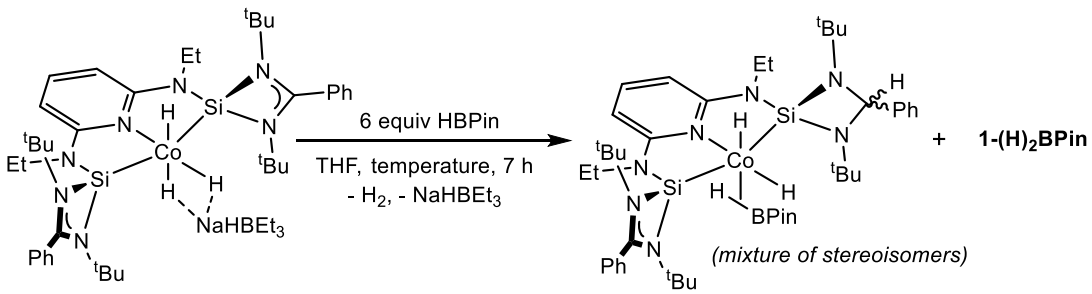

IIg. NMR monitoring of the reaction of 1-H_3·NaHBEt_3 with HBPin at 25 ºC, 50 ºC or 80 ºC. Formation of a mixture of 1-$(H)_2$BPin and [(^{Ph,H}SiNSi)CoH_2(HBPin)]. HBPin (52 µL, 0.3584 mmol) was added to a solution of **1-H_3·NaHBEt_3** (0.052 g, 0.0600 mmol) in THF-d_8 (0.25 mL) in a J. Young NMR tube in a nitrogen filled glovebox. The tube was sealed and brought out of the glovebox. The reaction was monitored by ^{1}H NMR at room temperature, 50 ºC or 80 ºC. When the reaction was run at 25 °C or 50 °C, a new mixture of stereoisomers with C_s symmetry (δ (hydride in THF-d_8) = -8.40 ppm) was concomitantly formed with **1-$(H)_2$BPin**. On the basis of 1D and 2D NMR characterization, the new cobalt complex, [(^{Ph,H}SiNSi)CoH_2(HBPin)], is proposed to be formed as a result of intramolecular hydride migration to the imine in the SiNSi pincer promoted by σ-bond coordination of HBPin. The amount of this complex decreased with increasing temperature (40% at 25 °C and 25% at 50 °C) and at 80 °C its formation was completely suppressed affording spectroscopically pure **1-$(H)_2$BPin** (Figure S41). The formation of this side-product at 25 °C and 50 °C could be attributed to competing σ-coordination of HBPin at temperatures where **1-H_3·NaHBEt_3** does not reach the required energy to surmount the H_2 reductive elimination barrier.

Diagnostic NMR signals of [(^{Ph,H}SiNSi)CoH_2(HBPin)] (minor component of the mixture). ^{1}H NMR (400 MHz, THF-d_8, 25 ºC): (only signals of the major stereoisomer of [(^{Ph,H}SiNSi)CoH_2(HBPin)] are assigned). δ 8.58 [br, 1H, Ph], 7.81 [br, 1H, CH Ph], 7.67 [br, 1H, CH Ph], 7.57 [br, 1H, CH Ph], 7.55 [br, 1H, CH Ph] 7.33 [br, 1H, CH Ph], 5.94, 5.91 [br, 1H, H3 and H5 py], 5.63 [s, 1H, N-CH-N], 1.35 [s, 24H, CH_3 2 *t*Bu and 2 CH_3 BPin], 1.22 [2 CH_3 BPin], 1.10 [s, 18H, CH_3 *t*Bu], -8.40 [s, 3H, CoH_2(*H*BPin)]. **^{13}C{^{1}H} NMR (400 MHz, C_6D_6, 25 ºC):** δ 174.9 [N-C-N silylene], 161.9, 161.6 [C2 and C6 py], 149.6 [C_{ipso} Ph silyl], 131.7 [CH Ph], 95.2, 93.0 [C3 and C5 py], 80.4, 78.7 [QC BPin], 74.7 [N-CH-N silyl], 54.8, 50.8 [QC *t*Bu], 39.0, 38.1 [CH_2-N], 30.9, 30.8 [CH_3 *t*Bu], 25.1, 24.2 [CH_3 BPin], 14.4, 14.3 [*C*H_3CH_2N].

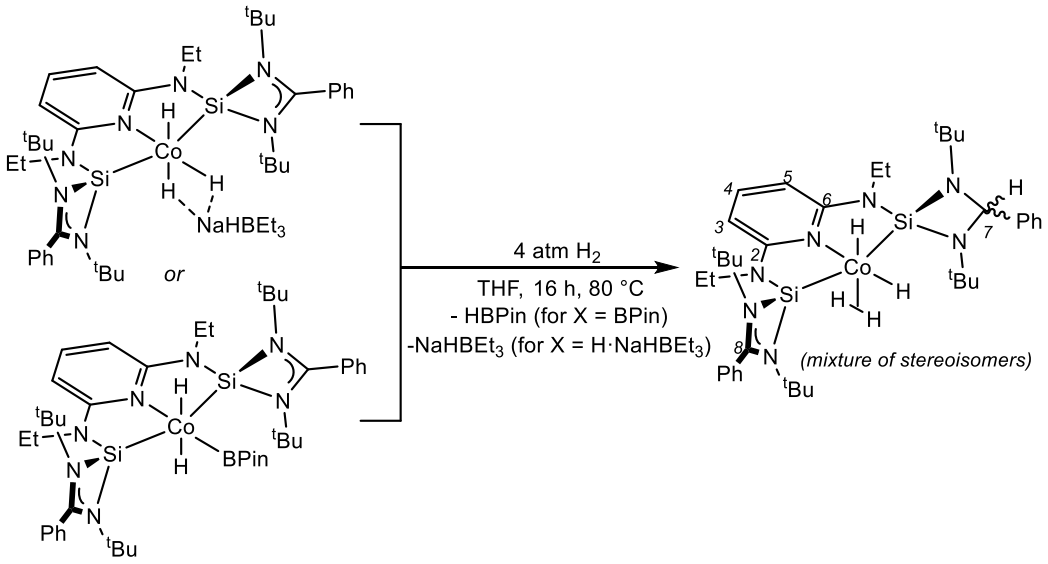

IIh. Preparation of [(^{Ph,H}SiNSi)CoH$_2$(H$_2$)] (3-H$_2$(H$_2$)). In a nitrogen filled glovebox, a thick-walled glass vessel was charged with 0.138 g (0.1593 mmol) of **1-H$_3$·NaHBEt$_3$** or 0.102 g (0.1172 mmol) of **1-(H)$_2$BPin**, 10 mL of THF and a magnetic stir bar. At the high vacuum line, the whole vessel was submerged in liquid nitrogen, the solution was frozen and degassed, and 4 atm of H_2 gas were admitted at 77 K. The solution was thawed and stirred at 80 ºC for 16 h. After cooling down to room temperature, the solution was frozen at the high vacuum line and the remaining H_2 was removed under vacuum. The vessel was brought into the glovebox and the solvent was removed under vacuum. The resulting brown residue was washed with pentane (2 x 3 mL) and dried under vacuum affording isolation of a brown powder that was identified as compound **3-H$_2$(H$_2$)** (0.032 g, 27% yield from **1-H$_3$·NaHBEt$_3$**).

^{1}H NMR (400 MHz, C$_6$D$_6$, 25 ºC): (only signals of the major stereoisomer are assigned). δ 8.50 [br, 1H, H$_o$ Ph], 7.24 [br, 1H, CH Ph], 7.23 [m, 1H, H4 py (obscured by residual C_6H_6)], 7.15 [m, 6H, 6 CH Ph obscured by residual C_6H_6], 6.84 [br, 1H, 1 CH Ph], 6.70 [br, 1H, 1 CH Ph], 6.07, 5.87 [br, 1H, H3 and H5 py], 5.82 [s, 1H, N-CH-N], 3.82 [q ($^3J_{HH}$ = 7.0), 2H, CH_2-N], 3.31 [m, 2H, CH_2-N], 1.42, 1.22 [s, 18H, CH_3 *t*Bu], 0.88 [t ($^3J_{HH}$ = 6.7), 3H, CH_3], 0.82 [t ($^3J_{HH}$ = 7.4), 3H, CH_3], -11.57 [s, 4H, $CoH_2(H_2)$]. **^{13}C{^{1}H} NMR (400 MHz, C$_6$D$_6$, 25 ºC):** δ 173.7 [N-C-N silylene], 163.0, 162.5 [C2 and C6 py], 150.1 [C_{ipso} Ph silyl], 135.1 [C4 py], 131.3 [CH_o Ph], 129.7, 128.8, 128.6,

128.3 [CH Ph], 96.5, 93.3 [C3 and C5 py], 76.8 [N-CH-N silyl], 54.8, 51.1 [*C*$(CH_3)_3$], 39.2, 38.5 [CH_2-N], 31.6, 30.8 [C(*C*$H_3)_3$], 14.9, 14.7 [*C*H_3CH_2N].

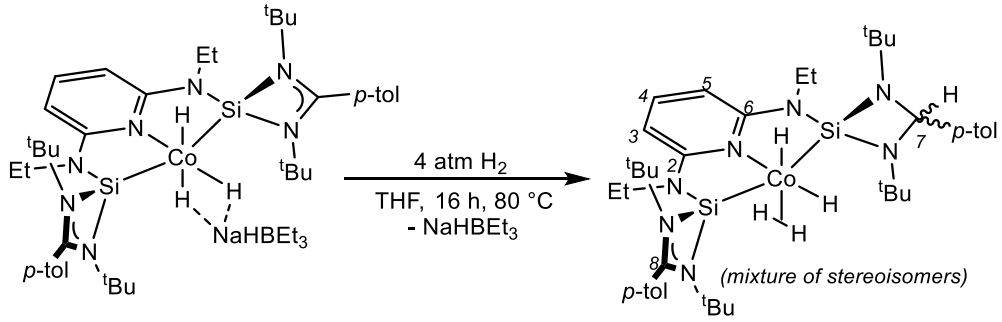

IIi. Preparation of [(^{ptol,H}SiNSi)Co$H_2(H_2)$] (4-$H_2(H_2)$). Compound **4-$H_2(H_2)$** was prepared in an analogous way to **3-$H_2(H_2)$** starting from **2-H_3·NaHBEt$_3$** (0.115 g, 0.1286 mmol). A brown powder was isolated and was identified as **4-$H_2(H_2)$.** Yield: 32% (0.032 g).

^{1}H NMR (400 MHz, C_6D_6, 25 ºC): (only signals of the major stereoisomer are assigned). *δ* 8.35 [d($^3J_{HH}$ = 7.6), 1H, H_o Ph], 7.35 [d($^3J_{HH}$ = 7.1), 1H, CH Ph], 7.22 [t($^3J_{HH}$ = 8.2), 1H, H4 py], 6.93 [d($^3J_{HH}$ = 7.9), 1H, CH Ph], 6.85 [m, 2H, 2 CH Ph], 6.76 [d($^3J_{HH}$ = 7.7), 1H, CH Ph], 6.71 [br, 1H, CH Ph], 6.05 [d($^3J_{HH}$ = 8.2), 1H, H3 py], 5.88 [d($^3J_{HH}$ = 8.2), 1H, H5 py], 5.86 [s, 1H, N-CH-N], 3.80 [q ($^3J_{HH}$ = 7.0), 2H, CH_2-N], 3.33 [m, 2H, CH_2-N], 2.23, 1.94 [s, 3H, CH_3 *p*-tol], 1.53, 1.32 [t ($^3J_{HH}$ = 6.7), 3H each, *C*H_3CH_2N], 1.42, 1.16 [s, 18H each, CH_3 *t*Bu], -11.59 [s, 4H, Co$H_2(H_2)$]. **^{13}C{^{1}H} NMR (400 MHz, C_6D_6, 25 ºC):** *δ* 174.2 [N-C-N silylene], 163.0, 162.5 [C2 and C6 py], 147.1 [C_{ipso} Ph silyl], 140.2 [*C*-CH_3 *p*-tol], 135.7 [*C*-CH_3 *p*-tol], 135.1 [C4 py], 131.3 [CH_o Ph], 128.8, 128.7, 128.6, 128.3, 128.2, 126.8 [7 CH Ph], 96.5, 93.3 [C3 and C5 py], 76.6 [N-CH-N silyl], 54.7, 51.1 [*C*$(CH_3)_3$ (*t*Bu)], 39.2, 38.5 [CH_2-N], 31.6, 30.9 [C(*C*$H_3)_3$ (*t*Bu)], 21.0, 20.8 [CH_3 *p*-tol], 14.9, 14.7 [*C*H_3CH_2N].

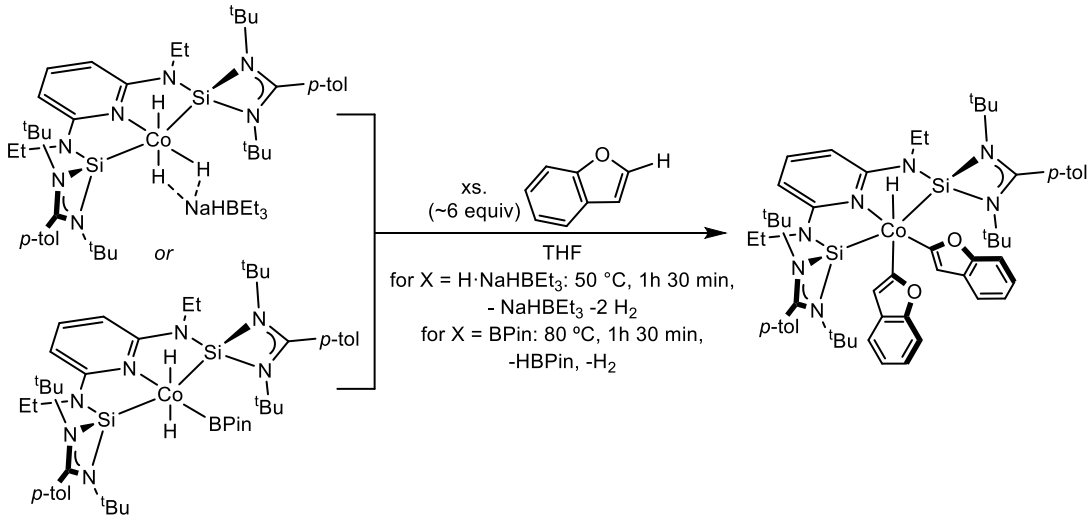

IIj. Preparation of *cis*-[(^ptol^SiNSi)CoH(Bf)$_2$] (2-H(Bf)$_2$). In a thick-walled glass vessel benzofuran (100 µL, 0.9075 mmol) was added to a solution of **2-H$_3$·NaHBEt$_3$** (0.133 g, 0.1487 mmol) or **2-(H)$_2$BPin** (0.136, 0.1514 mmol) in THF (10 mL) in a nitrogen filled glovebox. The resulting mixture was stirred at 50 ºC (for **2-H$_3$·NaHBEt$_3$**) or at 80 ºC (for **2-(H)$_2$BPin**) for 1 h and 30 minutes. The vessel was brought into the glovebox and the solvent was removed under vacuum. The resulting brown residue was suspended in diethyl ether (10 mL) and collected in a fine frit. The yellow solid was dried under vacuum yielding 0.069 g (from **2-H$_3$·NaHBEt$_3$**, 46% yield) or 0.061 g (from **2-(H)$_2$BPin**, 40% yield) of a compound that was identified as **2-H(Bf)$_2$**. Slow evaporation of a diethyl ether (10 mL) solution of **2-H(Bf)$_2$** at room temperature afforded orange single-crystals suitable for X-ray diffraction.

^{1}H NMR (400 MHz, C$_6$D$_6$, 25 ºC): δ 7.50 [m, 5H, CH *p*-tol and CH Bf (including C4 Bf)], 7.29 [m, 4H, H4 py and CH *p*-tol and Bf], 7.10 [m, 3H, and CH *p*-tol and Bf], 6.91 [m, 3H, CH *p*-tol and Bf], 6.78 [m, 4H, CH *p*-tol and Bf], 6.05 [d ($^3J_{HH}$ = 8.1), 2H, H3 and H5 py], 3.42 [q ($^3J_{HH}$ = 7.1), 4H, CH_2-N], 1.95 [s, 6H, CH_3 *p*-tol], 1.33 [t ($^3J_{HH}$ = 7.1), 6H, CH_3CH_2N], 1.28 [s, 18H, CH_3 2 *t*Bu], 0.95 [s, 18H, CH_3 2 *t*Bu], -11.41 [s, 1H, CoH]. **^{13}C{^{1}H} NMR (400 MHz, C$_6$D$_6$, 25 ºC):** δ 203.7 [Co-C *trans* to H], 194.6 [Co-C *trans* to py], 171.9 [N-C-N silylene], 164.7 [C2 and C6 py], 161.5, 159.4 [QC C-O Bf], 139.8 [QC *C*-CH_3 *p*-tol], 136.2 [C4 py], 134.2, 134.1 [QC Bf], 128.8 [QC *C*-CH_3 *p*-

tol], 128.5, 128.0, 127.9, 127.8 [CH *p*-tol], 120.0, 119.5, 116.8, 116.5, 116.2, 114.7, 114.2, 107.8, 106.6 [CH Bf], 96.2 [C3 and C5 py], 54.5, 54.2 [QC *t*Bu], 39.0 [CH_2-N], 30.8, 30.5 [CH_3 *t*Bu], 20.8 [CH_3 *p*-tol], 14.5 [CH_3CH_2N]. **^{29}Si{^{1}H} NMR (400 MHz, C_6D_6, 25 ºC):** δ 71.3.

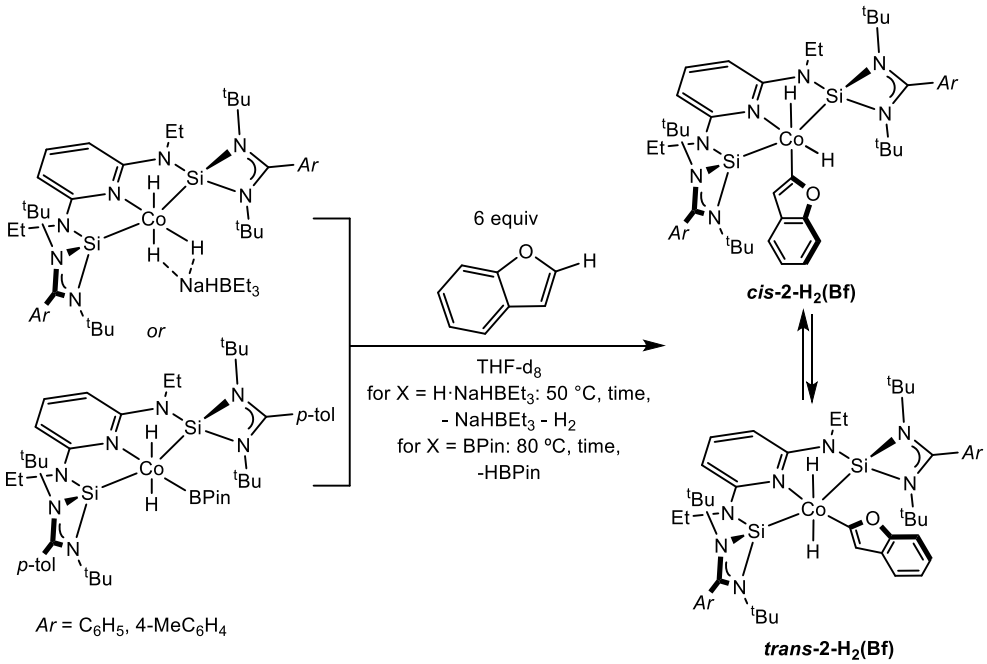

IIk. NMR monitoring of the reaction of 2-H_3·$NaHBEt_3$, 1-H_3·$NaHBEt_3$ or 2-$(H)_2$BPin with benzofuran. Observation of *cis*- and *trans*-[(^{Ar}SiNSi)CoH_2(Bf)] (*cis*-2-H_2(Bf) and *trans*-2-H_2(Bf)). Benzofuran (30 µL, 0.2722 mmol) was added to a solution of **2-H_3·$NaHBEt_3$** (0.040 g, 0.0447 mmol), **2-$(H)_2$BPin** (0.045 g, 0.0501 mmol) or **1-H_3·$NaHBEt_3$** in THF-d_8 (0.25 mL) in a J. Young NMR tube in a nitrogen filled glovebox. The tube was sealed, brought out of the glovebox and heated up to 50 ºC (**1-H_3·$NaHBEt_3$** and **2-H_3·$NaHBEt_3$**) or 80 ºC (**2-$(H)_2$BPin**). The reaction was monitored by ^{1}H NMR at room temperature allowing identification of the formation of a mixture *cis*- and *trans*-[(^{Ar}SiNSi)CoH_2(Bf)] (Figures S74 and S75). The reaction between **1-H_3·$NaHBEt_3$** and benzofuran was monitored in THF-d_8 at 50 ºC for 45 minutes, the tube was brought into the glovebox and the volatiles were removed under vacuum. After washing with diethyl ether (2 x 3 mL) a yellow powder was isolated as an spectroscopically pure compound that was identified as *cis*-[(^{Ph}SiNSi)CoH_2(Bf)] (***cis*-1-H_2(Bf)**) and was fully characterized by NMR spectroscopy.

^{1}H NMR (400 MHz, THF-d_8, 25 ºC): δ hydride ligands: -10.05 [s, 2H, ***trans*-2-H$_2$(Bf)**], -11.68 [s, 1H, ***cis*-2-H(Bf)$_2$**], -14.57 [d($^2J_{HH}$ = 19.0), 1H, ***cis*-2-H$_2$(Bf)**], -21.57 [d($^2J_{HH}$ = 19.0), 1H, ***cis*-2-H$_2$(Bf)**].

Characterization of *cis*-1-H$_2$(Bf): ^{1}H NMR (400 MHz, C$_6$D$_6$, 25 ºC): δ 7.96 [br, 2H, CH Ph], 7.57 [d ($^3J_{HH}$ = 7.1), 1H, CH Bf], 7.30 [m, 2H, H4 py and CH Bf], 7.00 [m, 9H, CH Ph and Bf], 6.03 [br, 2H, H3 and H5 py], 5.61 [br, 1H, CH Bf], 3.27 [m, 4H, CH_2-N], 1.24 [br, 24H, CH_3CH_2N and CH_3 2 *t*Bu], 0.84 [s, 18H, CH_3 2 *t*Bu], -15.05 [d($^2J_{HH}$ = 17.0), 1H, CoH], -23.50 [d($^2J_{HH}$ = 17.0), 1H, CoH]. **^{13}C{^{1}H} NMR (400 MHz, C$_6$D$_6$, 25 ºC):** δ 205.7 [Co-C], 172.2 [N-C-N silylene], 165.0 [C2 and C6 py], 160.4 [QC Ph], 135.9 [C4 py], 133.1, 131.5 [QC Bf], 130.0, 129.9, 128.9, 128.8 [CH Ph], 121.0, 117.8, 115.0, 112.1, 107.4 [CH Bf], 96.4 [C3 and C5 py], 55.0, 54.0 [QC *t*Bu], 38.9 [CH_2-N], 30.9, 30.7 [CH_3 *t*Bu], 14.6 [CH_3CH_2N].

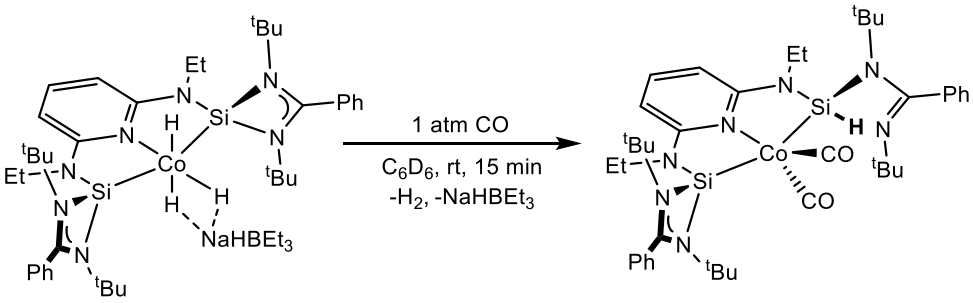

IIm. Preparation of [(^{Ph}SiNSiH)Co(CO)$_2$] (5-(CO)$_2$). A J. Young NMR tube was charged with 0.052 g (0.0600 mmol) of **1-H$_3$·NaHBEt$_3$** and 0.25 mL of C_6D_6. At the high vacuum line, the solution was frozen and degassed and 1 atm of CO gas was admitted at 77 K. The solution was thawed and a color change from orange to yellow was observed. The tube was brought into the glovebox and the volatiles were removed under vacuum. After washing with pentane (2 x 3 mL) a pale-yellow solid was isolated in 75% yield (0.036 g) and was identified as **5-(CO)$_2$**. Crystallization from pentane at -35 ºC afforded pale yellow crystals suitable for X-ray diffraction.

^{1}H NMR (400 MHz, C$_6$D$_6$, 25 ºC): δ 7.52 [br, 2H, 2 CH Ph], 7.20 [m, H4 py and 6 CH Ph (obscured by residual C_6H_6)], 6.89 [br, 1H, 1 CH Ph], 6.67 [br, 1H, 1 CH Ph], 6.49 [s, 1H, Si-H], 5.90 [br, 1H, H3 py], 5.85 [br, 1H, H5 py], 4.21 [dq ($^2J_{HH}$ = 13.5, $^3J_{HH}$ = 6.4), 1H, 1H CH_2-N], 3.38 [dq ($^2J_{HH}$ =

13.5, $^{3}J_{HH}$ = 6.4), 1H, 1H CH_2-N], 3.26 [m, 2H, 2H CH_2-N], 1.54 [s, 9H, 3 CH_3 *t*Bu], 1.35 [t ($^{3}J_{HH}$ = 6.8), 3H, 1 C*H*$_3$$CH_2$-N], 1.29 [s, 9H, 3 CH_3 *t*Bu], 1.27 [br, 12H, 3 CH_3 *t*Bu and 1 C*H*$_3$$CH_2$-N], 1.10 [s, 9H, 3 CH_3 *t*Bu]. **^{13}C{^{1}H} NMR (400 MHz, C_6D_6, 25 ºC):** δ 206.7, 205.6 [2 CO], 172.6 [N-C-N silylene], 163.4 [C2 py], 163.0 [N-C=N silyl], 162.4 [C6 py], 138.8 [C_{ipso} Ph] 131.0 [C4 py], 130.2, 129.1, 129.0 [CH Ph], 97.2 [C3 py], 93.1 [C5 py], 54.4, 54.3, 54.3, 53.6 [*C*$(CH_3)_3$], 42.4, 38.2 [CH_2-N], 32.4, 32.1, 30.5, 30.3 [C(*C*$H_3)_3$], 14.8, 13.3 [*C*H_3CH_2N].

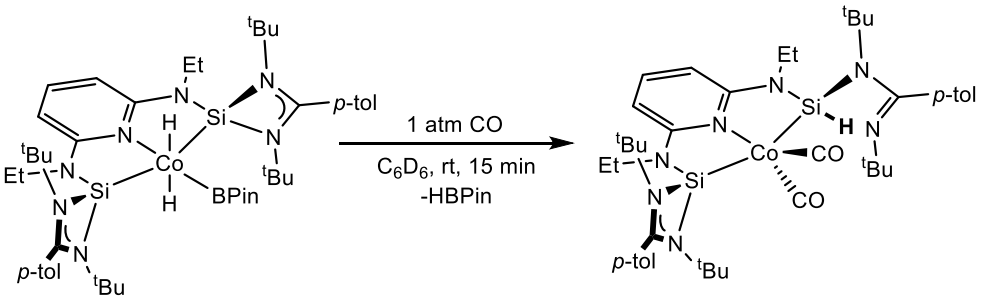

IIn. Preparation of [(ptolSiNSiH)Co(CO)$_2$] (6-(CO)$_2$). Compound **6-(CO)$_2$** was prepared in an analogous way to **5-(CO)$_2$** starting from **2-H$_2$BPin** (0.058 g, 0.0646 mmol). Yield: 71% (0.038 g). **NMR (400 MHz, C_6D_6, 25 ºC):** δ 7.47 [d($^{3}J_{HH}$ = 7.5), 2H, 2 CH *p*-tol], 7.25 [t ($^{3}J_{HH}$ = 8.0), 1H, H4 py], 6.85 [m, 3H, 3 CH *p*-tol], 6.74 [d ($^{3}J_{HH}$ = 7.7), 1H, 1 CH *p*-tol], 6.65 [m, 2H, 2 CH *p*-tol], 6.50 [s, 1H, Si-H], 5.91 [d ($^{3}J_{HH}$ = 8.2), 1H, H3 py], 5.86 [d ($^{3}J_{HH}$ = 7.8), 1H, H5 py], 4.24 [dq ($^{2}J_{HH}$ = 14.0, $^{3}J_{HH}$ = 6.8), 1H, 1H CH_2-N], 3.39 [dq ($^{2}J_{HH}$ = 14.0, $^{3}J_{HH}$ = 5.3), 1H, 1H CH_2-N], 3.30 [m, 2H, 2H CH_2-N], 2.02 [s, 3H, 1 CH_3 *p*-tol], 1.95 [s, 3H, 1 CH_3 *p*-tol], 1.57 [s, 9H, 3 CH_3 *t*Bu], 1.33 [br, 24H, 6 CH_3 *t*Bu and 2 C*H*$_3$$CH_2$-N], 1.14 [s, 9H, 3 CH_3 *t*Bu], 0.98 [s, 9H, 3 CH_3 *t*Bu].

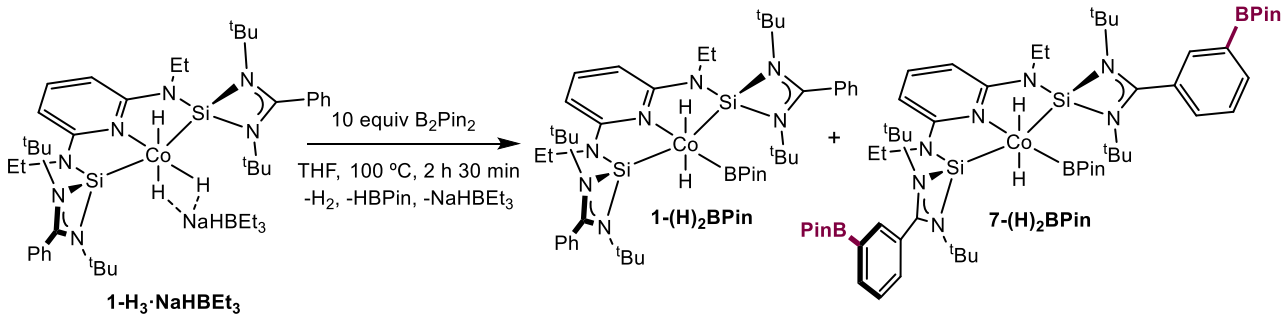

IIo. Reaction of 1-H_3·NaHBEt$_3$ with B_2Pin_2. Formation of the mixture of 1-$(H)_2$BPin and [(^{BPin,Ph}SiNSi)CoH_2(BPin)] (7-$(H)_2$BPin). In a nitrogen filled glovebox, B_2Pin_2 (210 g, 0.8270 mmol) was added to a solution of **1-H_3·NaHBEt$_3$** (0.072 g, 0.0831 mmol) in THF-d_8 (10 mL) in a J. Young NMR tube. The resulting mixture was heated up to 100 ºC for 2 h and 30 min. After cooling down the NMR spectra were registered.

Diagnostic signals of 7-$(H)_2$BPin.

^{1}H NMR (400 MHz, C6D6, 25 ºC): 7.91 [s, H_o ^{BPin}Ph], -11.40 [CoH_2].

^{13}C{^{1}H} NMR (400 MHz, C6D6, 25 ºC): δ 171.2 [N-C-N silylene], 132.0 [br, C-BPin Ph].

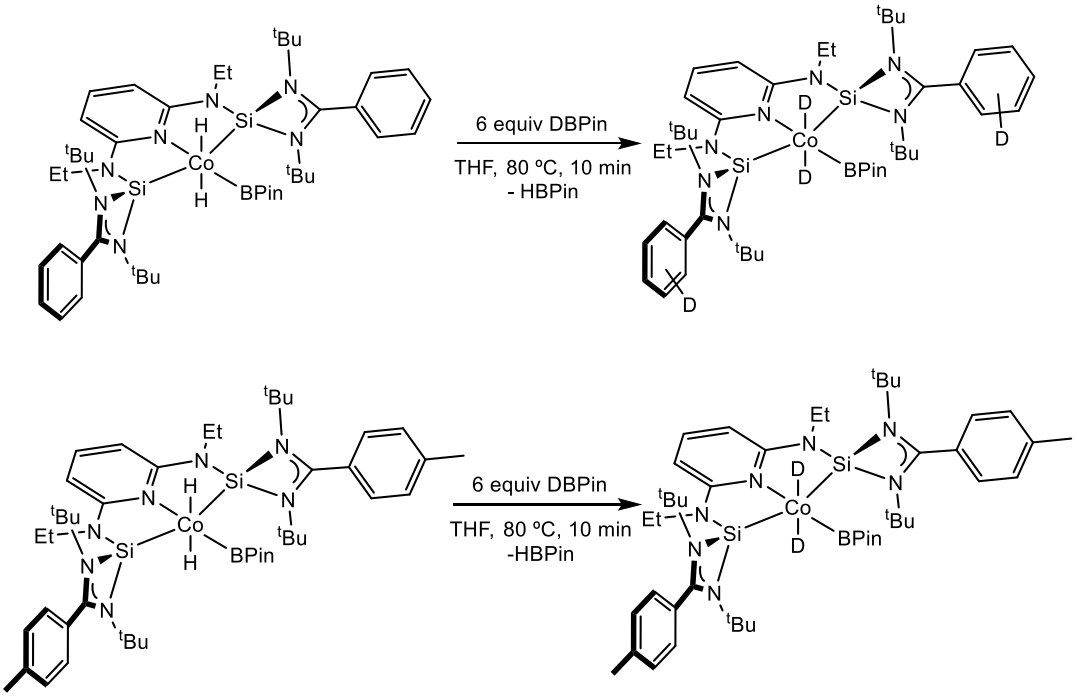

IIp. Reaction of 1-$(H)_2$BPin or 2-$(H)_2$BPin with DBPin. In a nitrogen filled glovebox, DBPin (37 µL, 0.2550 mmol) was added to a solution of **1-$(H)_2$BPin** (0.035 g, 0.0402 mmol) or **2-$(H)_2$BPin** (0.038 g, 0.0423 mmol) in THF (0.30 mL) in a J. Young NMR tube. The resulting mixture was heated up to 80 ºC for 10 min. After cooling down the sample, the ^{2}H NMR spectrum was registered. The sample was brought into the glovebox and the volatiles were removed under vacuum. The resulting orange residue was dissolved in C_6D_6 and the ^{1}H NMR spectrum was registered.

III. Catalyst Resting-State Determination as a Function of Time

IIIa. For the borylation of 2-methylfuran with HBPin

In a nitrogen-filled glovebox, a J. Young NMR tube was charged with HBPin (37 µL, 0.2550 mmol), 2-methylfuran (22 µL, 0.2484 mmol), **1-H_3·NaHBEt_3** (0.011 g, 0.0127 mmol), mesitylene (10 µL, 0.0719 mmol) and 0.50 mL of THF-d_8. The tube was sealed, brought out of the glovebox and heated to 80 °C in an oil bath. The progress of the reaction as well as the identity of the catalyst resting state as a function of time was monitored by registering the ^{1}H NMR spectrum (at 23 °C) at different time points (Figures S46-S49). The approximate % yield of 5-BPin-2-methylfuran was calculated from the relative integrations of characteristic peaks for 2-methylfuran (C4 proton) and 5-BPin-2-methylfuran (C4 proton).

IIIb. For the borylation of 2,6-lutidine with B_2Pin_2

In a nitrogen-filled glovebox, a scintillation vial was charged with B_2Pin_2 (0.064 g, 0.2510 mmol), 2,6-lutidine (29 µL, 0.2503 mmol), 0.50 mL of THF-d_8 and **1-H_3·NaHBEt_3** (0.033 g, 0.0381 mmol), **2-H_3·NaHBEt_3** (0.034 g, 0.0380 mmol) or **2-$(H)_2$BPin** (0.034 g, 0.0379 mmol). Mesitylene (10 µL, 0.0719 mmol) was also added to the catalytic reaction with **2-$(H)_2$BPin** to monitor catalyst concentration. The tube was sealed, brought out of the glovebox and was heated to 100 °C in an oil bath. The progress of the reaction as well as the identity of the catalyst resting state as a function of time was monitored by registering the ^{1}H NMR spectrum (at 23 °C) at different time points (Figures S91-S94 for **1-H_3·NaHBEt_3**, Figures S107-S108 for **2-H_3·NaHBEt_3** and Figures S109-S110 for **2-$(H)_2$BPin**). The approximate % yield of 4-BPin-2,6-dimethylpyridine was calculated from the relative integrations of characteristic peaks for 2,6-lutidine (C3 protons) and 4-BPin-2,6-lutidine (C3 protons).

IV. General Catalytic Procedures

IVa. General procedure for the borylation of 2-methylfuran and benzofuran

In a nitrogen-filled glovebox a glass vessel with a J. Young seal was charged with a magnetic stir bar, HBPin (37 µL, 0.2550 mmol), 2-methylfuran (22 µL, 0.2484 mmol) or benzofuran (27 µL, 0.2451 mmol), mesitylene (10 µL, 0.0719 mmol), 0.50 mL of THF and **1-H_3·NaHBEt_3** (0.011 g, 0.0127 mmol) or **2-H_3·NaHBEt_3** (0.012 g, 0.0134 mmol) or **2-$(H)_2$BPin** (0.012 g, 0.0134 mmol). The tube was sealed and the resulting mixture was stirred at 80 ºC for 24 hours. The reaction was then quenched by exposing it to air, the crude reaction mixture was diluted with THF and passed through a plug of silica gel in a Pasteur pipette and then analyzed by GC chromatography without additional purification.

IVb. General procedure for the borylation of 2,6-lutidine

In a nitrogen-filled glovebox a glass vessel with a J. Young seal was charged with a magnetic stir bar, B_2Pin_2 (0.064 g, 0.2510 mmol), 2,6-lutidine (29 µL, 0.2503 mmol), mesitylene (10 µL, 0.0719 mmol), 0.50 mL of THF and **1-H_3·NaHBEt_3** (0.011 g, 0.0127 mmol) or **2-H_3·NaHBEt_3** (0.012 g, 0.0134 mmol) or **2-$(H)_2$BPin** (0.012 g, 0.0134 mmol),. The tube was sealed and the resulting mixture was stirred at 100 ºC for 24 hours. The reaction was then quenched by exposing it to air, the crude reaction mixture was diluted with THF and passed through a plug of silica gel in a Pasteur pipette and then analyzed by GC chromatography without additional purification.

V. Spectroscopic Data and Additional Information.

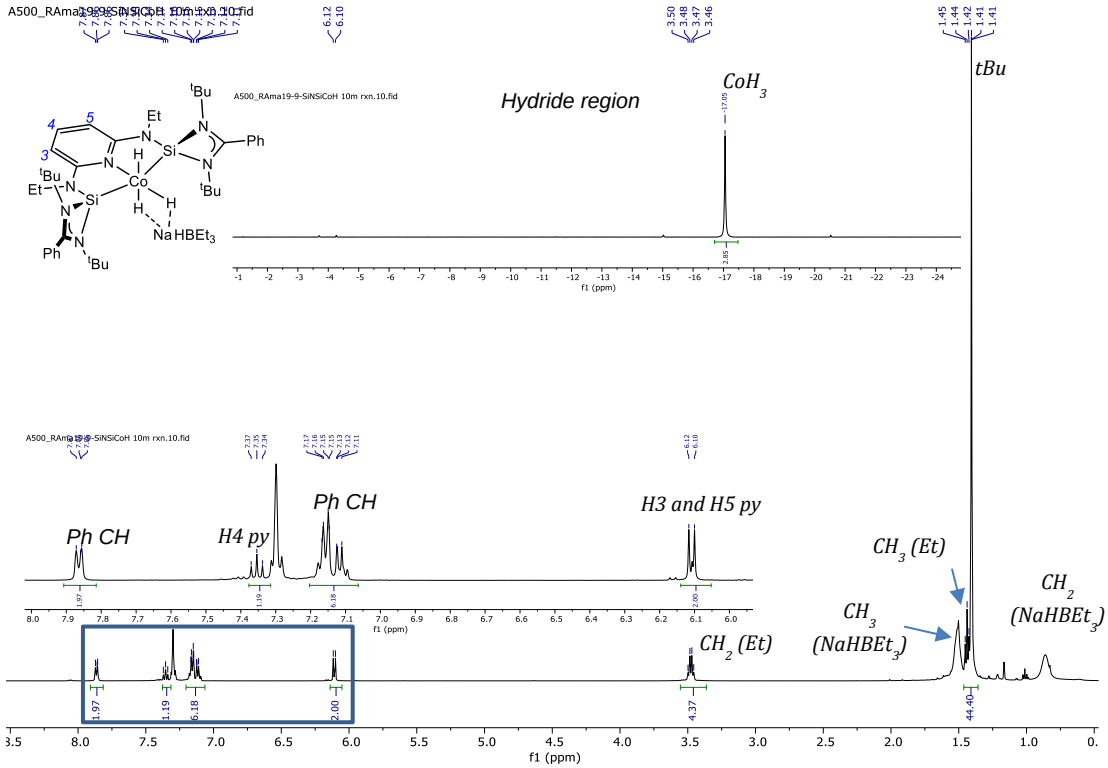

Figure S1. ^{1}H NMR spectrum of **1-H$_3$·NaHBEt$_3$** in C_6D_6 at 300 K. The inset is an expanded view of the hydride region.

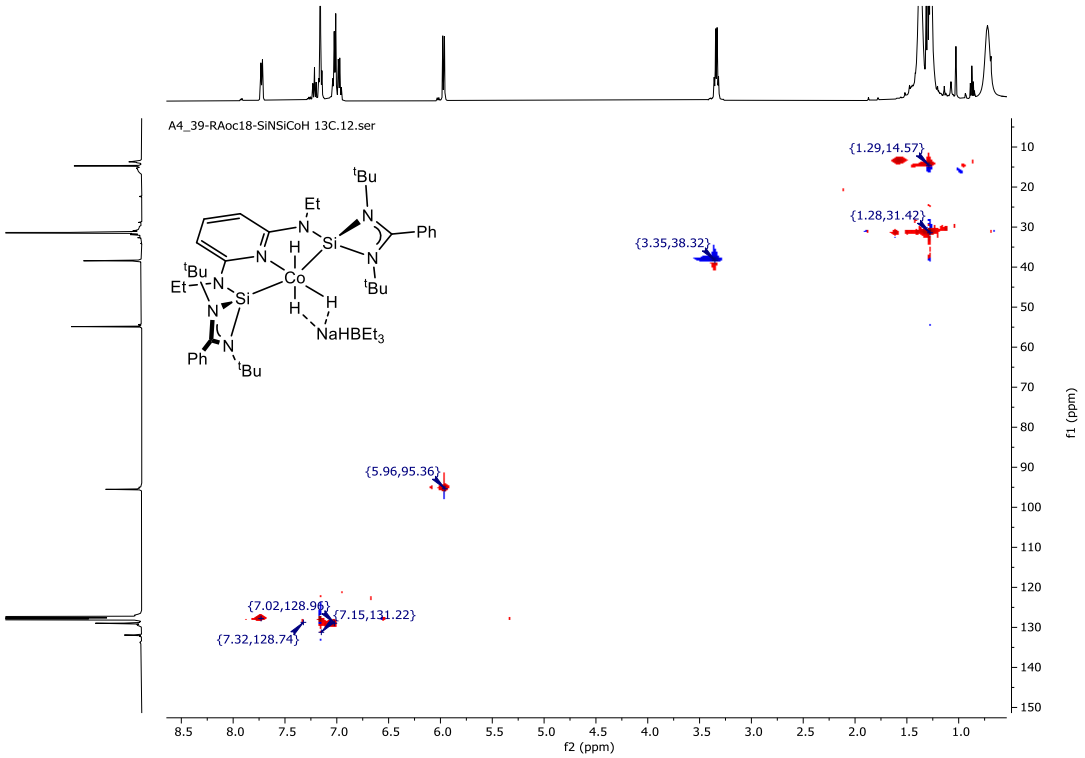

Figure S2. ^{1}H,^{13}C-HSQC NMR spectrum of **1-H$_3$·NaHBEt$_3$** in C_6D_6 at 300 K.

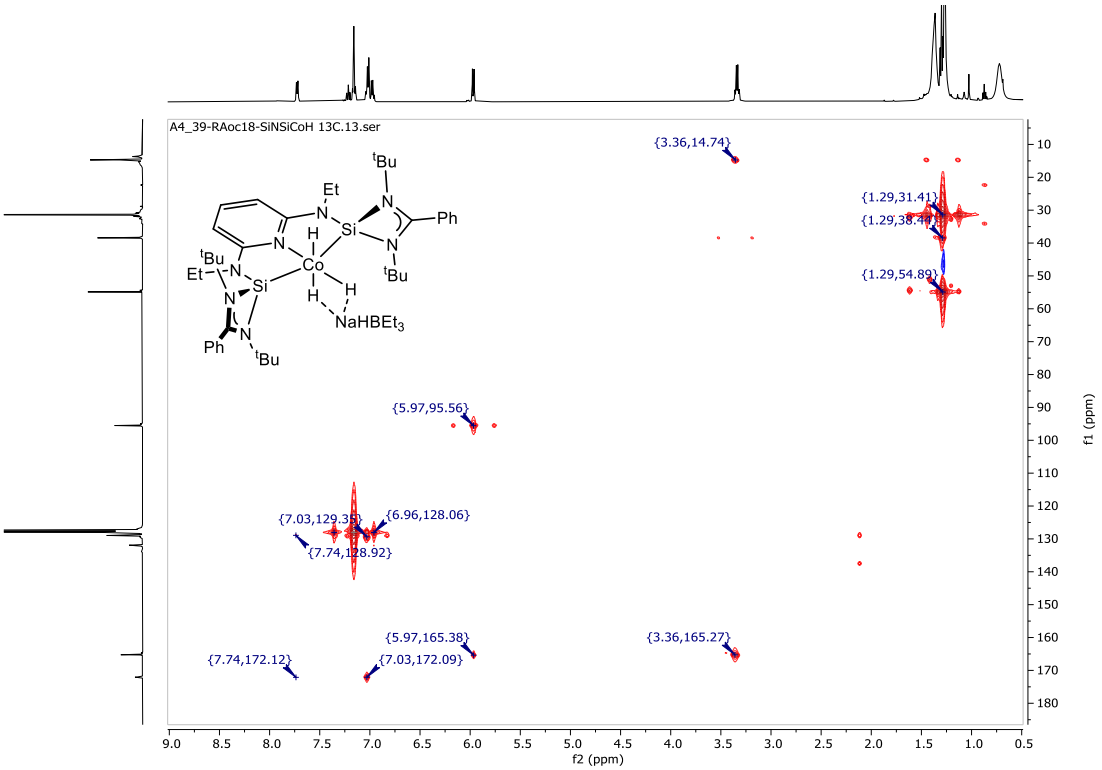

Figure S3. $^{1}H,^{13}C$-HMBC NMR spectrum of **1-H$_3$·NaHBEt$_3$** in C_6D_6 at 300 K.

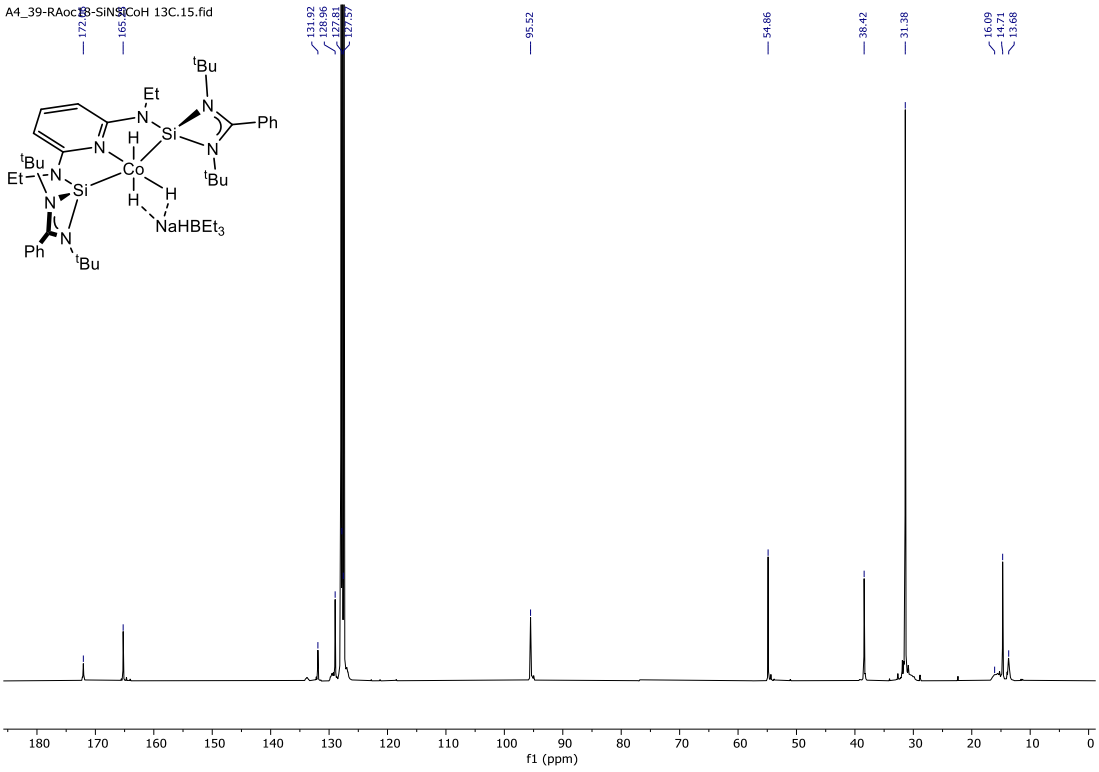

Figure S4. ^{13}C NMR spectrum of **1-H$_3$·NaHBEt$_3$** in C_6D_6 at 300 K.

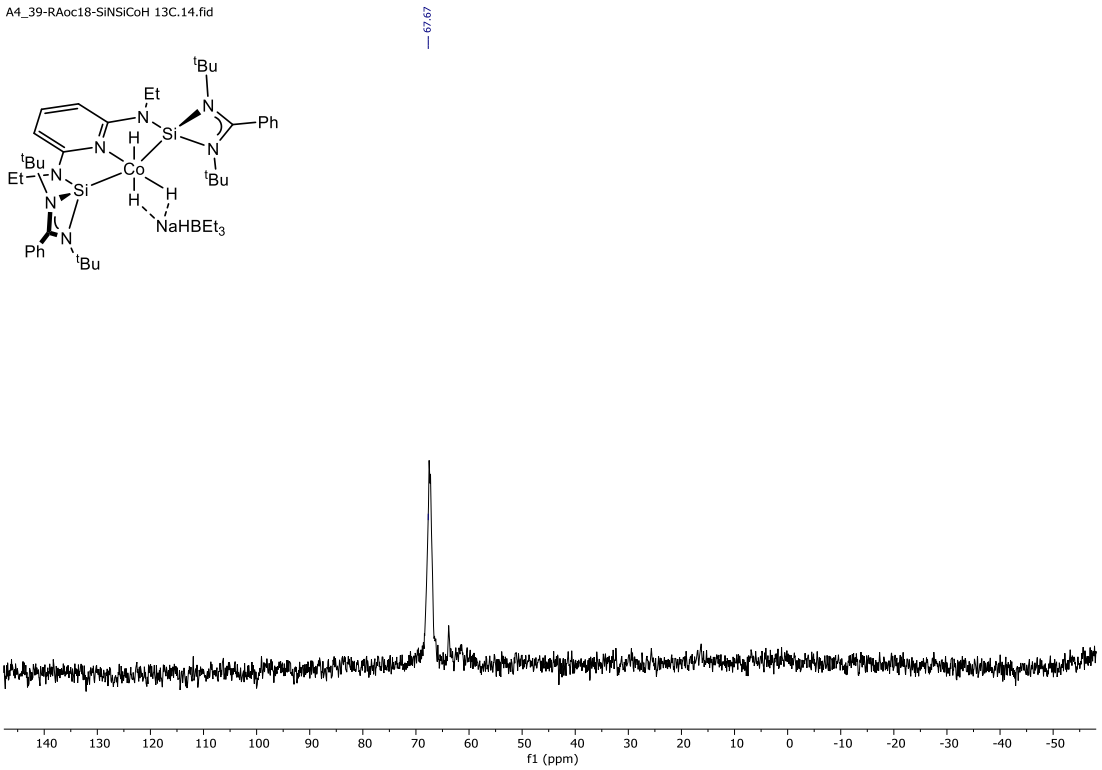

Figure S5. ^{29}Si NMR spectrum of **1-H$_3$·NaHBEt$_3$** in C_6D_6 at 300 K.

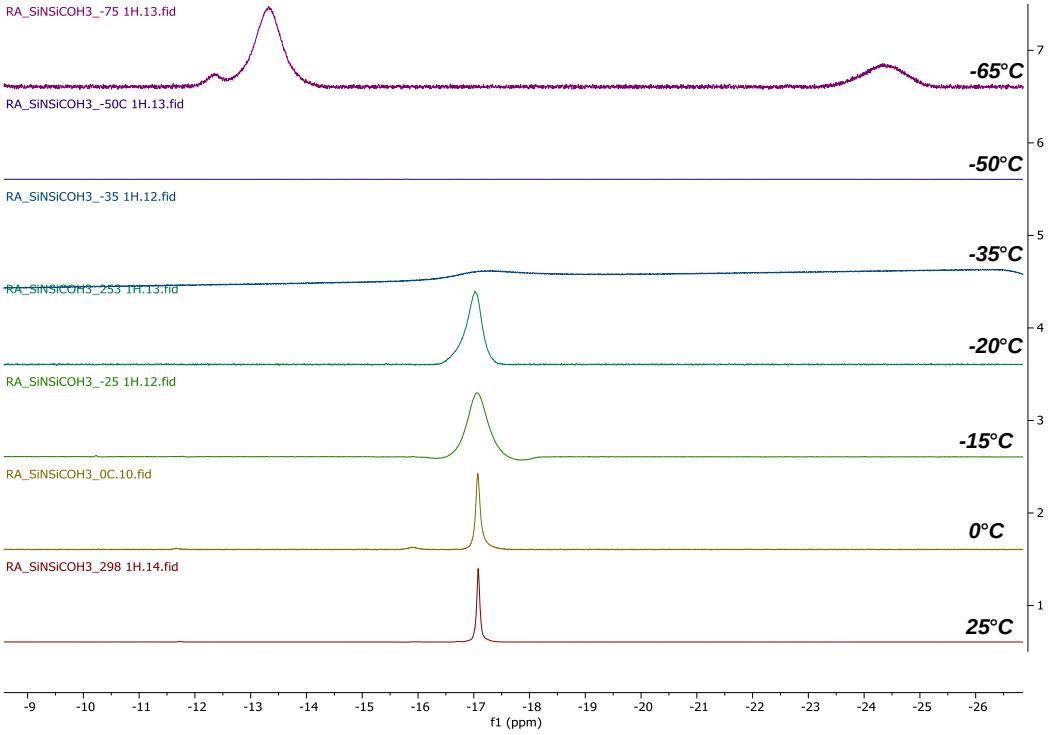

Figure S6. VT-^{1}H NMR spectrum of **1-H$_3$·NaHBEt$_3$** in toluene-d_8 (hydride region).

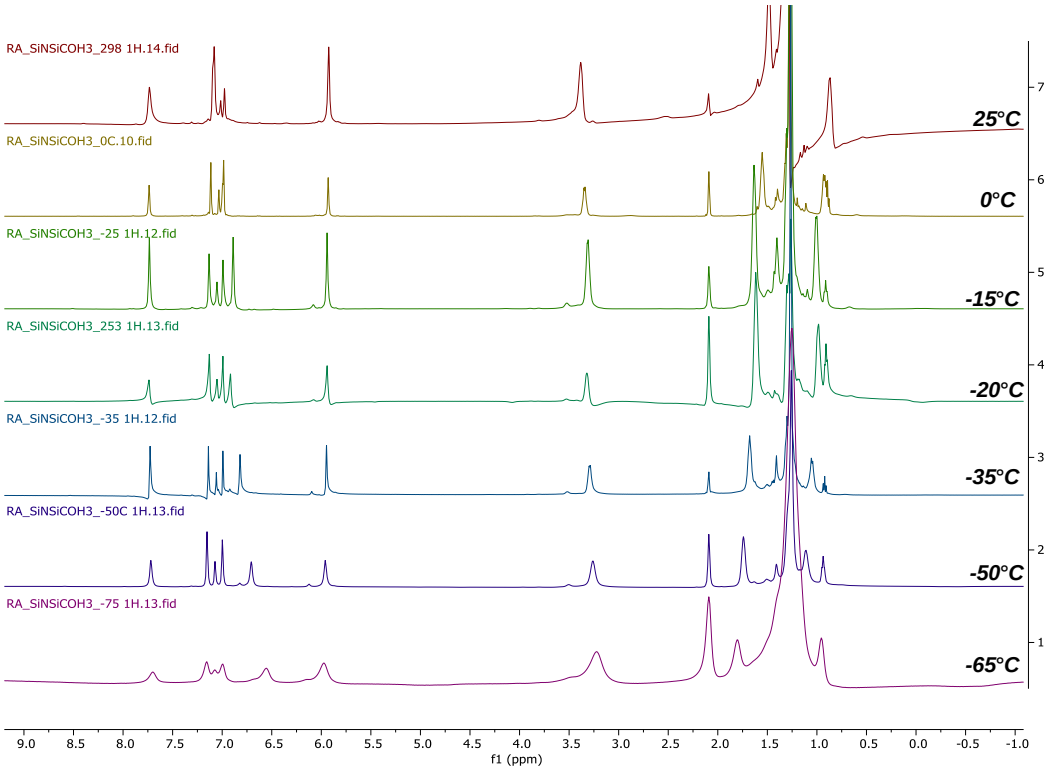

Figure S7. VT-^{1}H NMR spectrum of **1-H$_3$·NaHBEt$_3$** in toluene-d_8 (aromatic region).

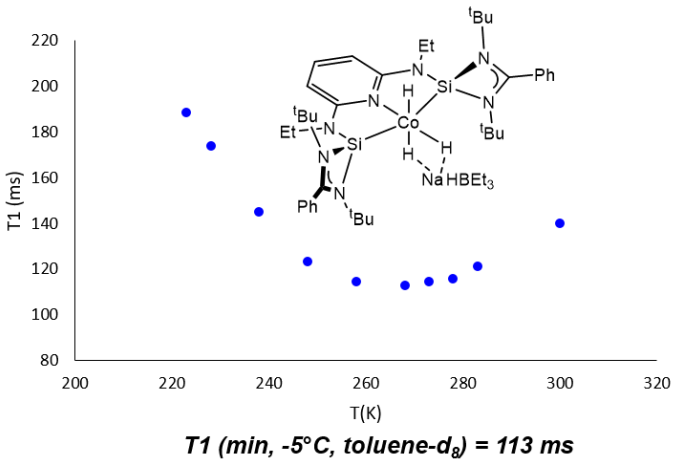

T1 (min, -5°C, toluene-d$_8$) = 113 ms

T (K)	T$_1$ (ms)
300	140
283	121
278	116
273	114
268	113
258	114
248	123
238	145
228	174
223	188

Figure S8. T_1 values for the hydride ligands in **1-H$_3$·NaHBEt$_3$** in toluene-d_8 at different temperatures.

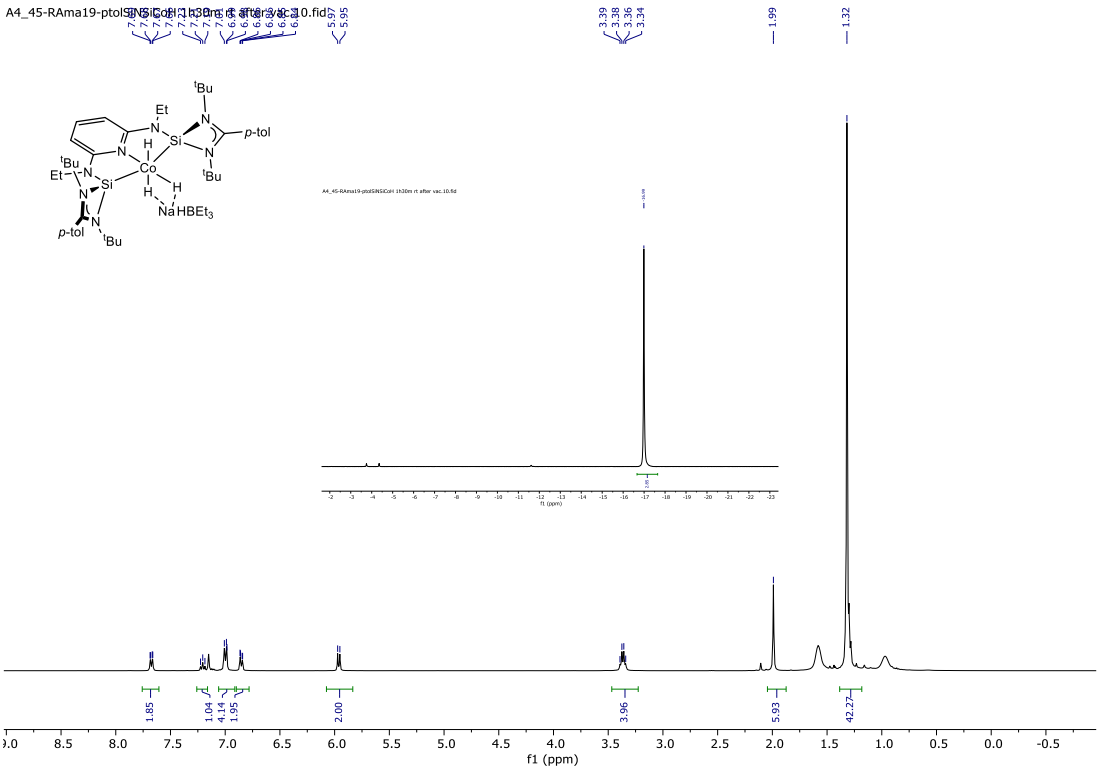

Figure S9. ^{1}H NMR spectrum of **2-H$_3$·NaHBEt$_3$** in C_6D_6 at 300 K. The inset is an expanded view of the hydride region.

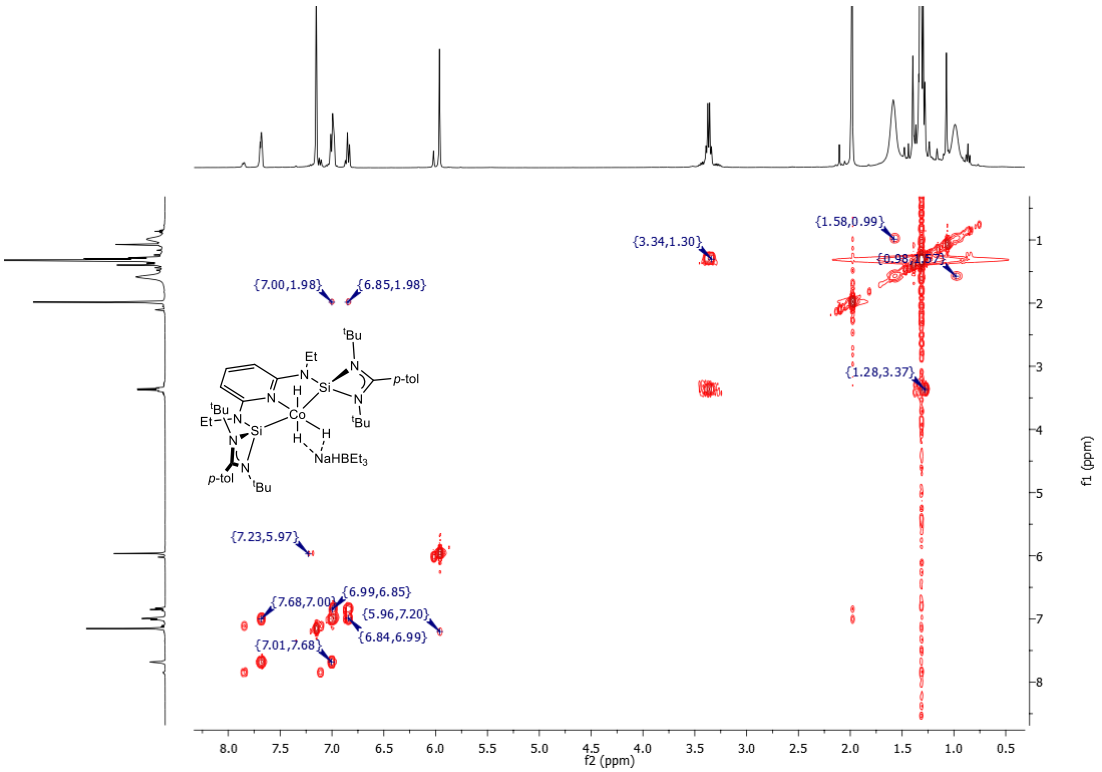

Figure S10. ^{1}H, ^{1}H-COSY NMR spectrum of **2-H$_3$·NaHBEt$_3$** in C_6D_6 at 300 K.

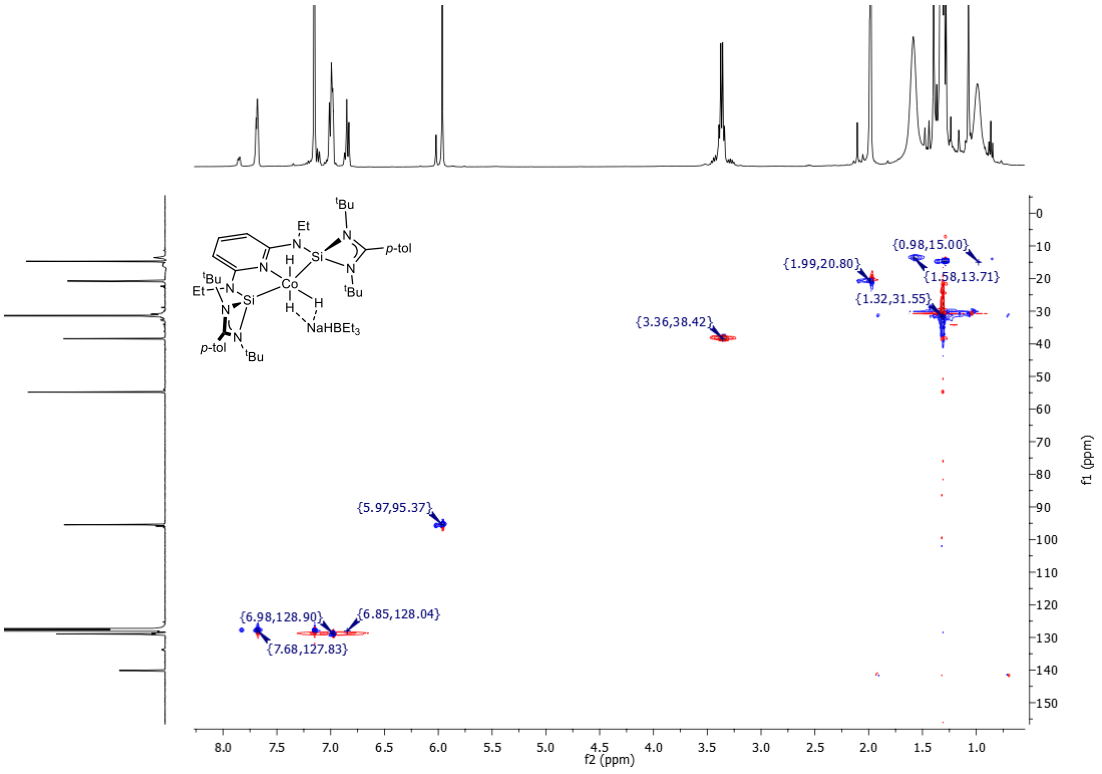

Figure S11. ^{1}H, ^{13}C-HSQC NMR spectrum of **2-H₃·NaHBEt₃** in C_6D_6 at 300 K.

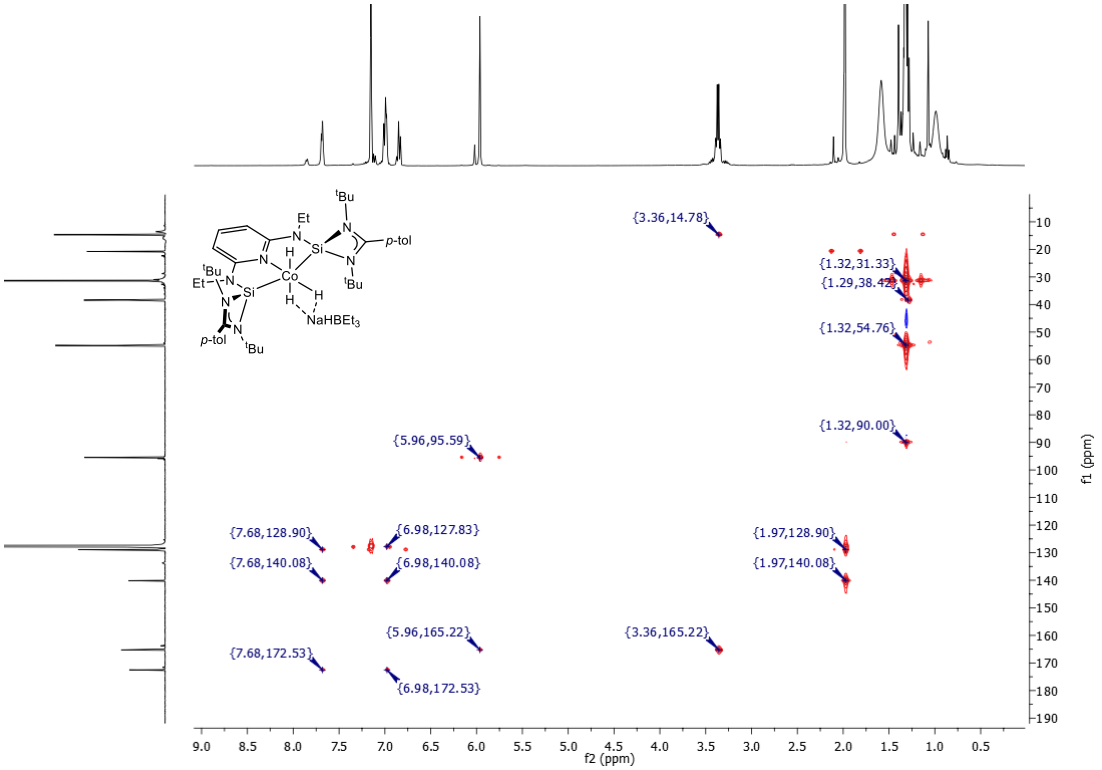

Figure S12. ^{1}H, ^{13}C-HMBC NMR spectrum of **2-H₃·NaHBEt₃** in C_6D_6 at 300 K.

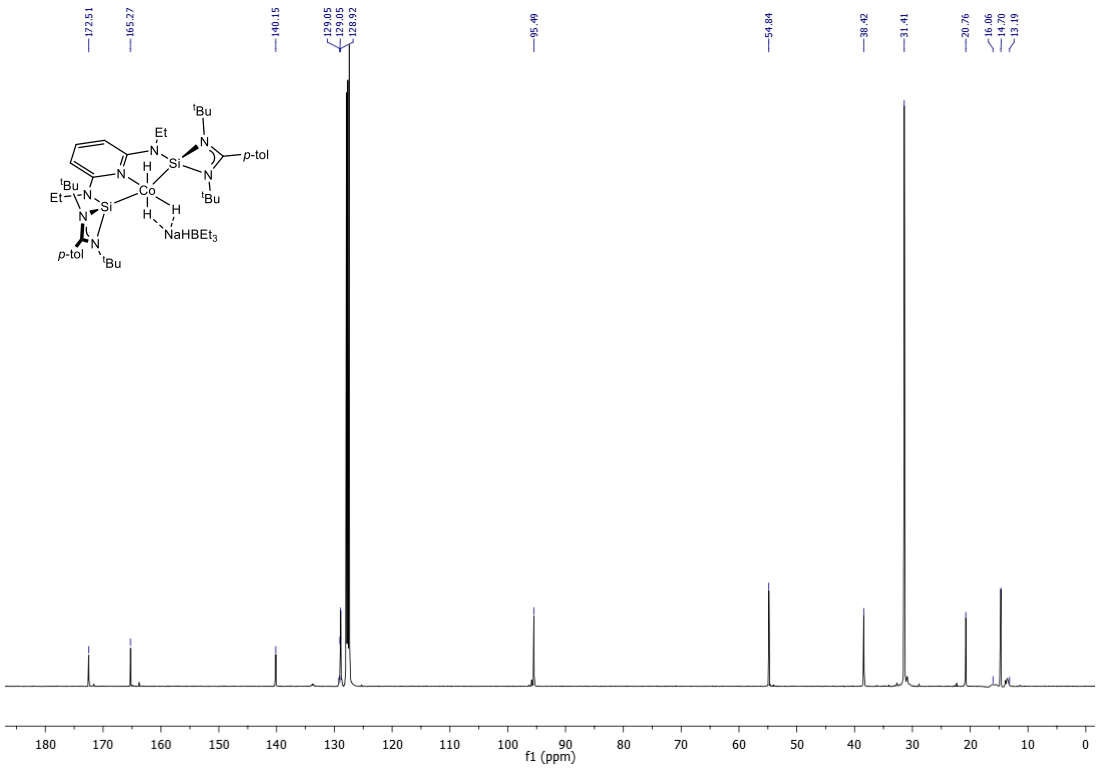

Figure S13. ^{13}C NMR spectrum of **2-H$_3$·NaHBEt$_3$** in C_6D_6 at 300 K.

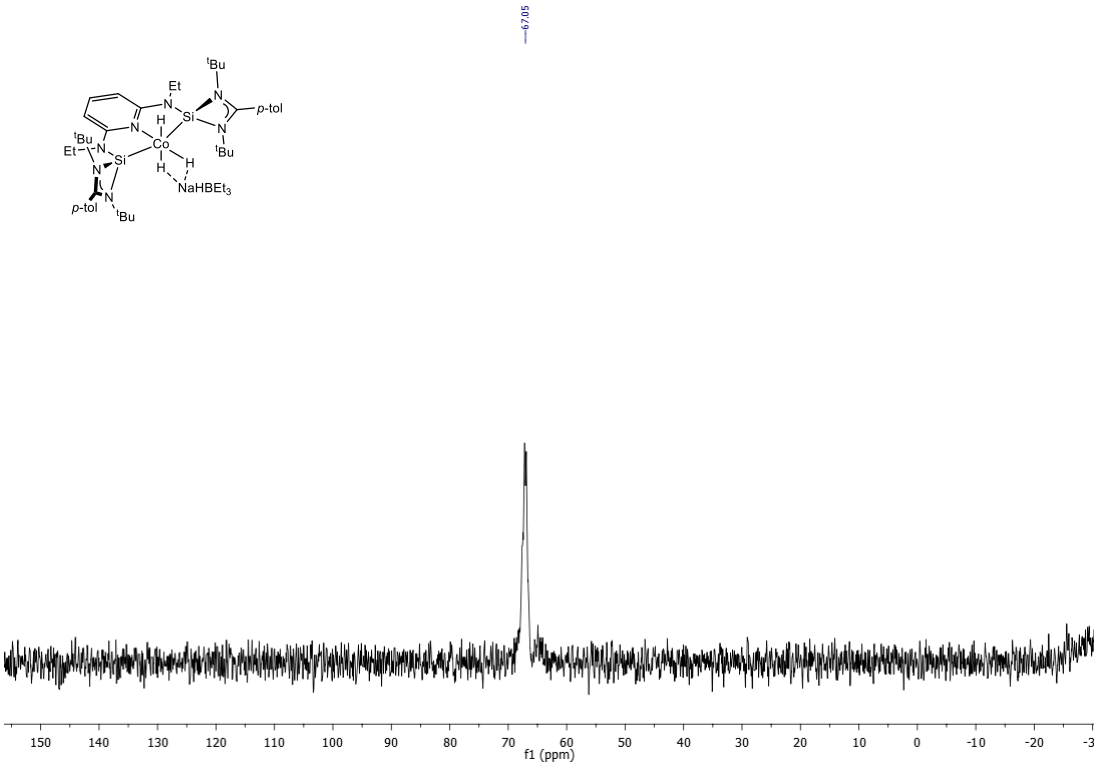

Figure S14. ^{29}Si NMR spectrum of **2-H$_3$·NaHBEt$_3$** in C_6D_6 at 300 K.

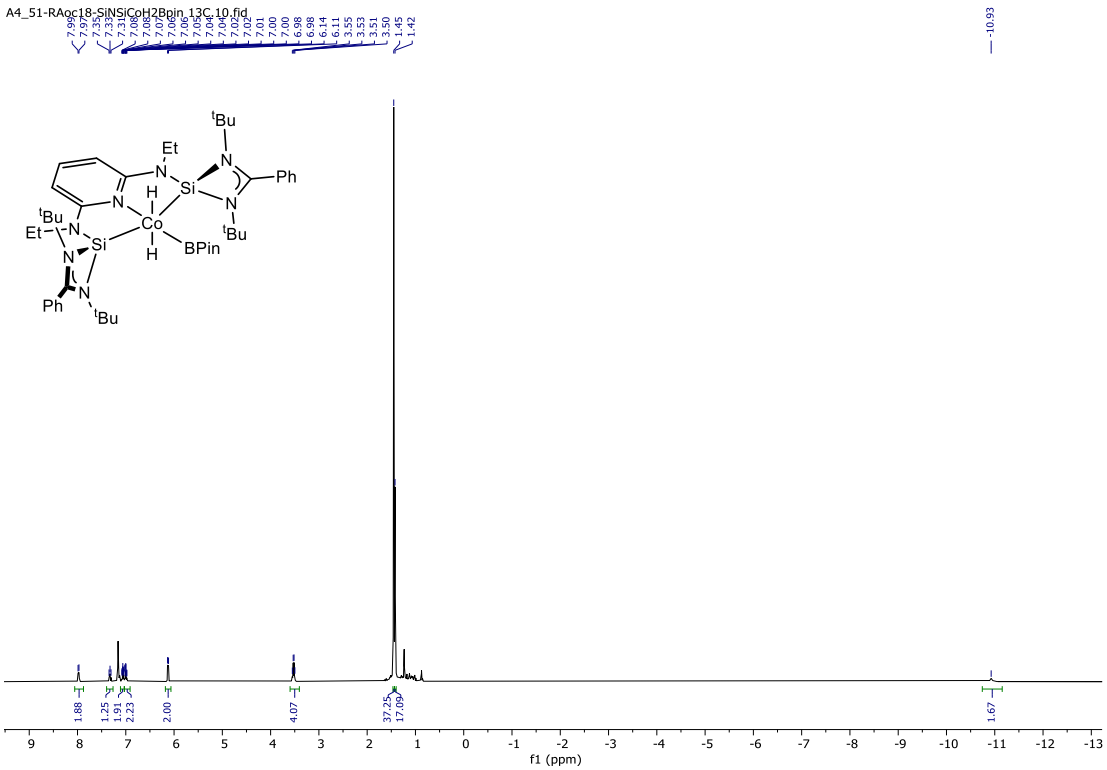

Figure S15. ^{1}H NMR spectrum of **1-(H)$_2$BPin** in C_6D_6 at 300 K.

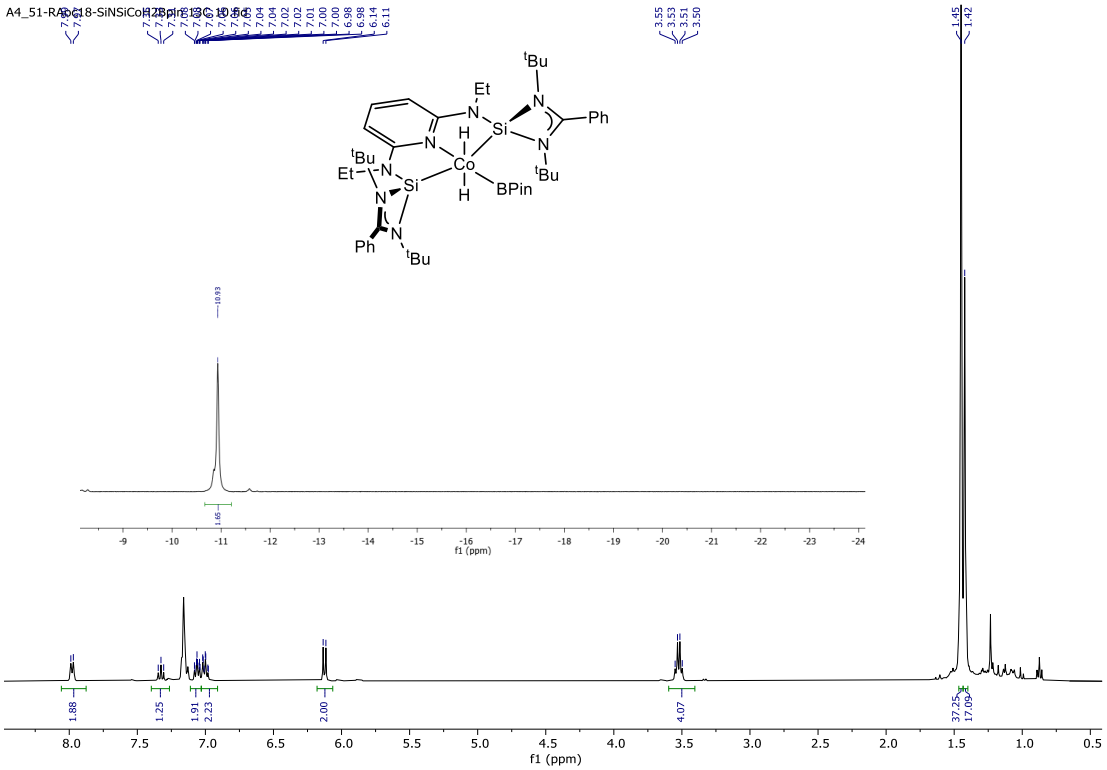

Figure S16. ^{1}H NMR spectrum of **1-(H)$_2$BPin** in C_6D_6 at 300 K. The inset is an expanded view of the hydride region.

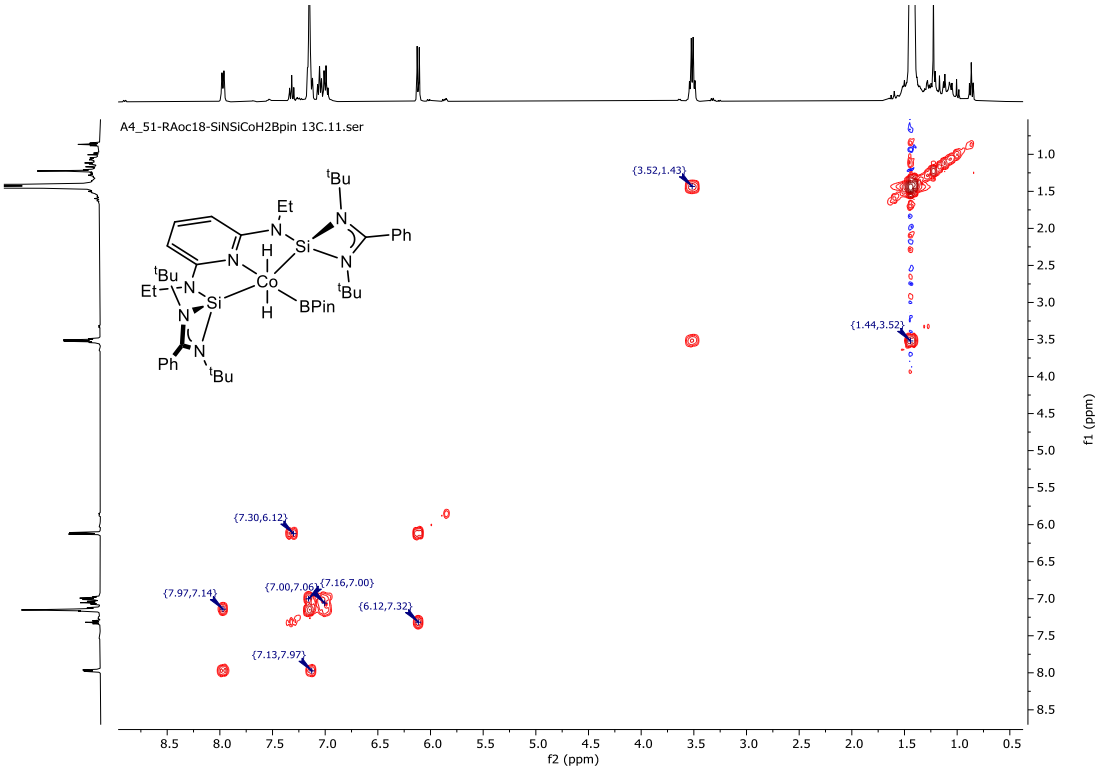

Figure S17. ^{1}H, ^{1}H-COSY NMR spectrum of **1-(H)$_2$BPin** in C_6D_6 at 300 K.

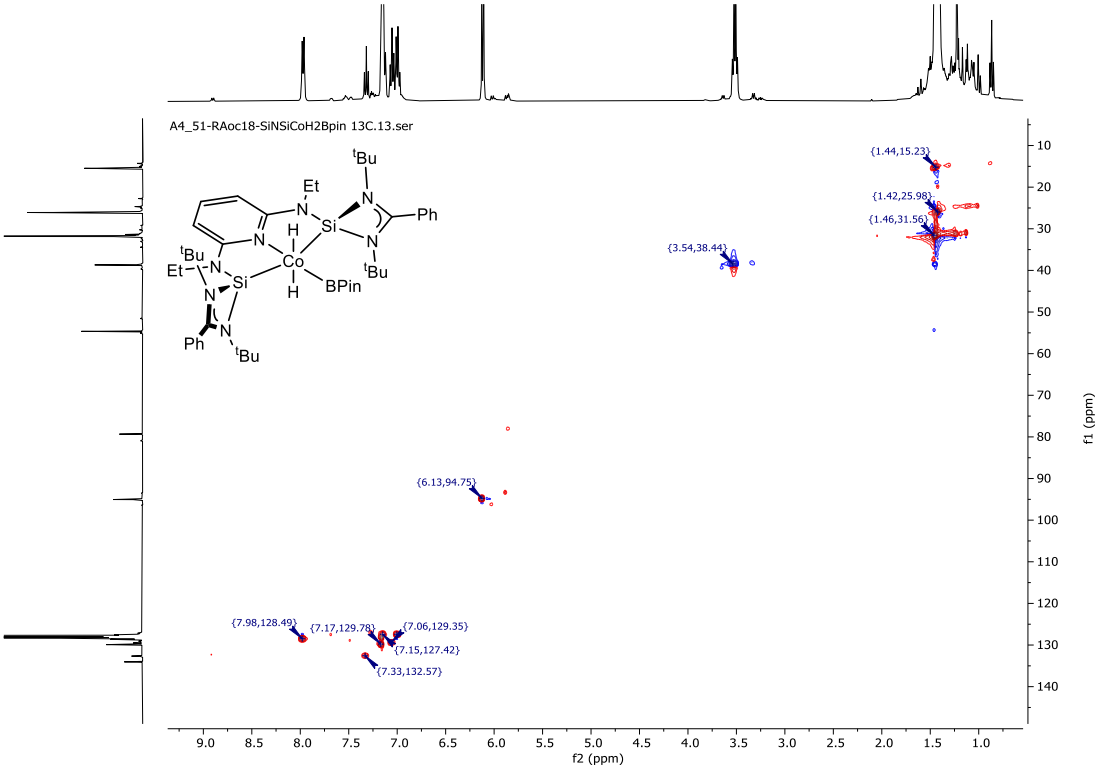

Figure S18. ^{1}H, ^{13}C-HSQC NMR spectrum of **1-(H)$_2$BPin** in C_6D_6 at 300 K.

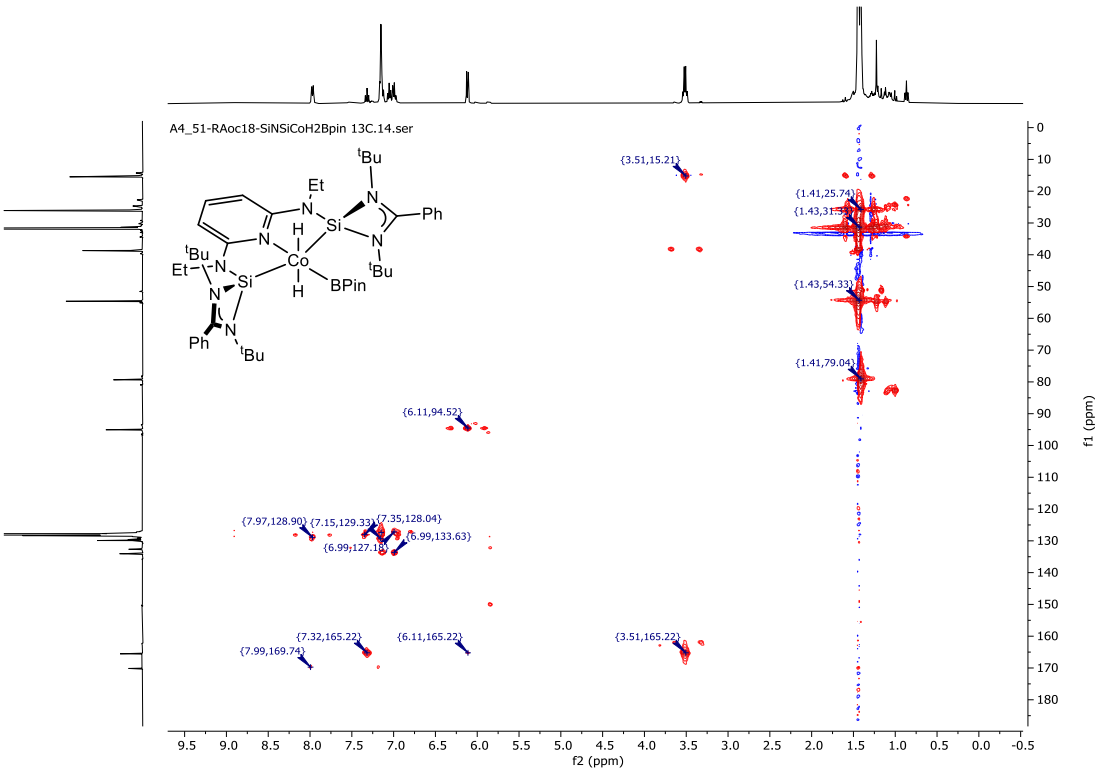

Figure S19. ^{1}H, ^{13}C-HMBC NMR spectrum of **1-(H)$_2$BPin** in C_6D_6 at 300 K.

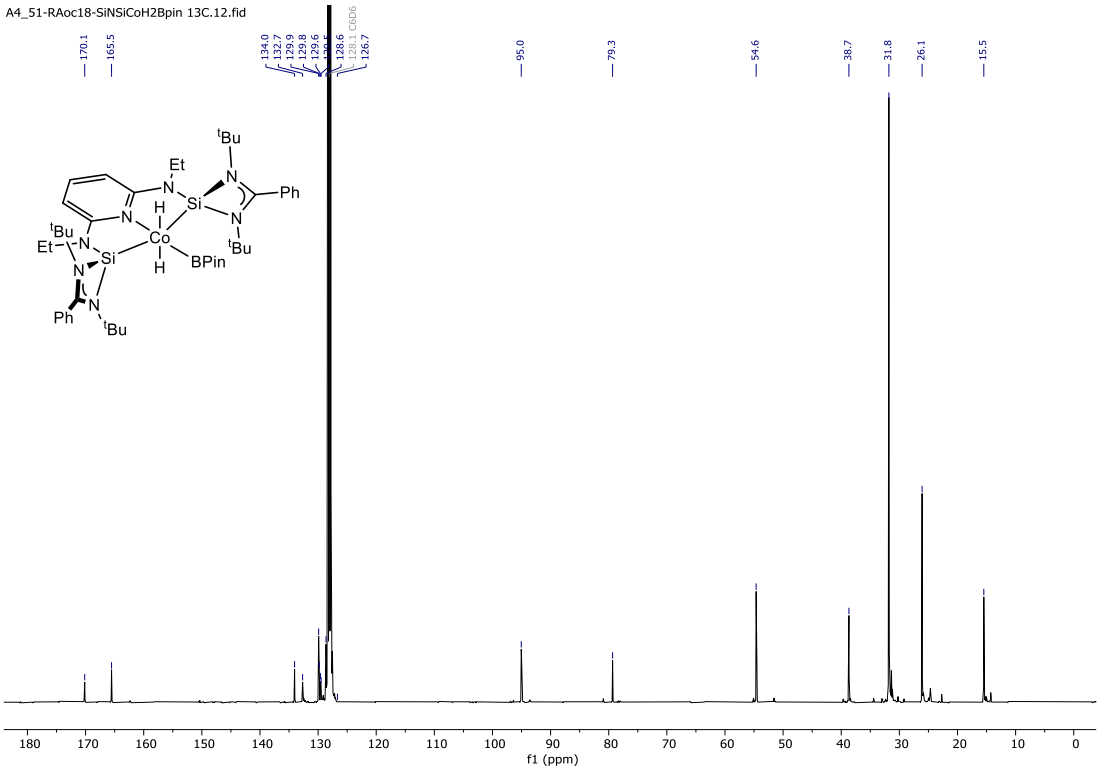

Figure S20. ^{13}C NMR spectrum of **1-(H)$_2$BPin** in C_6D_6 at 300 K.

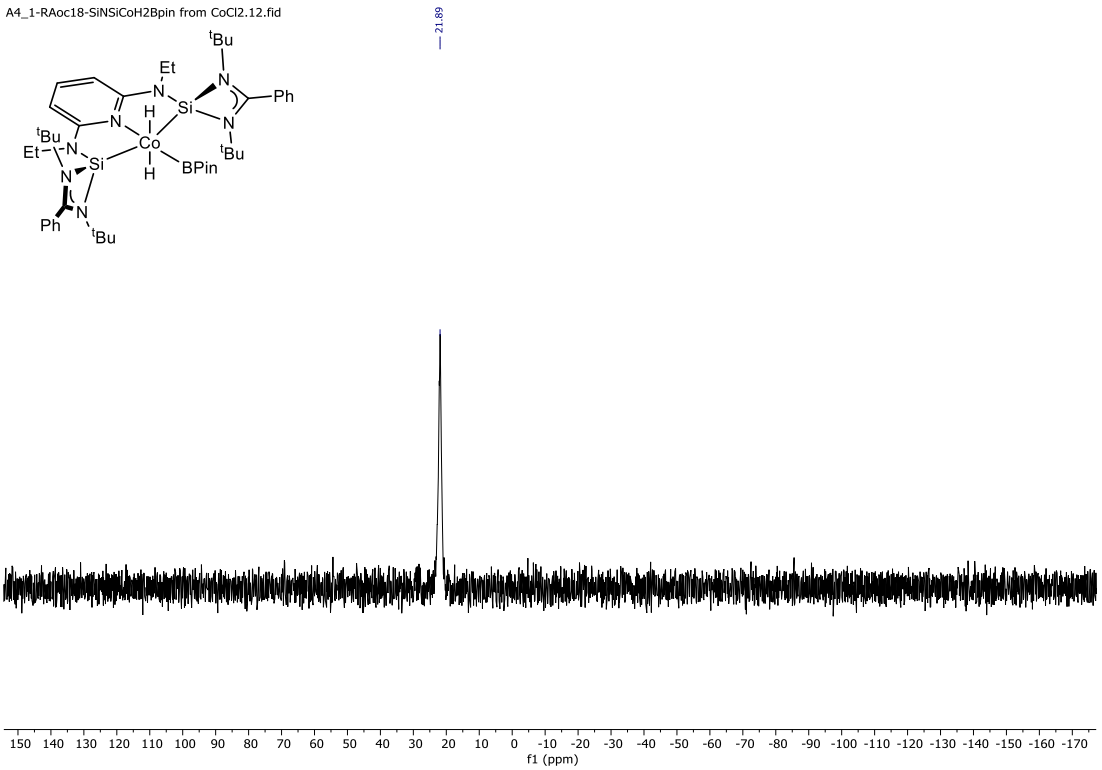

Figure S21. ^{11}B NMR spectrum of **1-(H)$_2$BPin** in C_6D_6 at 300 K.

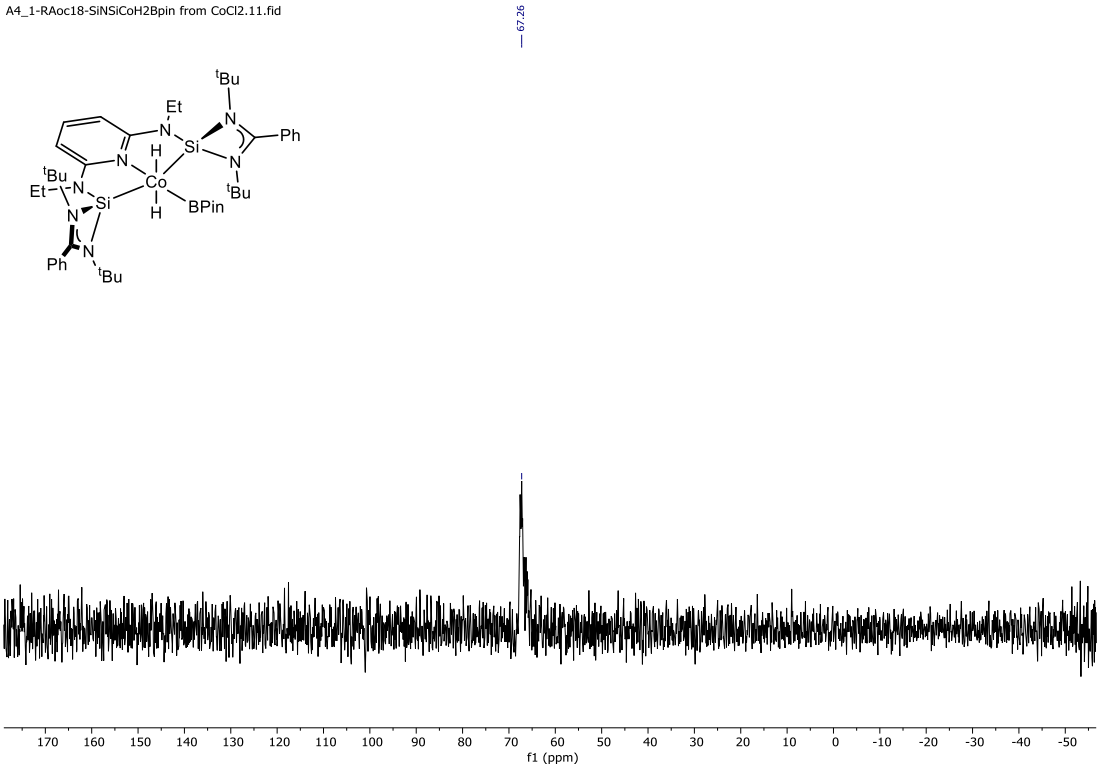

Figure S22. ^{29}Si NMR spectrum of **1-(H)$_2$BPin** in C_6D_6 at 300 K.

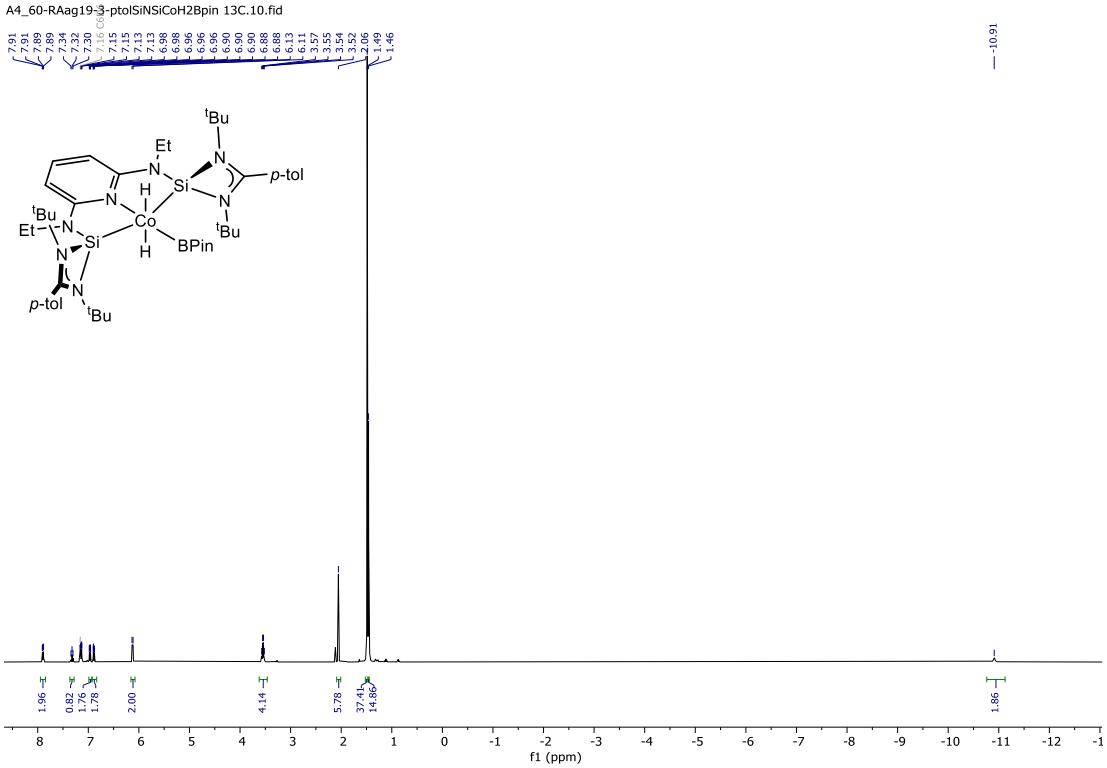

Figure S23. ^{1}H NMR spectrum of **2-(H)$_2$BPin** in C_6D_6 at 300 K.

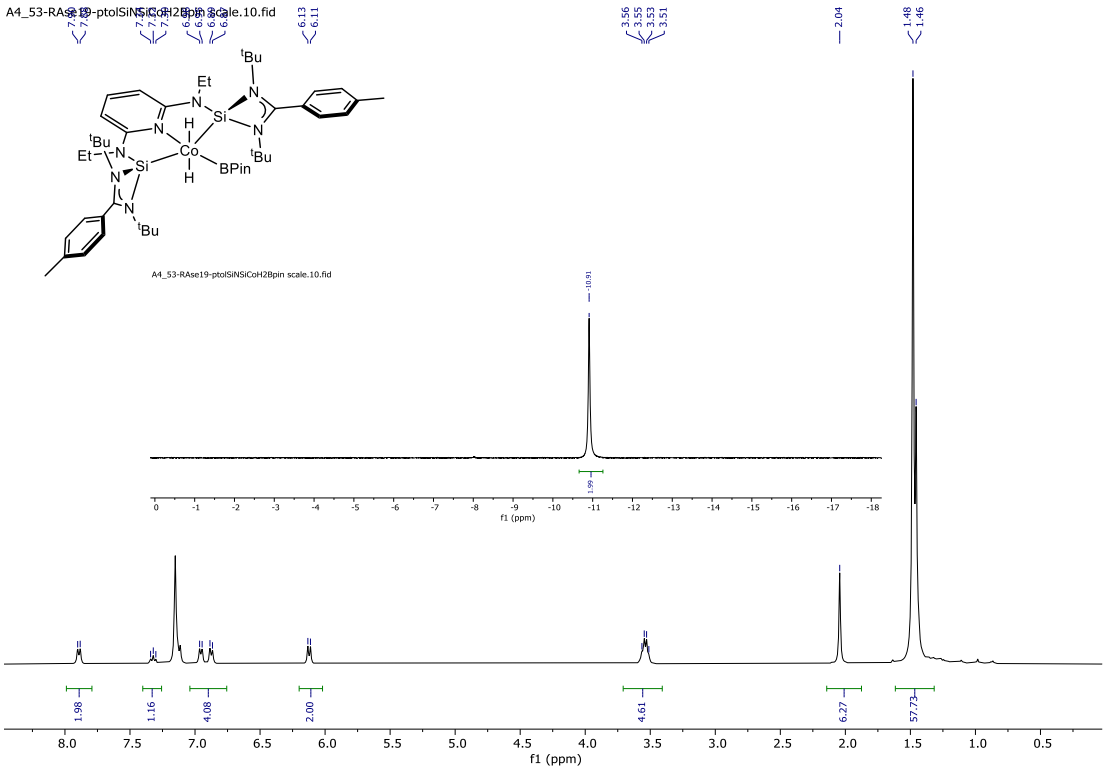

Figure S24. ^{1}H NMR spectrum of **2-(H)$_2$BPin** in C_6D_6 at 300 K. The inset is an expanded view of the hydride region.

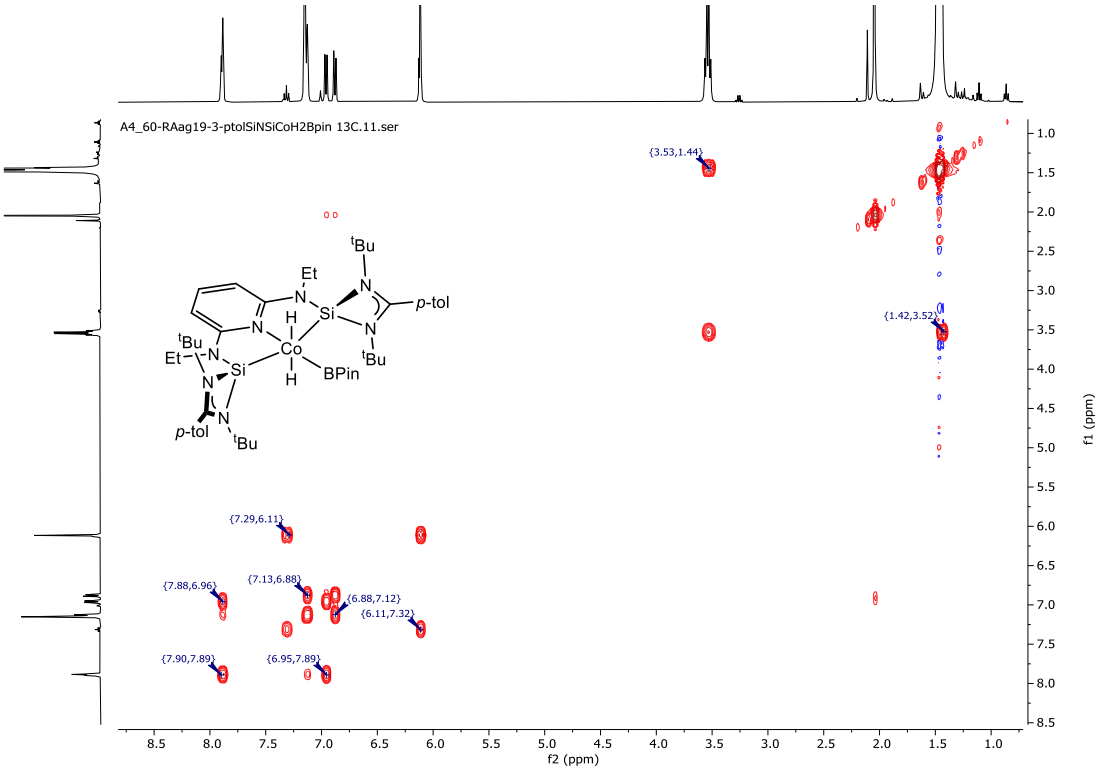

Figure S25. ^{1}H, ^{1}H-COSY NMR spectrum of **2-(H)$_2$BPin** in C_6D_6 at 300 K.

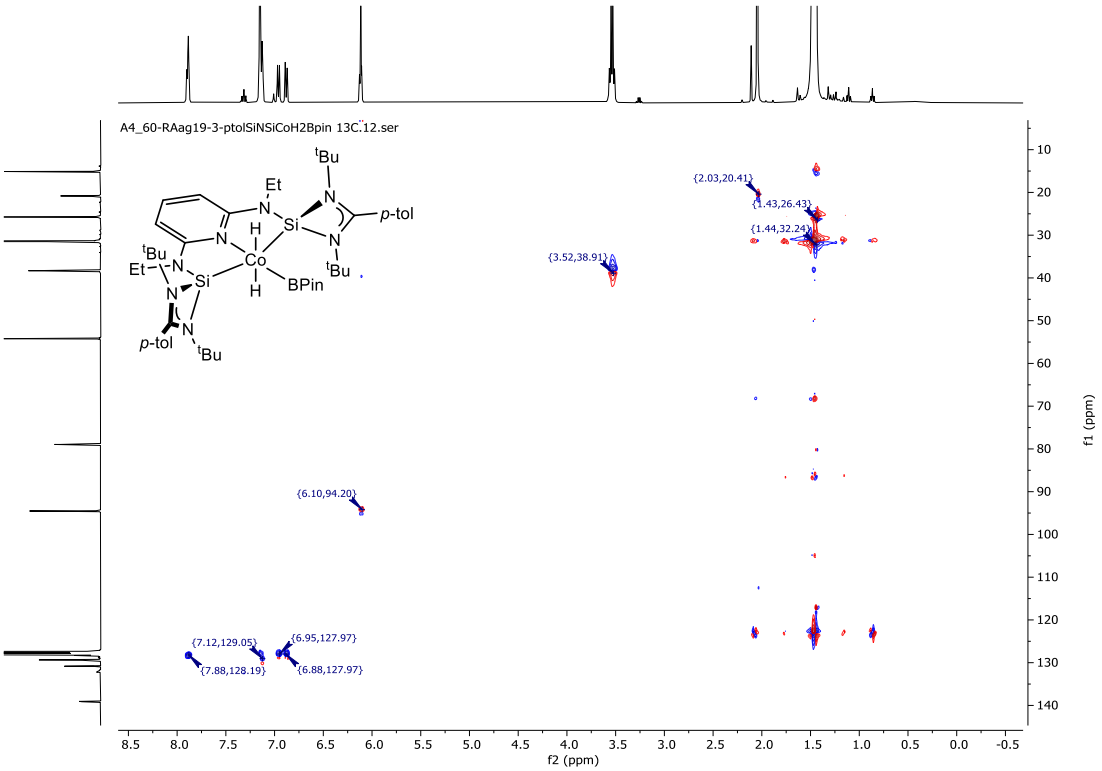

Figure S26. ^{1}H, ^{13}C-HSQC NMR spectrum of **2-(H)$_2$BPin** in C_6D_6 at 300 K.

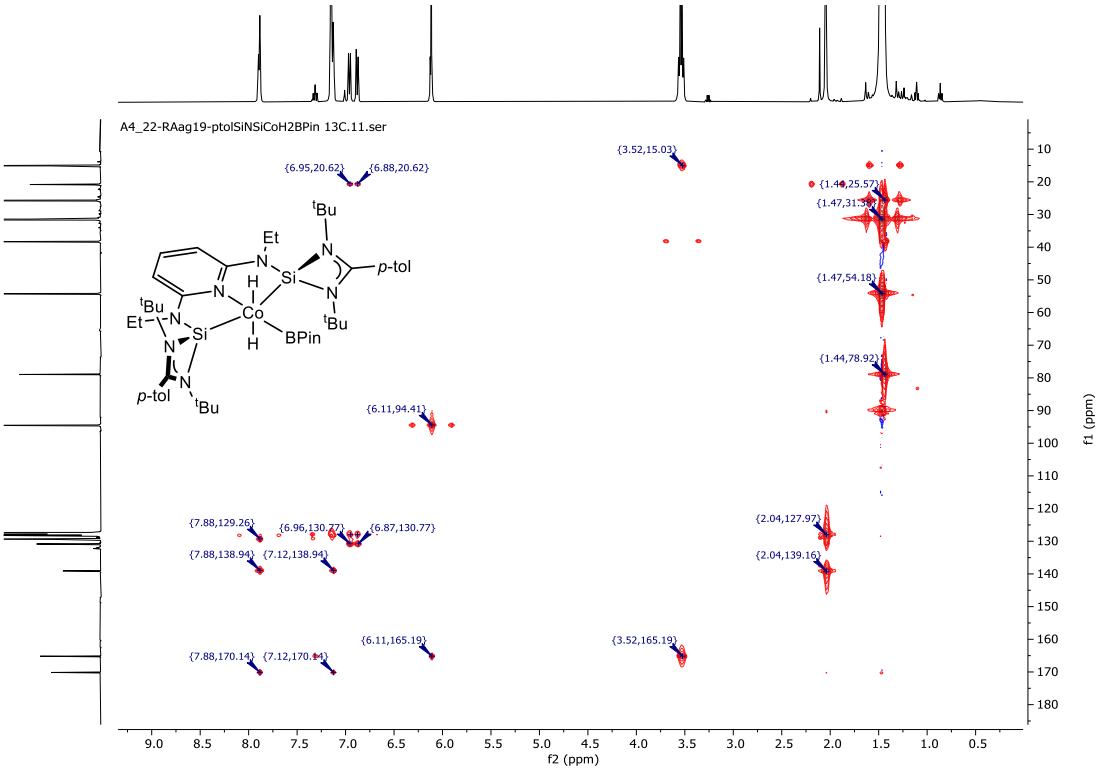

Figure S27. ^{1}H, ^{13}C-HMBC NMR spectrum of **2-(H)$_2$BPin** in C_6D_6 at 300 K.

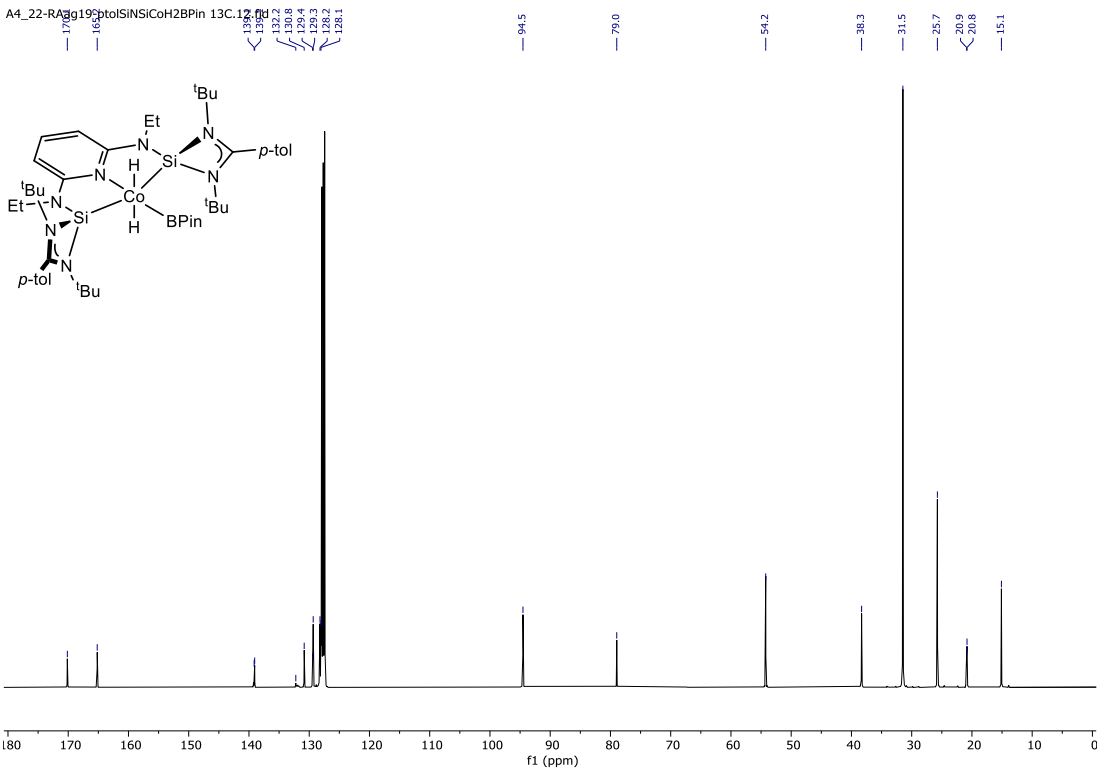

Figure S28. ^{13}C NMR spectrum of **2-(H)$_2$BPin** in C_6D_6 at 300 K.

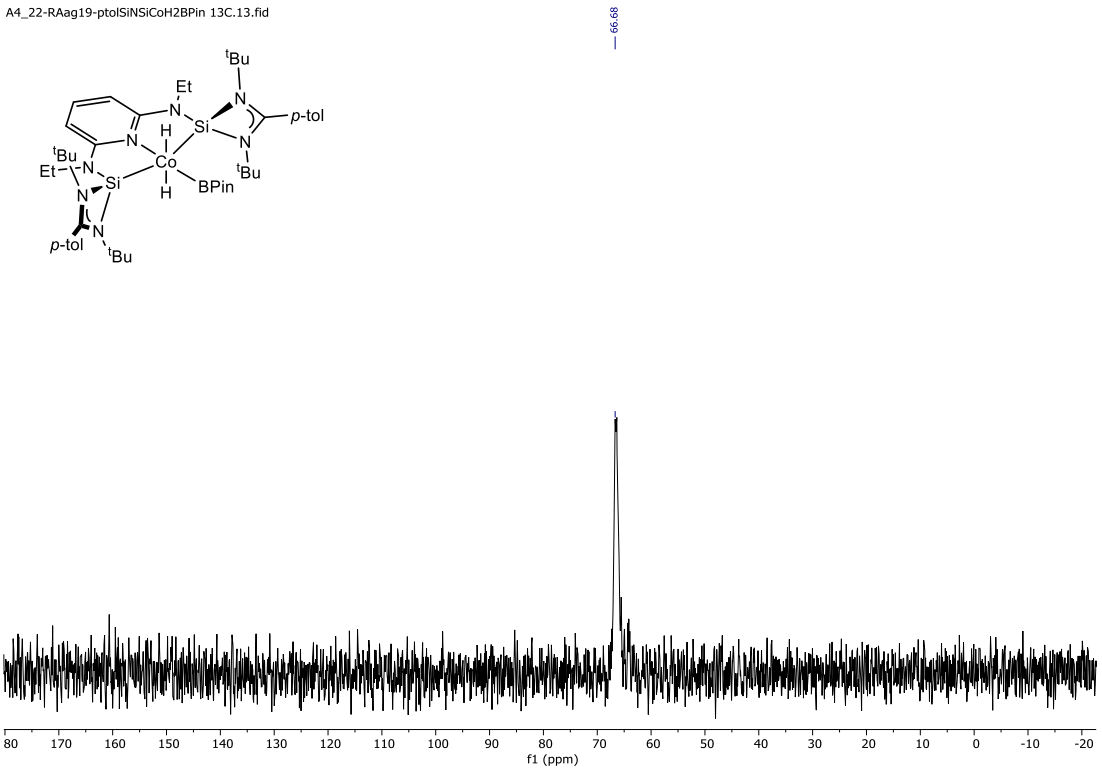

Figure S29. ^{29}Si NMR spectrum of **2-(H)$_2$BPin** in C_6D_6 at 300 K.

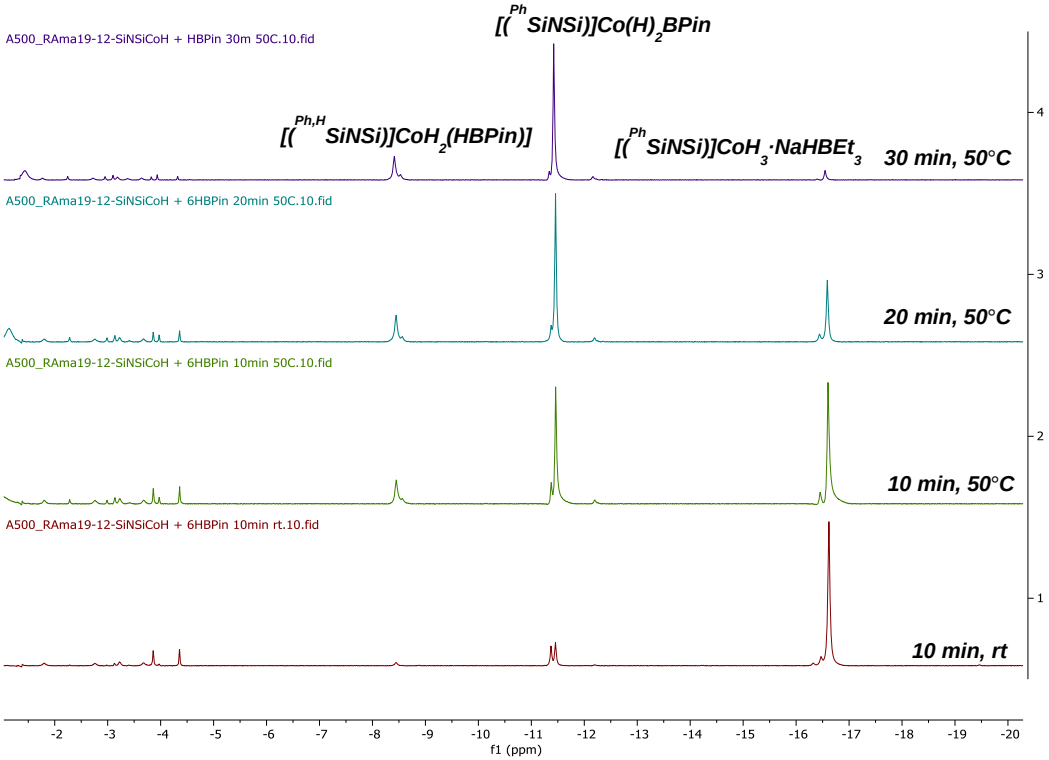

Figure S30. ^{1}H NMR monitoring for the reaction of **1-H$_3$·NaHBEt$_3$** with HBPin in THF-d_8 at 50ºC showing formation of **1-H$_2$BPin** and [(^{Ph,H}SiNSi)CoH$_2$(HBPin)] (hydride region).

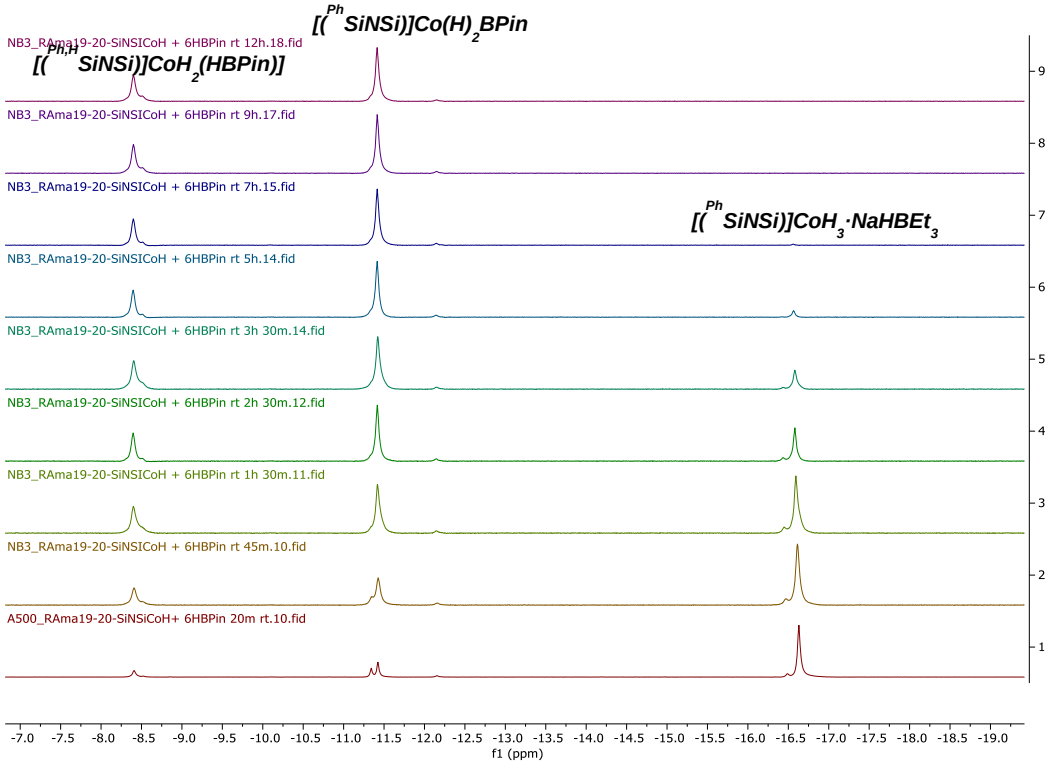

Figure S31. ^{1}H NMR monitoring for the reaction of **1-H$_3$·NaHBEt$_3$** with HBPin in THF-d_8 at room temperature showing formation of **1-H$_2$BPin** and [(^{Ph,H}SiNSi)CoH$_2$(HBPin)] (hydride region).

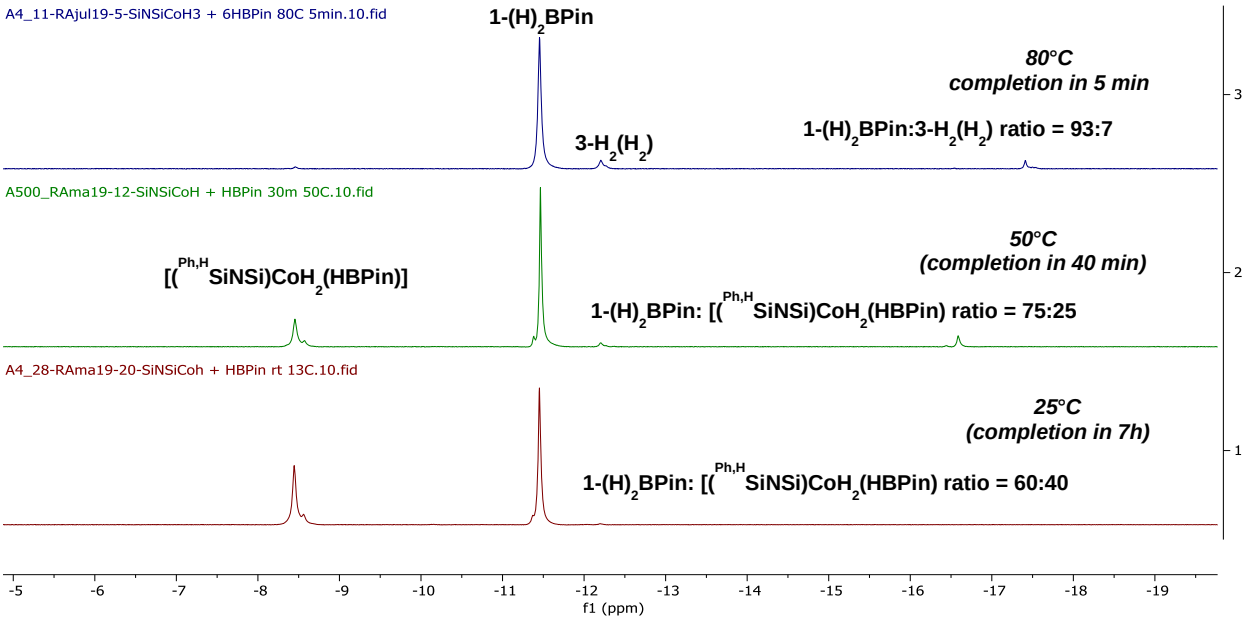

Figure S32. ^{1}H NMR spectra for the reaction of **1-H$_3$·NaHBEt$_3$** with HBPin in THF-d_8 at different temperatures showing formation of **1-H$_2$BPin** and [(^{Ph,H}SiNSi)CoH$_2$(HBPin)] in different ratios (hydride region).

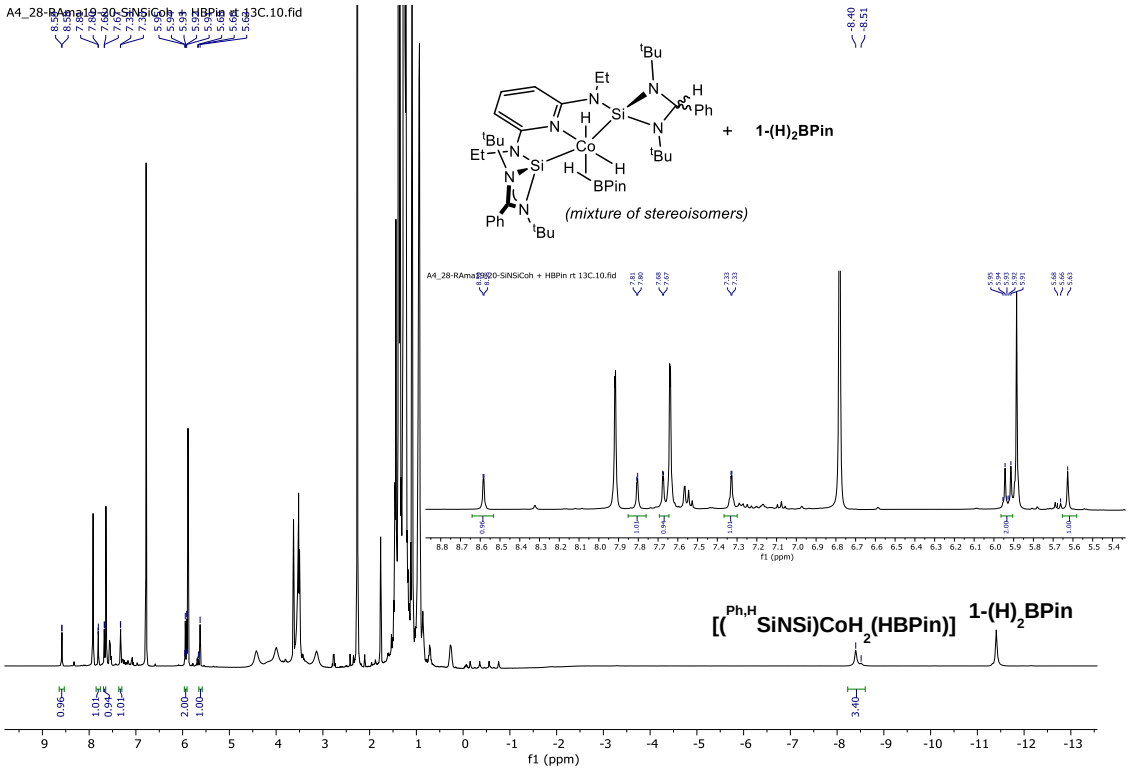

Figure S33. ^{1}H NMR spectrum of a mixture of **1-(H)$_2$BPin** and [(^{Ph,H}SiNSi)CoH$_2$(HBPin)] (60:40 ratio) in THF-d_8 in the presence of HBPin at 300 K. The inset is an expanded view of the aromatic region.

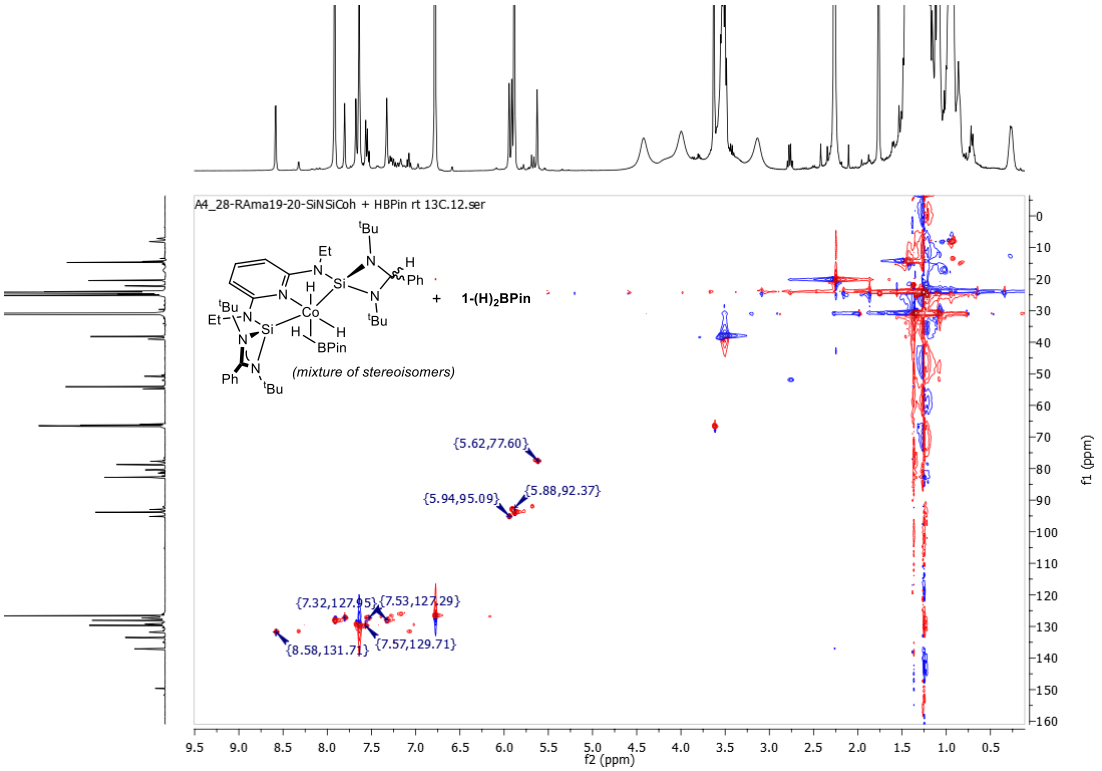

Figure S34. ^{1}H, ^{13}C-HSQC NMR spectrum of a mixture of **1-(H)$_2$BPin** and [(^{Ph,H}SiNSi)CoH$_2$(HBPin)] (60:40 ratio) in THF-d_8 in the presence of HBPin at 300 K.

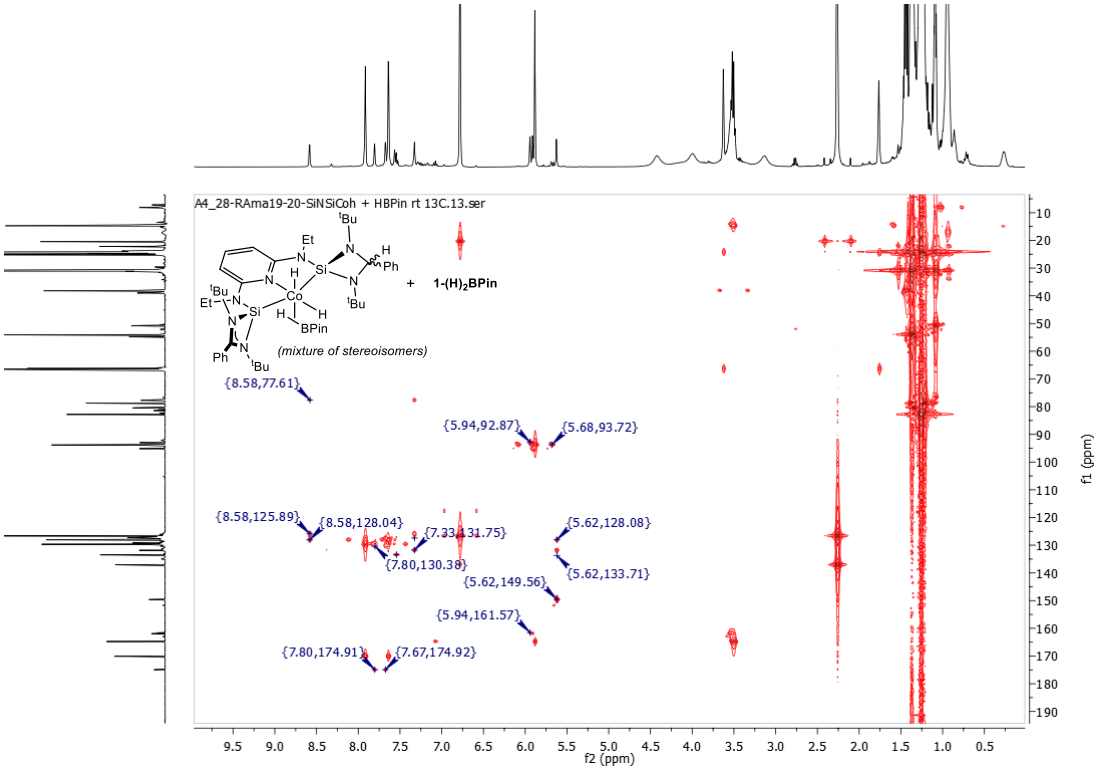

Figure S35. ^{1}H, ^{13}C-HMBC NMR spectrum of a mixture of **1-(H)$_2$BPin** and [(^{Ph,H}SiNSi)CoH$_2$(HBPin)] (60:40 ratio) in THF-d_8 in the presence of HBPin at 300 K.

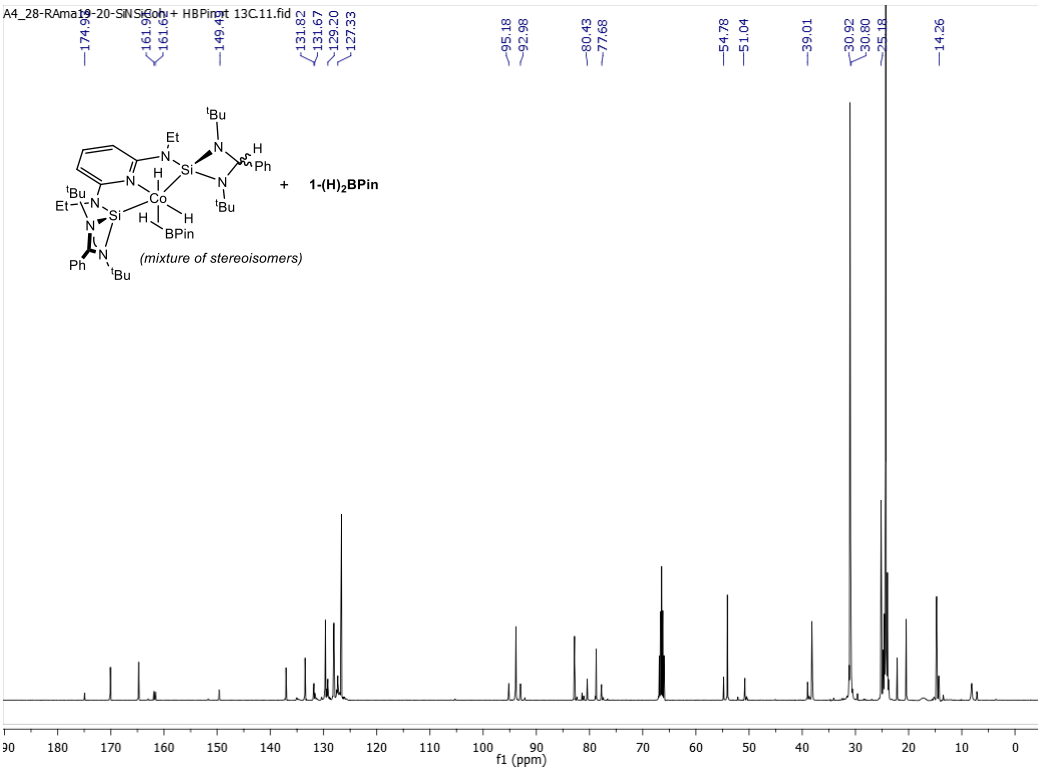

Figure S36. ^{13}C NMR spectrum of a mixture of **1-(H)$_2$BPin** and [(^{Ph,H}SiNSi)CoH$_2$(HBPin)] (60:40 ratio) in THF-d_8 in the presence of HBPin at 300 K.

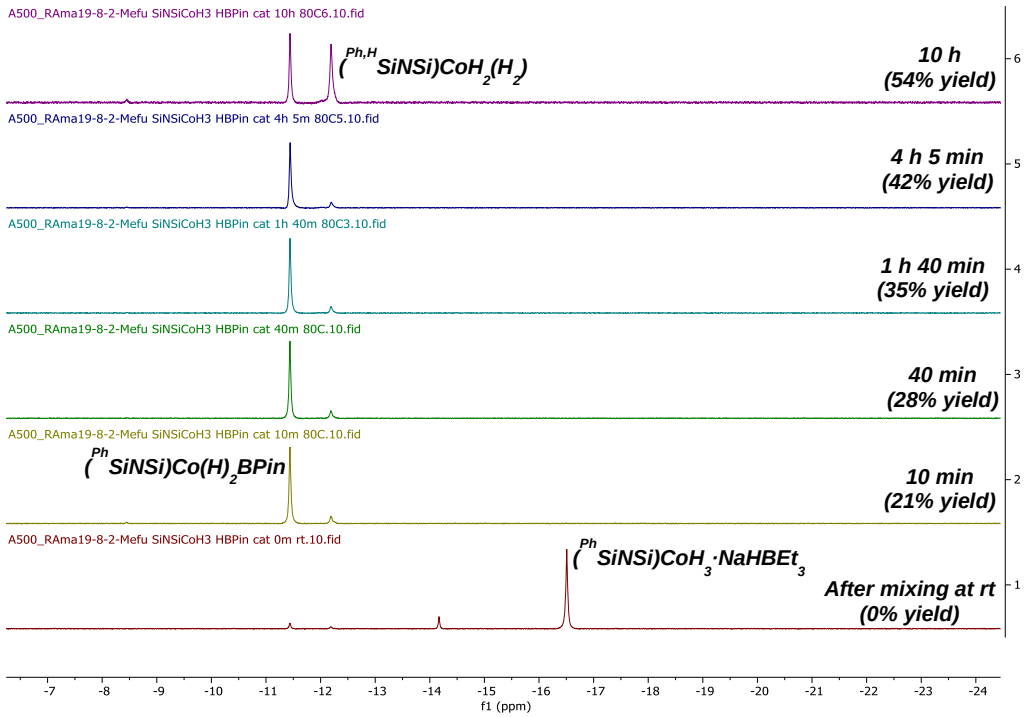

Figure S37. ^{1}H NMR monitoring of the catalytic borylation of 2-methylfuran with 1 equiv HBPin and 5 mol% of **1-H$_3$·NaHBEt$_3$** in THF-d_8 at 80 ºC (hydride region).

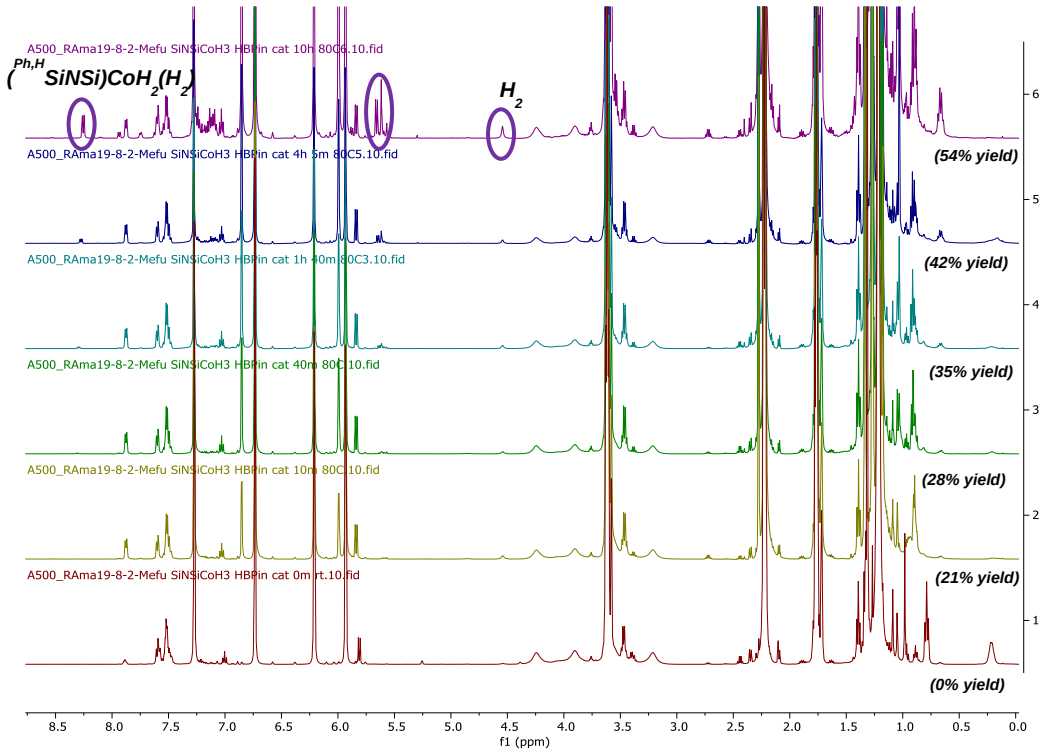

Figure S38. ^{1}H NMR monitoring of the catalytic borylation of 2-methylfuran with 1 equiv HBPin and 5 mol% of **1-H$_3$·NaHBEt$_3$** in THF-d_8 at 80 ºC (aromatic region).1. after mixing at rt, 2. 10 min at 80 ºC, 3. 40 min at 80 ºC, 4. 1 h 40 min at 80 ºC, 5. 4 h 5 min at 80 ºC, 6. 10 h at 80 ºC.

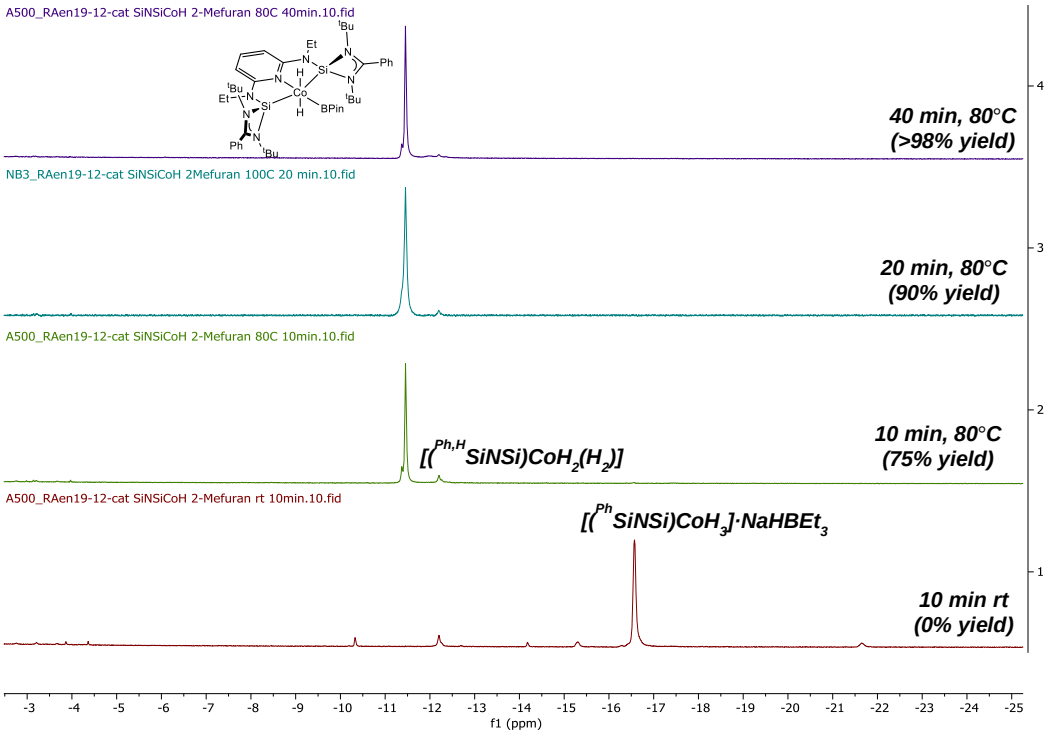

Figure S39. ^{1}H NMR monitoring of the catalytic borylation of 2-methylfuran with 0.5 equiv of B_2Pin_2 and 15 mol% of **1-H$_3$·NaHBEt$_3$** in THF-d_8 at 80 ºC (hydride region).

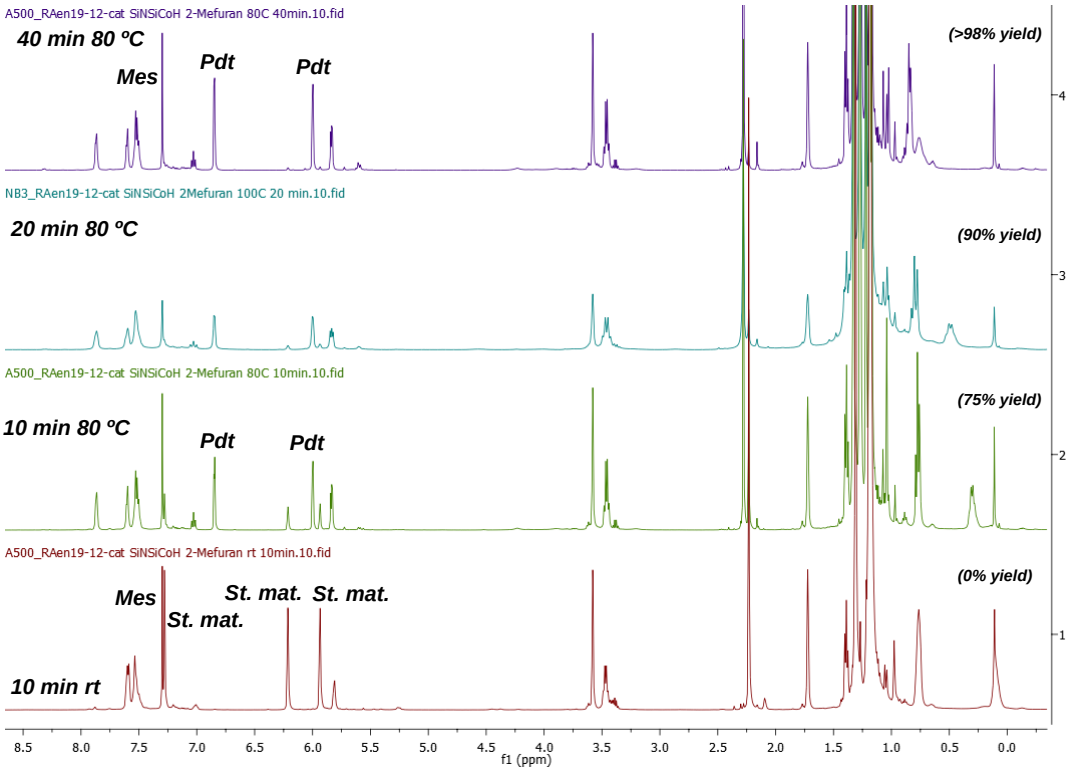

Figure S40. ^{1}H NMR monitoring of the catalytic borylation of 2-methylfuran with 0.5 equiv of B_2Pin_2 and 15 mol% of **1-H$_3$·NaHBEt$_3$** in THF-d_8 at 80 ºC (aromatic region). St. mat. = starting material, Pdt = product and Mes = mesitylene (internal standard).

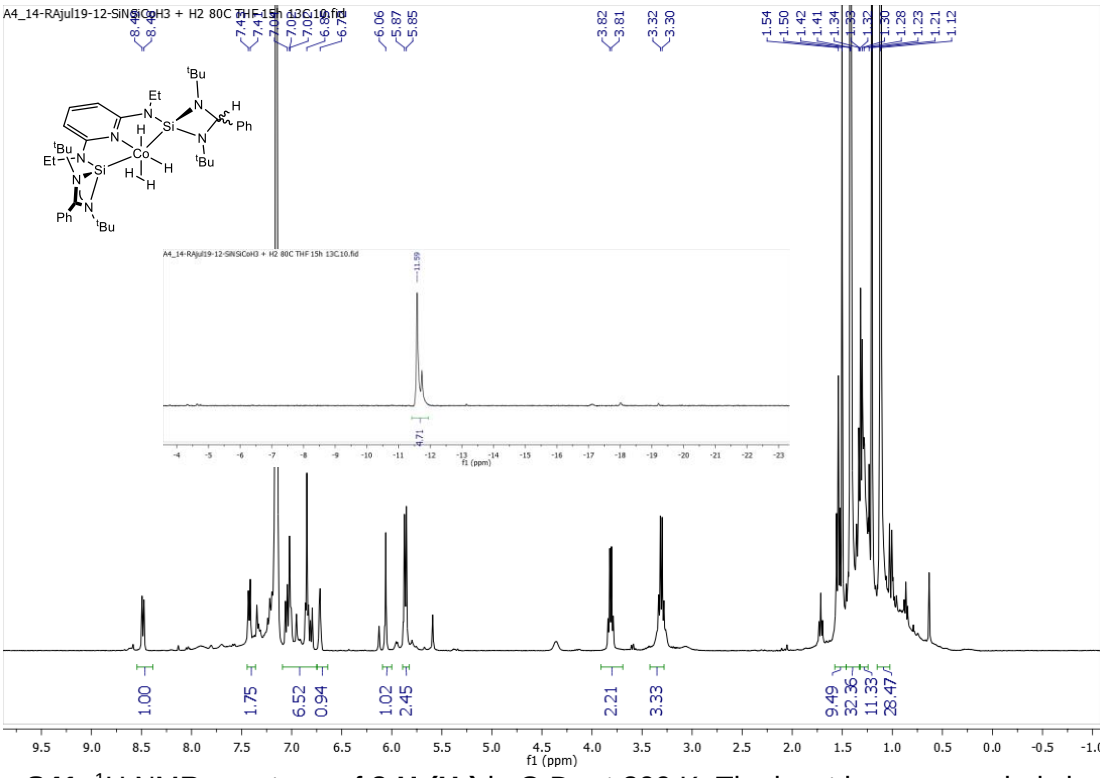

Figure S41. ^{1}H NMR spectrum of **3-H$_2$(H$_2$)** in C_6D_6 at 300 K. The inset is an expanded view of the hydride region.

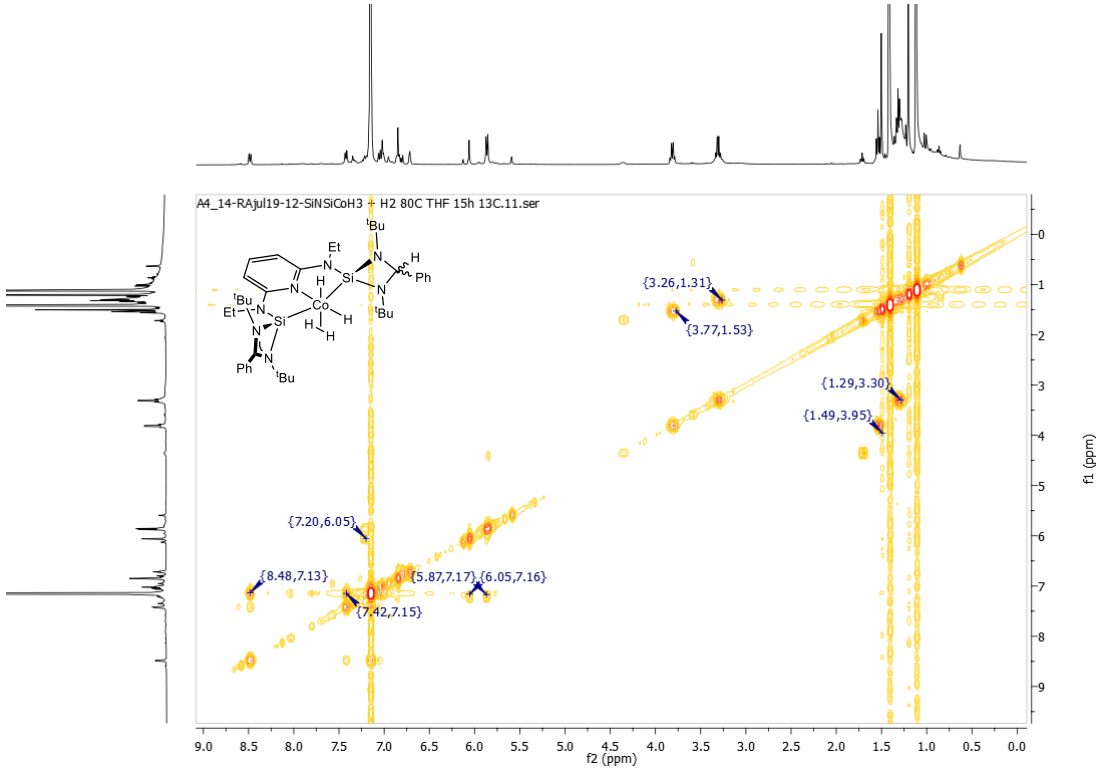

Figure S42. ^{1}H, ^{1}H-COSY NMR spectrum of **3-H$_2$(H$_2$)** in C_6D_6 at 300 K.

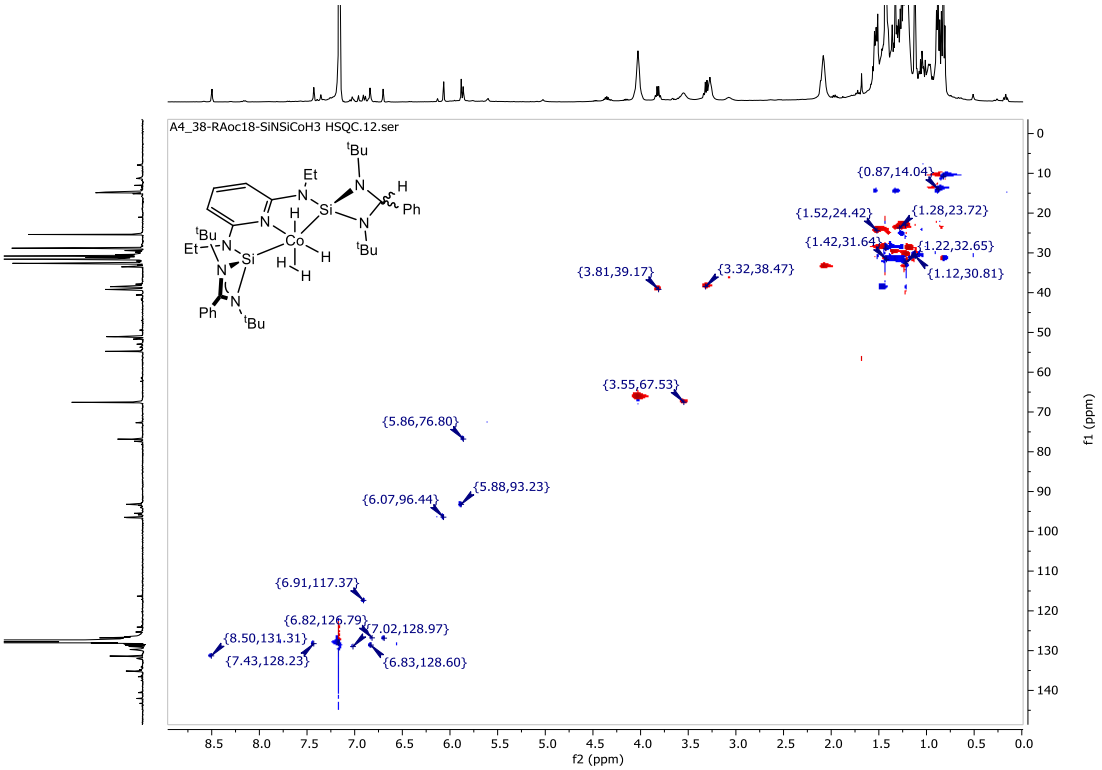

Figure S43. ^{1}H, ^{13}C-HSQC NMR spectrum of **3-H_2(H_2)** in C_6D_6 at 300 K.

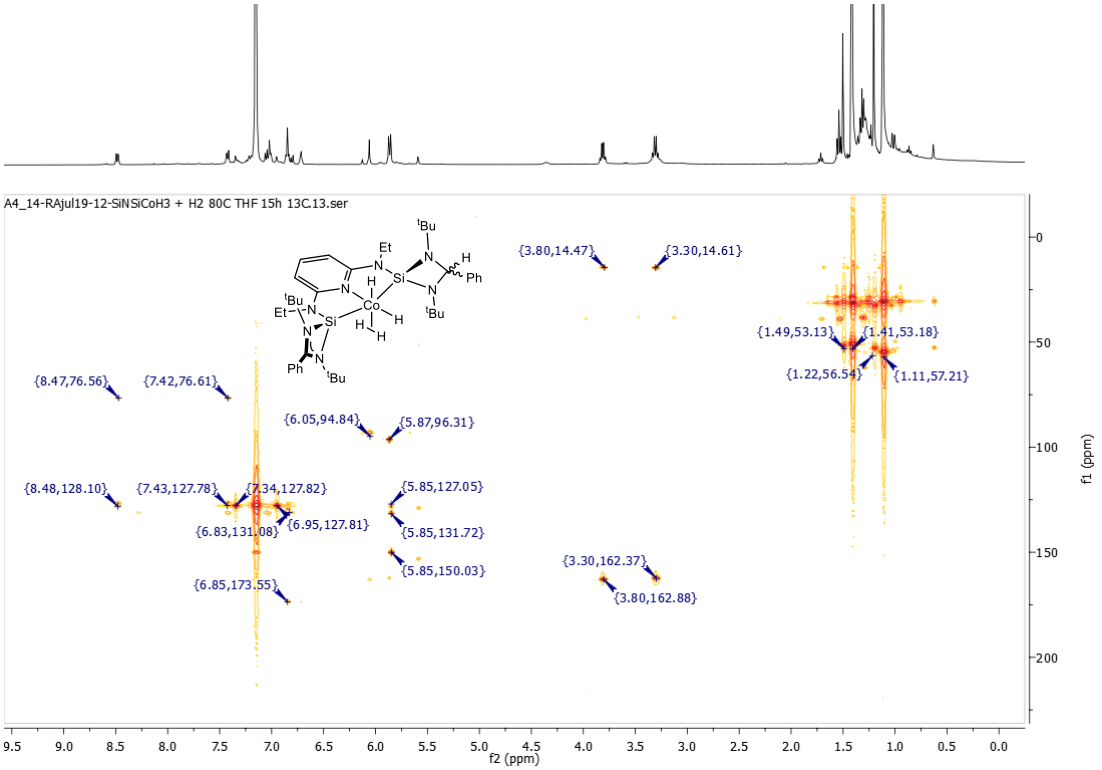

Figure S44. ^{1}H, ^{13}C-HMBC NMR spectrum of **3-H_2(H_2)** in C_6D_6 at 300 K.

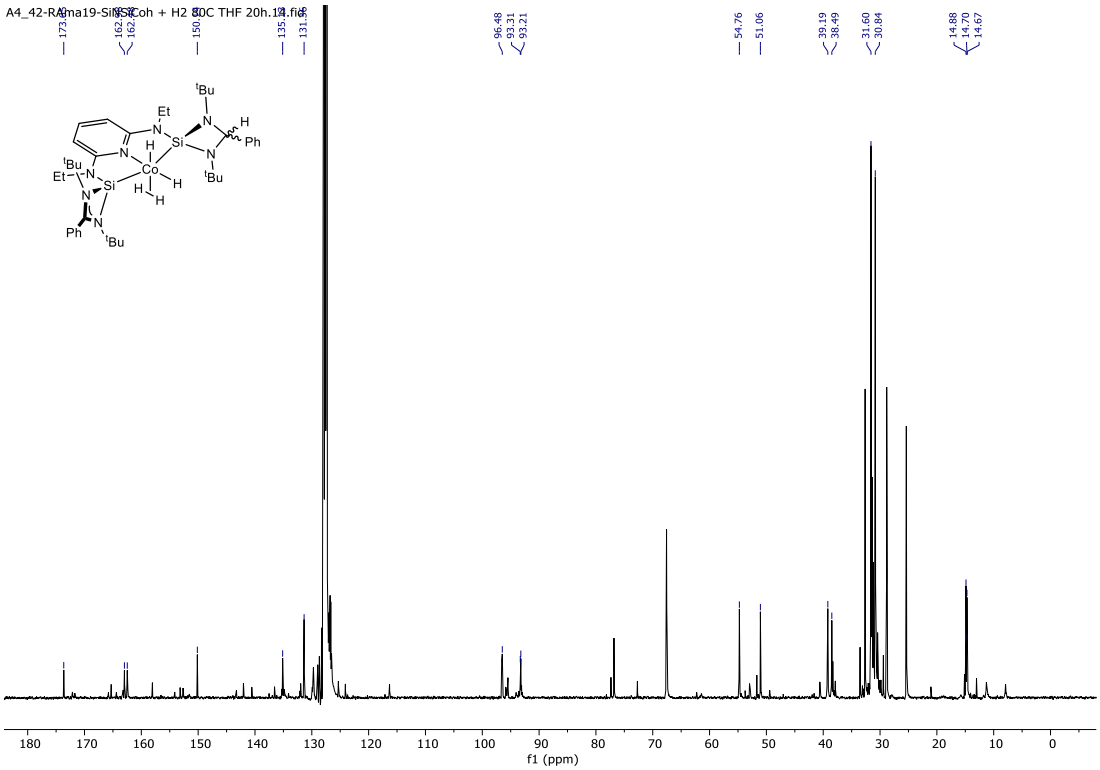

Figure S45. ^{13}C NMR spectrum of **3-H_2(H_2)** in C_6D_6 at 300 K.

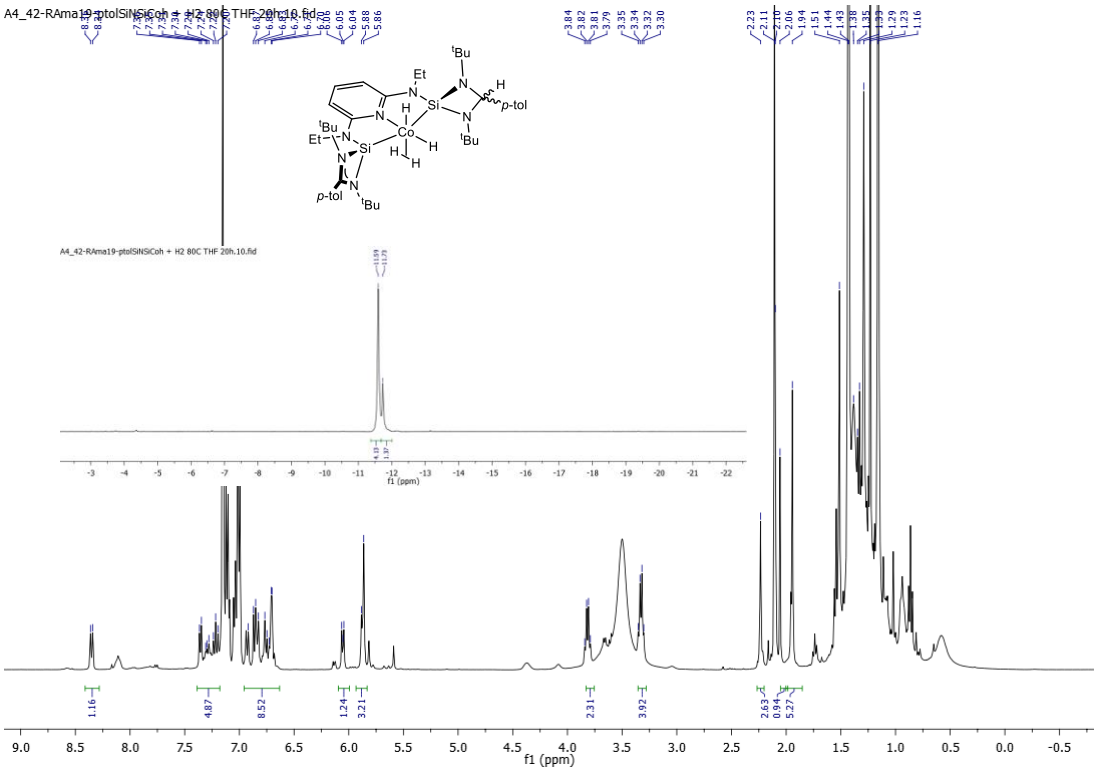

Figure S46. ^{1}H NMR spectrum of **4-H_2(H_2)** in C_6D_6 at 300 K. The inset is an expanded view of the hydride region.

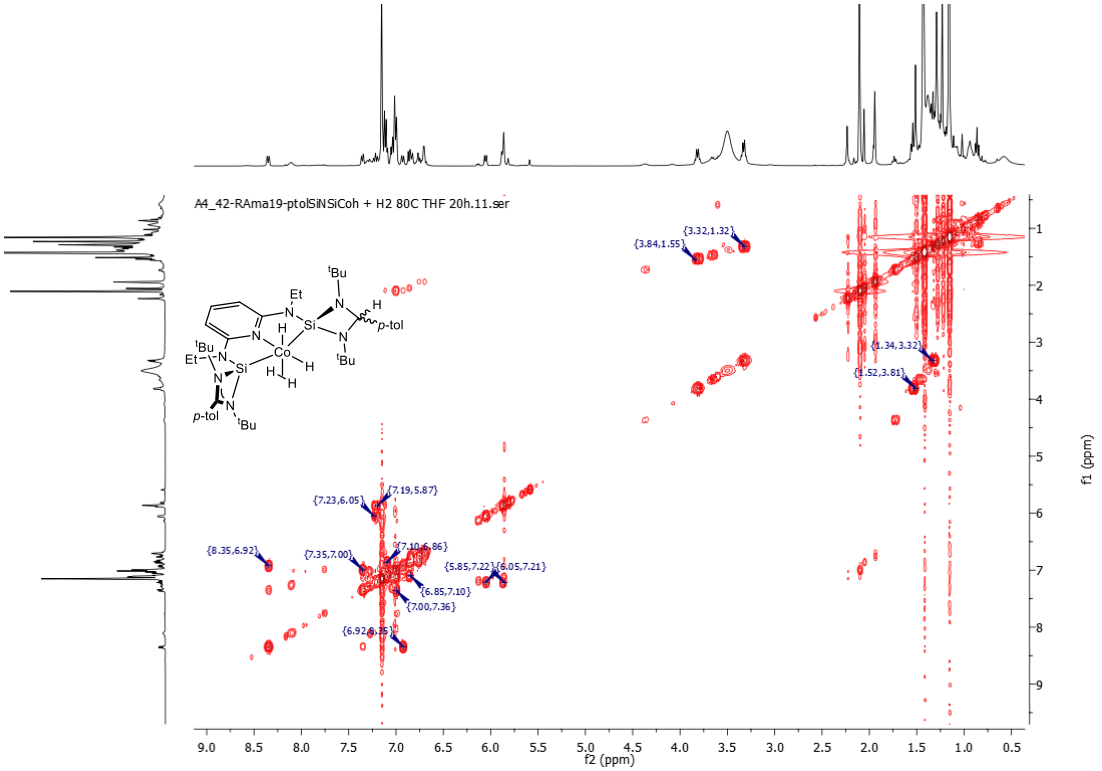

Figure S47. ^{1}H-^{1}H COSY NMR spectrum of **4-H$_2$(H$_2$)** in C_6D_6 at 300 K.

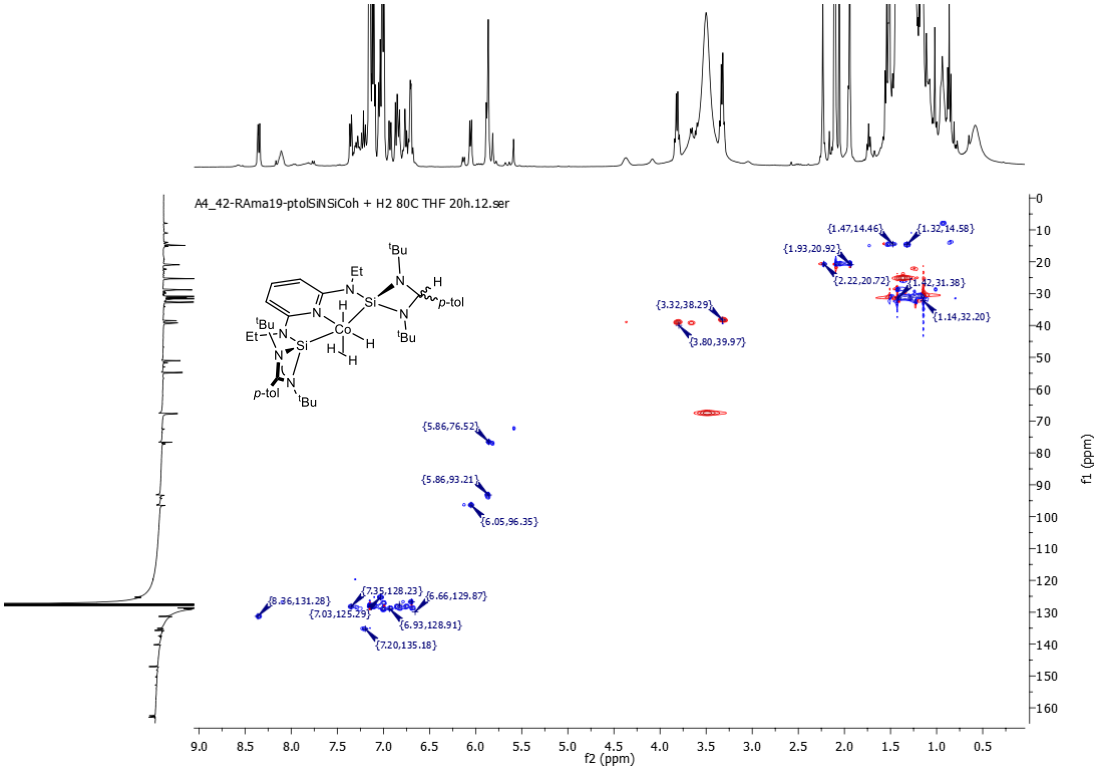

Figure S48. ^{1}H-^{13}C HSQC NMR spectrum of **4-H$_2$(H$_2$)** in C_6D_6 at 300 K.

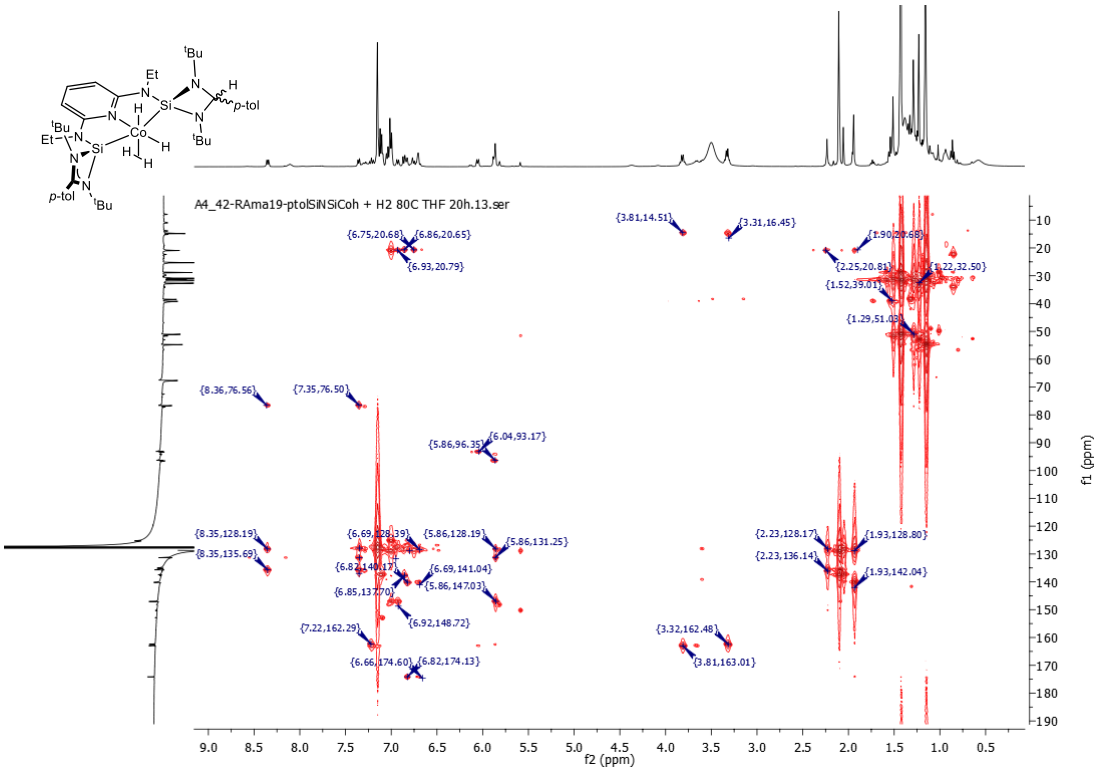

Figure S49. ^{1}H-^{13}C HMBC NMR spectrum of **4-H_2(H_2)** in C_6D_6 at 300 K.

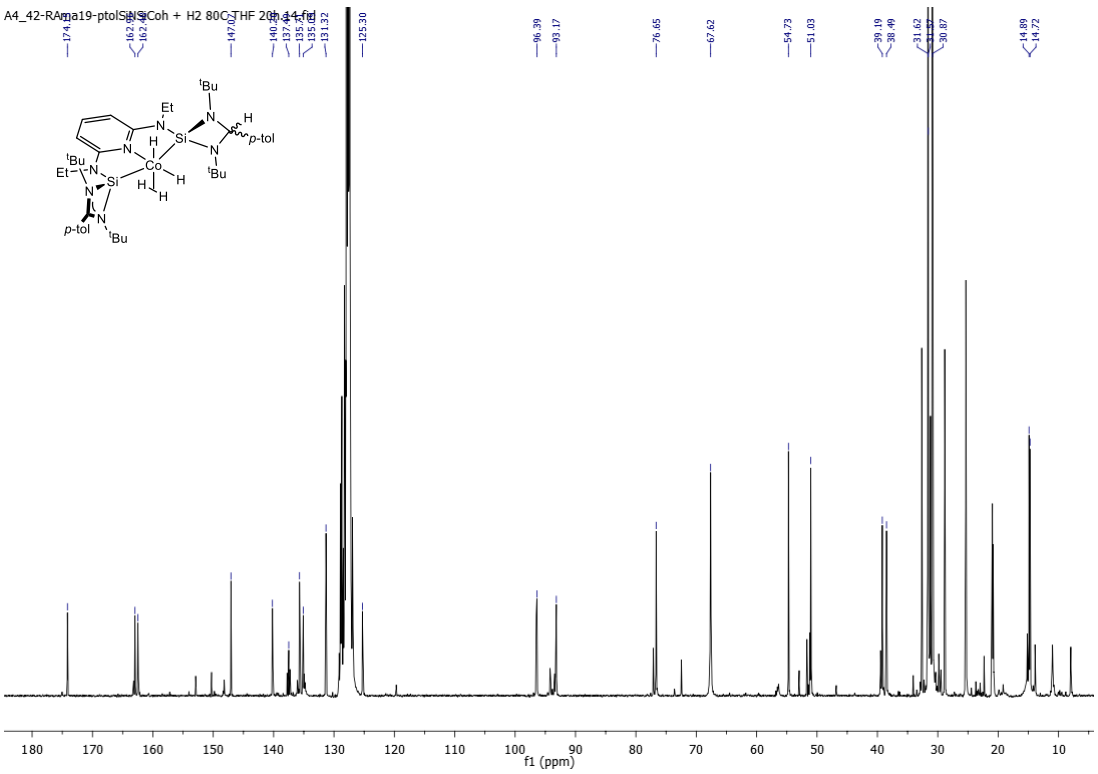

Figure S50. ^{13}C NMR spectrum of **4-H_2(H_2)** in C_6D_6 at 300 K.

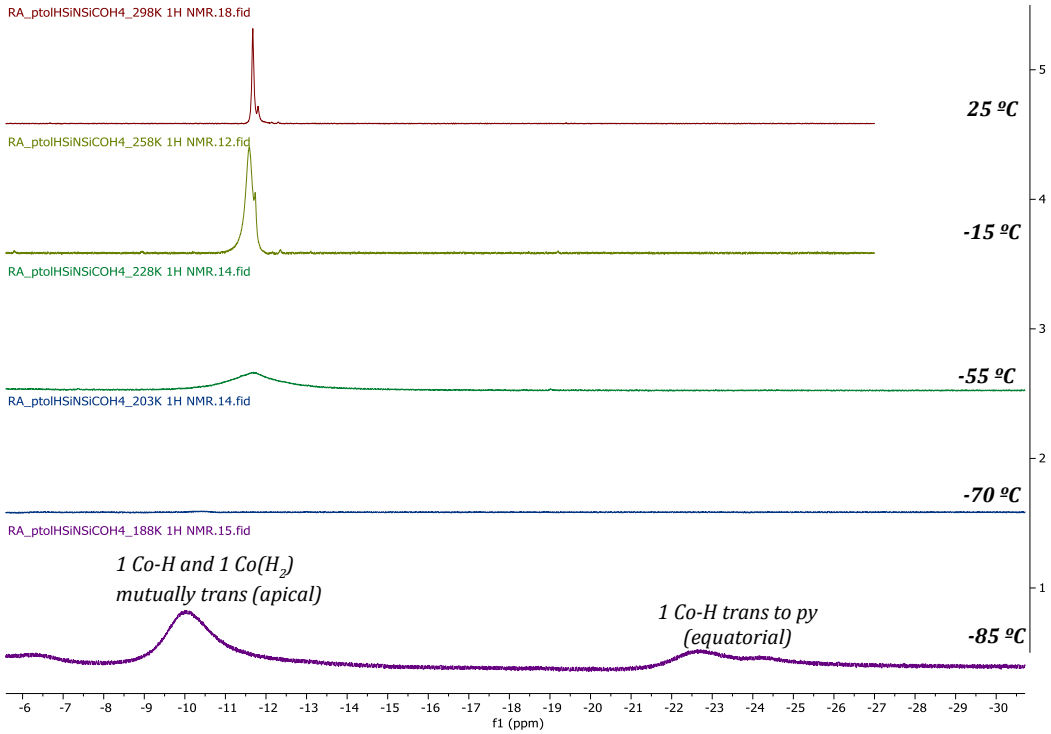

Figure S51. ^{1}H-VT NMR spectra of **4-H$_2$(H$_2$)** in toluene-d_8 (hydride region).

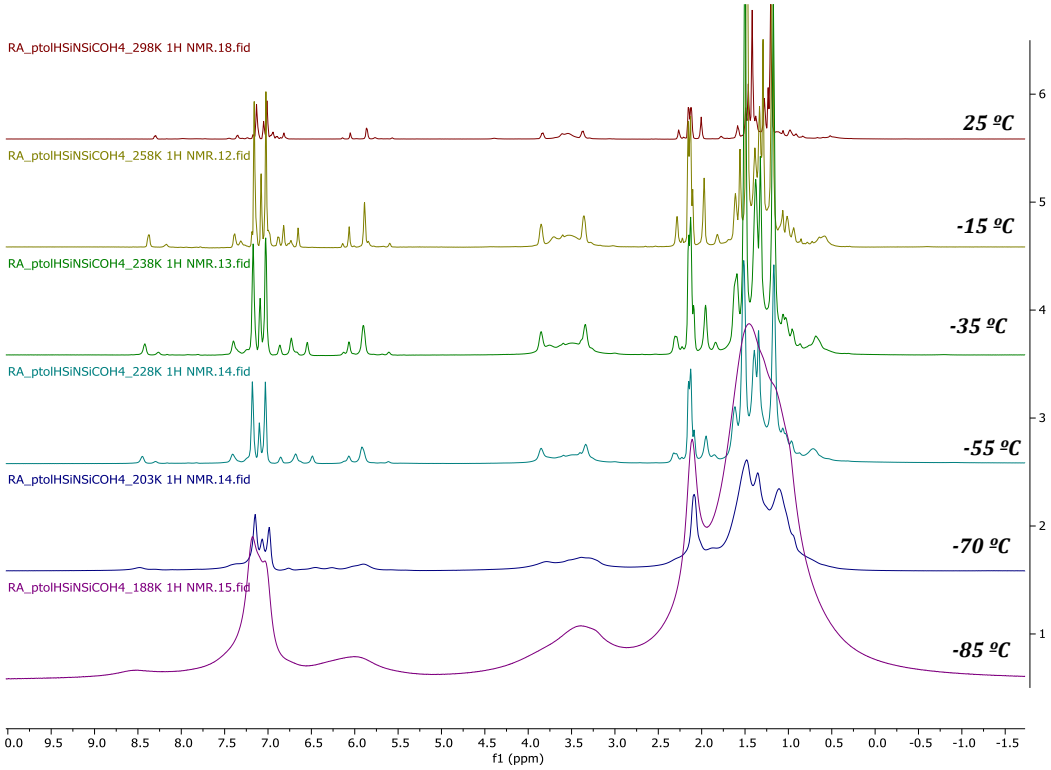

Figure S52. ^{1}H-VT NMR spectra of **4-H$_2$(H$_2$)** in toluene-d_8 (aromatic region).

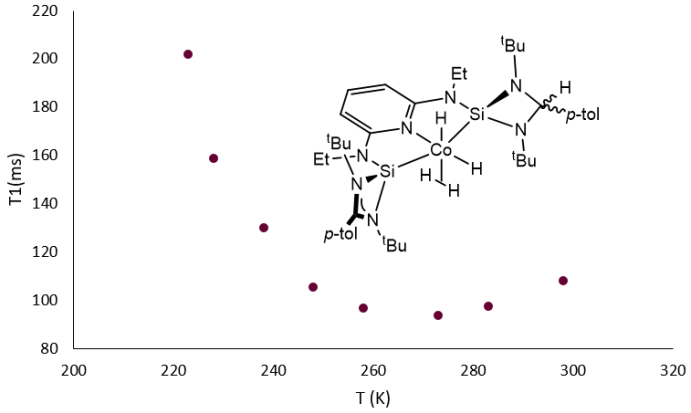

T (K)	T_1 (ms)
298	108
283	97
273	94
258	97
248	105
238	130
228	159
223	202

Figure S53. T_1 values for the hydride ligands in **4-H_2(H_2)** in toluene-d_8 at different temperatures.

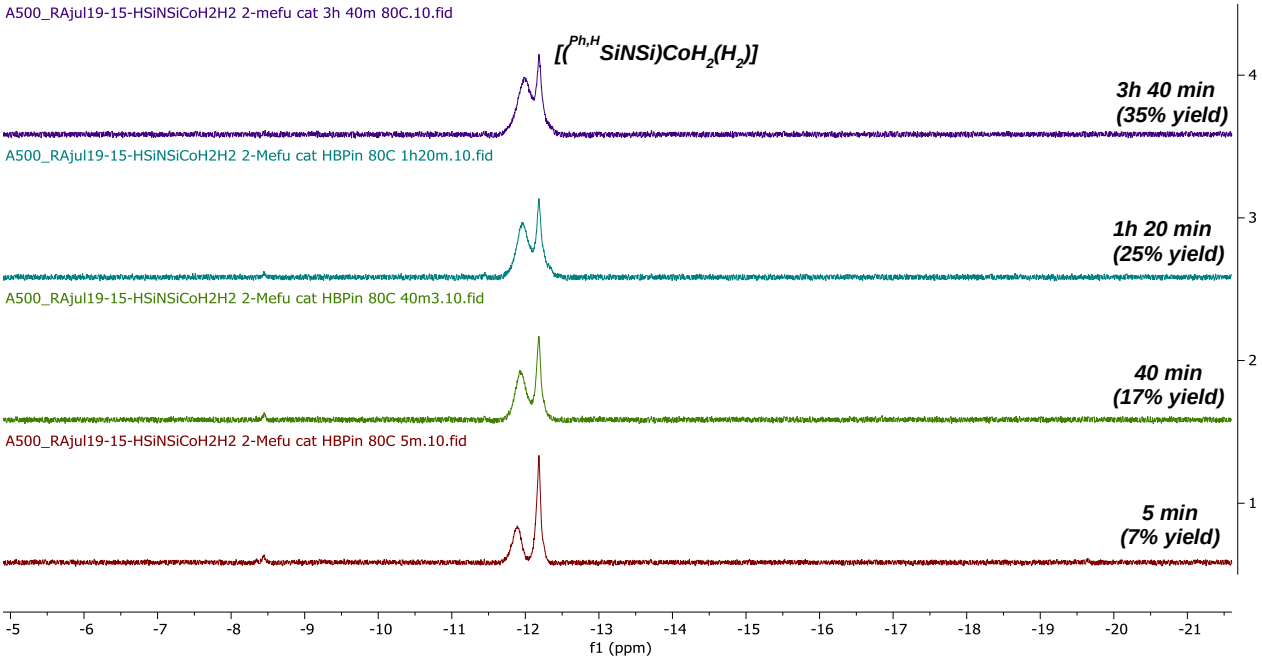

Figure S54. ^{1}H NMR monitoring of the borylation of 2-methylfuran with 1 equiv of HBPin and 5 mol% of **3-H_2(H_2)** as precatalyst (hydride region).

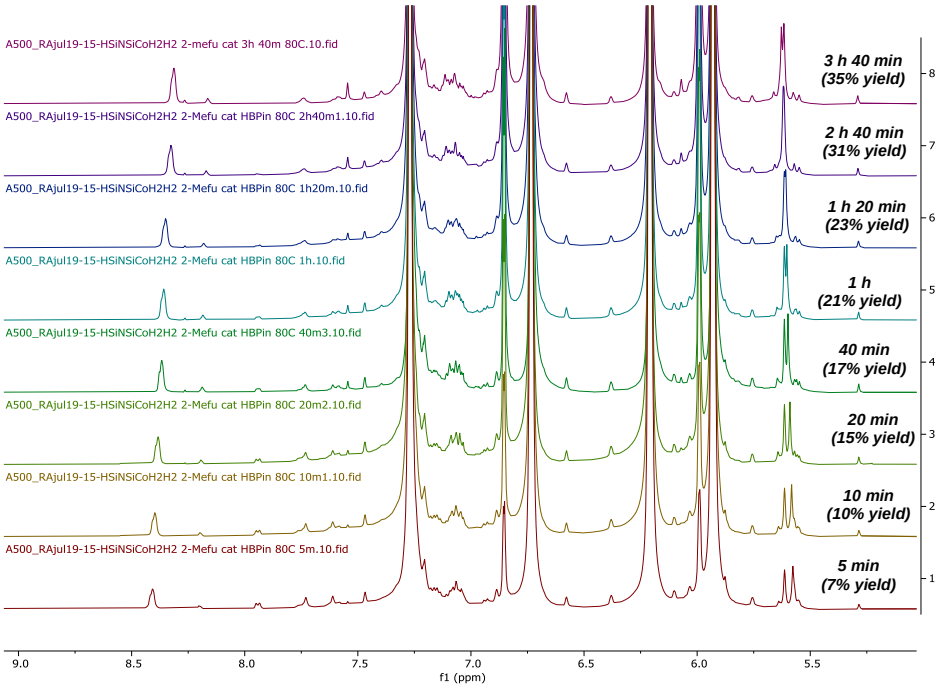

Figure S55. ^{1}H NMR monitoring of the borylation of 2-methylfuran with 1 equiv of HBPin and 5 mol% of **3-H_2(H_2)** as precatalyst (aromatic region).

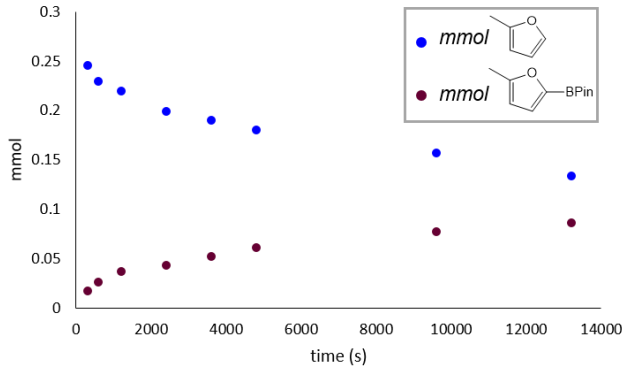

Figure S56. Reaction profile of the borylation of 2-methylfuran with 1 equiv of HBPin and 5 mol% of **3-H_2(H_2)** as precatalyst from NMR integration.

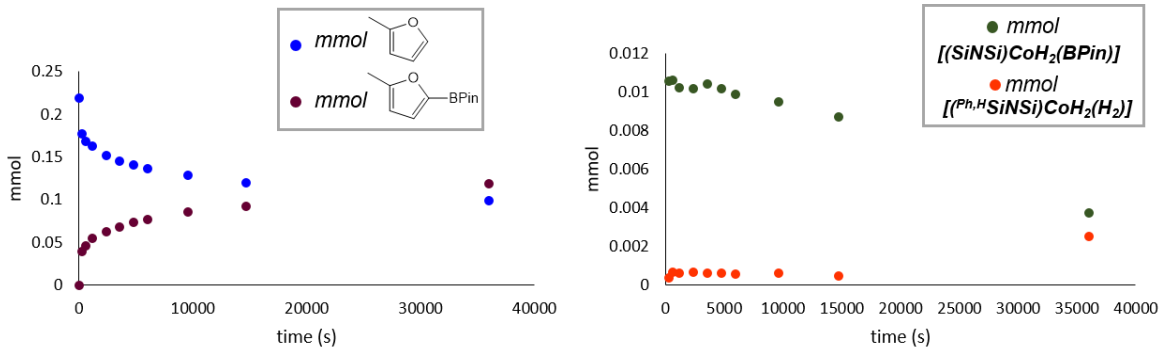

Figure S57. Reaction profile of the borylation of 2-methylfuran with 1 equiv of HBPin and 5 mol% of **1-H$_3$·NaHBEt$_3$** as precatalyst from NMR integration. Left graph shows starting material and product monitoring and right graph shows catalyst deactivation over time.

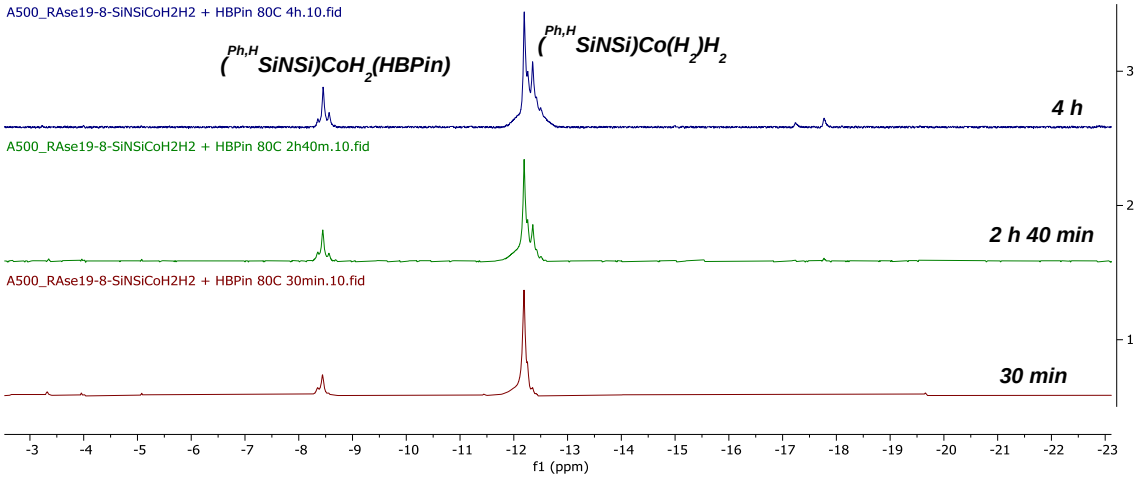

Figure S58. ^{1}H NMR monitoring of the reaction of **3-H$_2$(H$_2$)** with 6 equiv of HBPin in THF-d_8 at 80 ºC (hydride region).

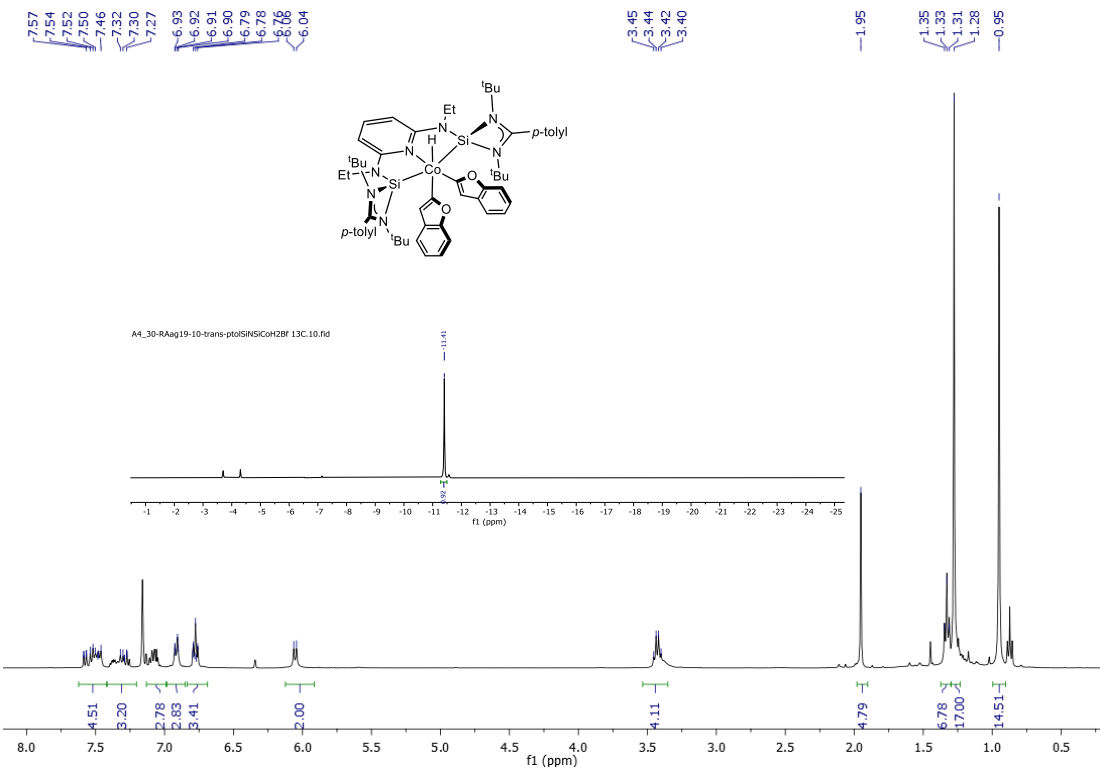

Figure S59. ^{1}H NMR spectrum of **2-H(Bf)$_2$** in C_6D_6 at 300 K. The inset is an expanded view of the hydride region.

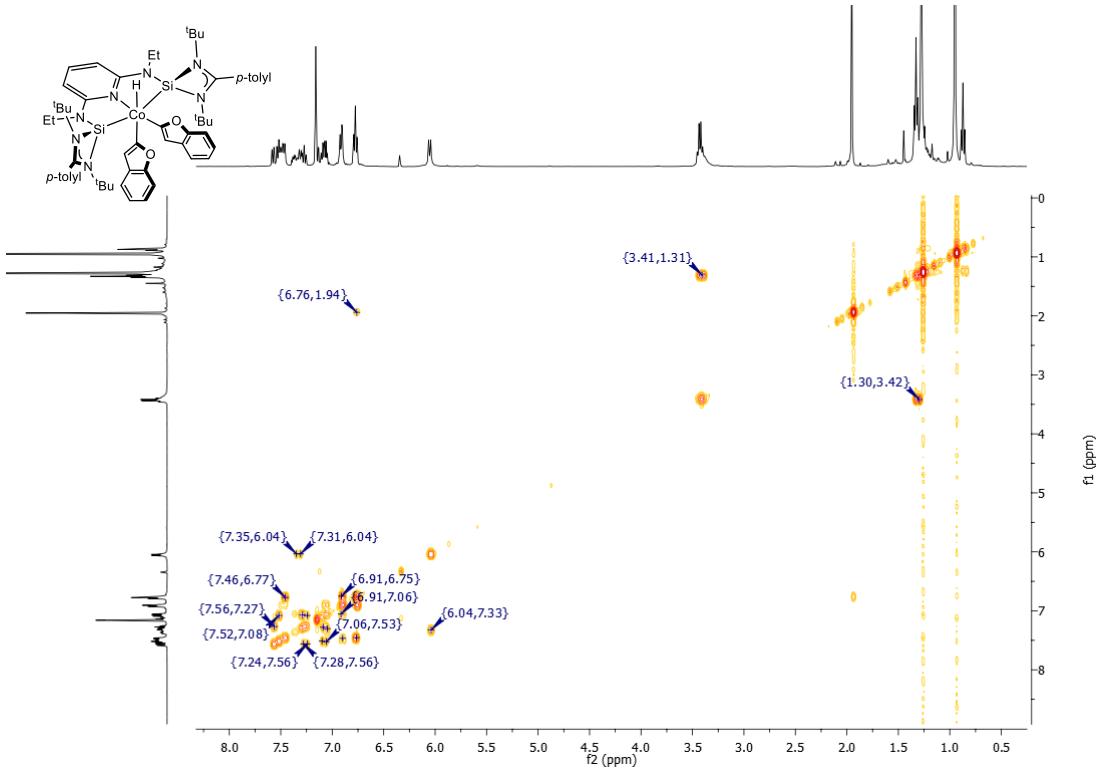

Figure S60. ^{1}H-^{1}H COSY NMR spectrum of **2-H(Bf)$_2$** in C_6D_6 at 300 K.

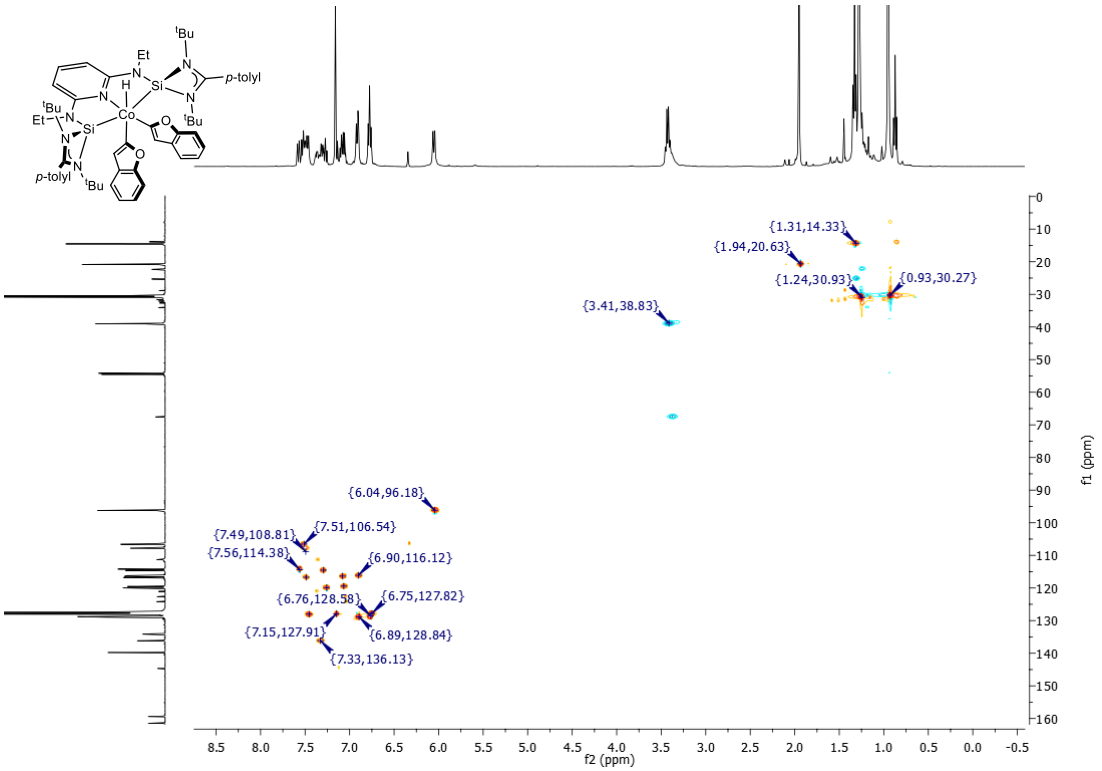

Figure S61. ^{1}H-^{13}C HSQC NMR spectrum of **2-H(Bf)$_2$** in C_6D_6 at 300 K.

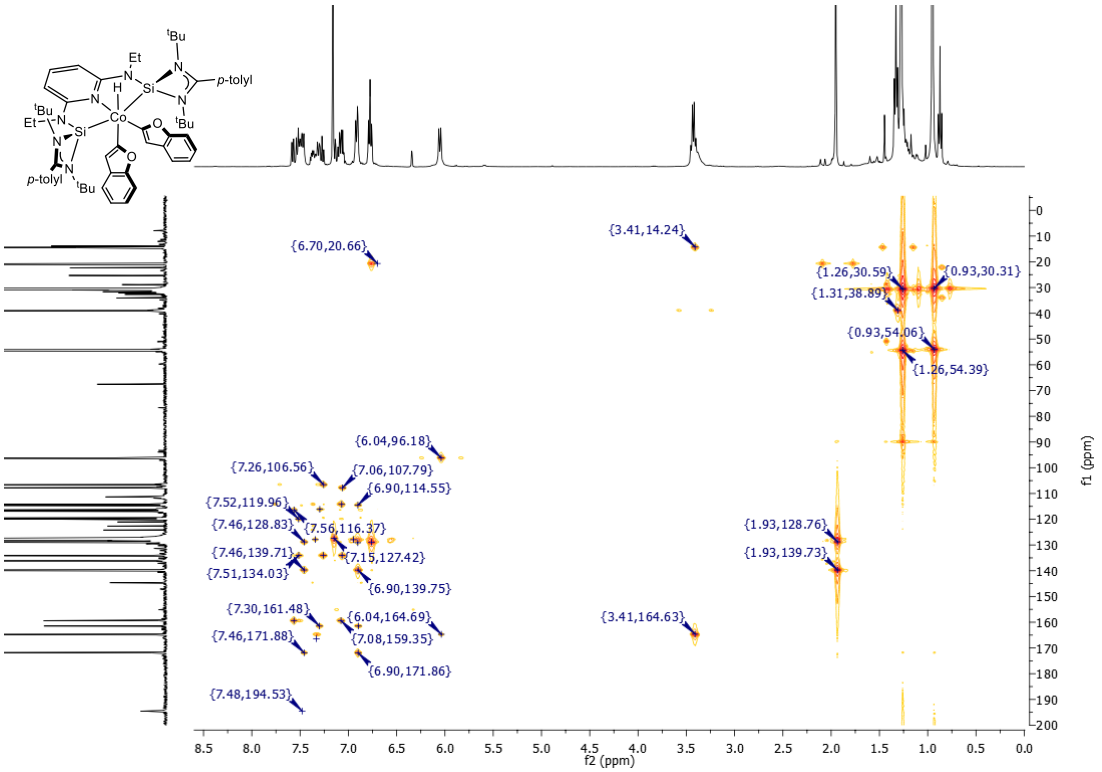

Figure S62. ^{1}H-^{13}C HMBC NMR spectrum of **2-H(Bf)$_2$** in C_6D_6 at 300 K.

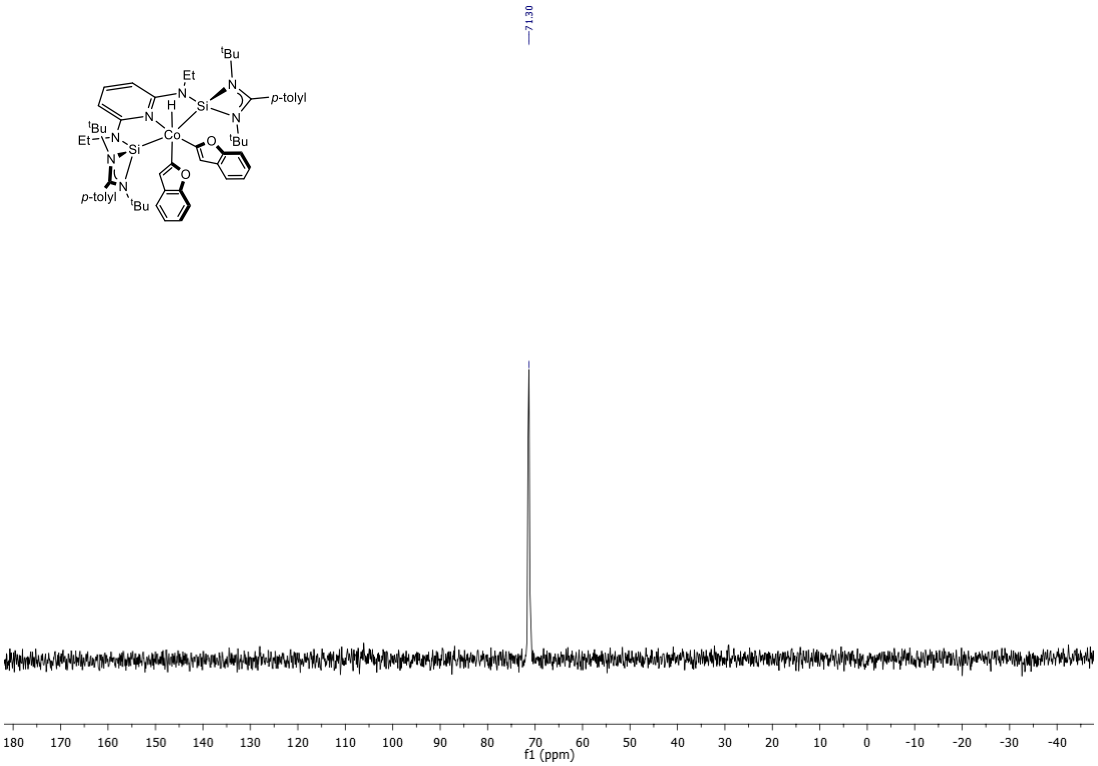

Figure S63. ^{29}Si NMR spectrum of **2-H(Bf)$_2$** in C_6D_6 at 300 K.

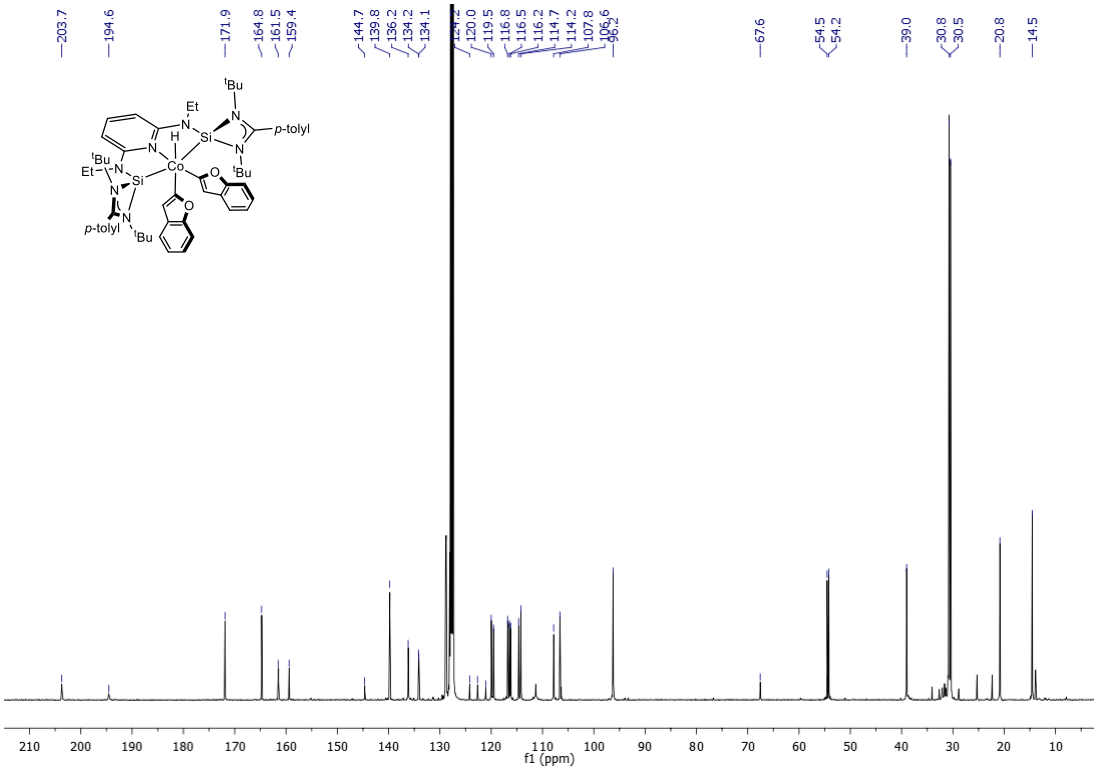

Figure S64. ^{13}C NMR spectrum of **2-H(Bf)$_2$** in C_6D_6 at 300 K.

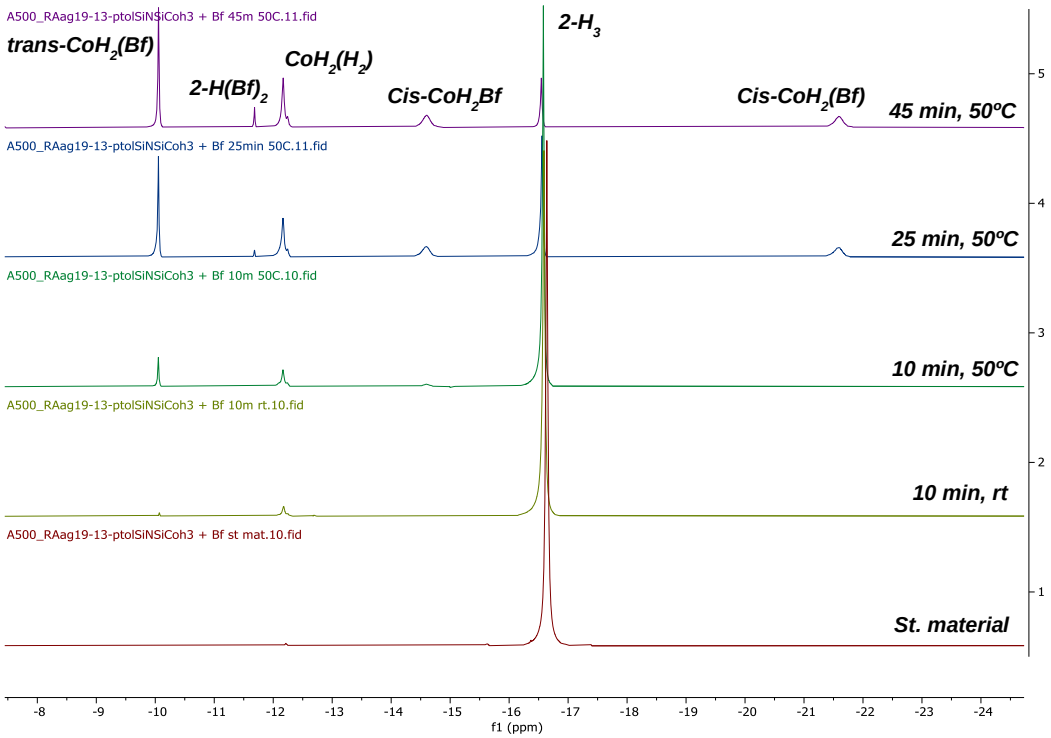

Figure S65. ^{1}H NMR monitoring (10 - 45 min) of the reaction of **2-H$_3$·NaHBEt$_3$** with 6 equiv of benzofuran in THF-d_8 at 50 ºC (hydride region).

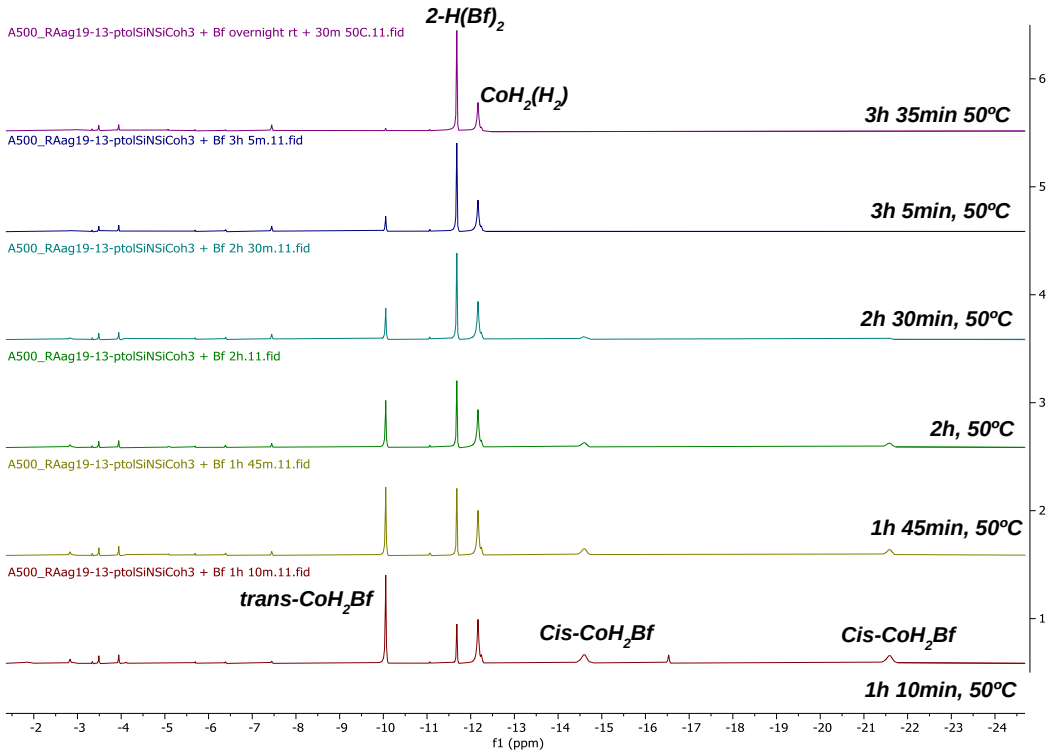

Figure S66. ^{1}H NMR monitoring (1 h 10 min – 3 h 35 min) of the reaction of **2-H$_3$·NaHBEt$_3$** with 6 equiv of benzofuran in THF-d_8 at 50 ºC (hydride region).

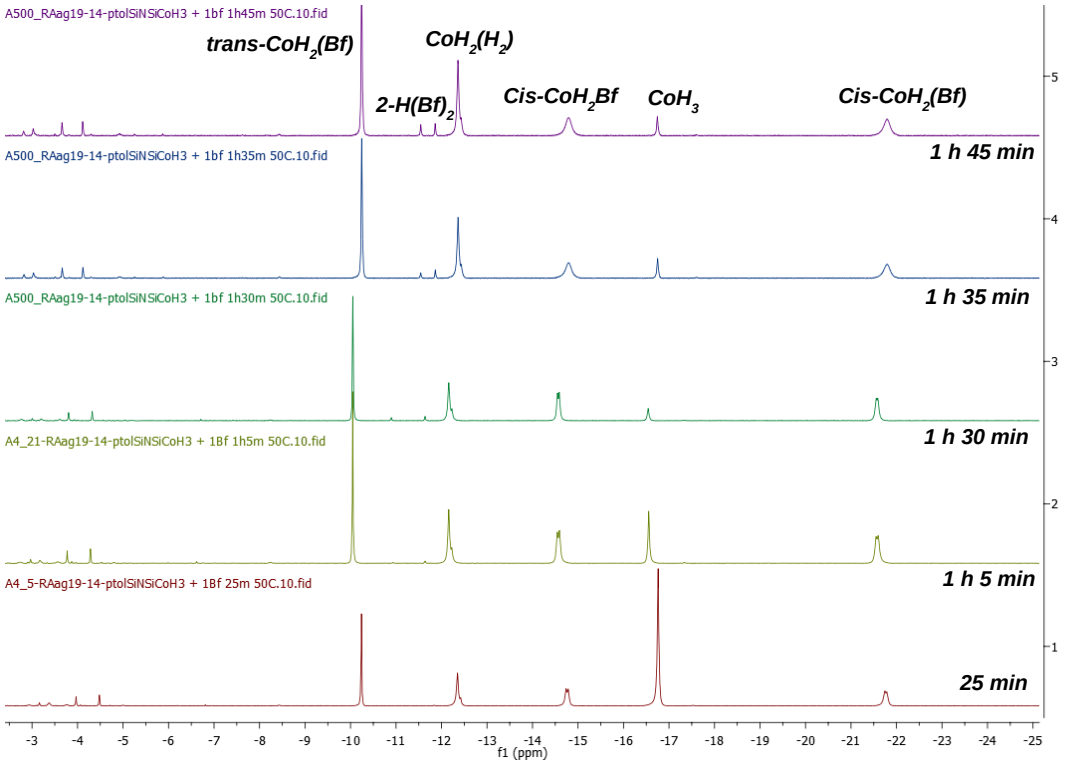

Figure S67. ^{1}H NMR monitoring (25 min – 1 h 35 min) of the reaction of **2-H$_3$·NaHBEt$_3$** with 1 equiv of benzofuran in THF-d_8 at 50 ºC (hydride region).

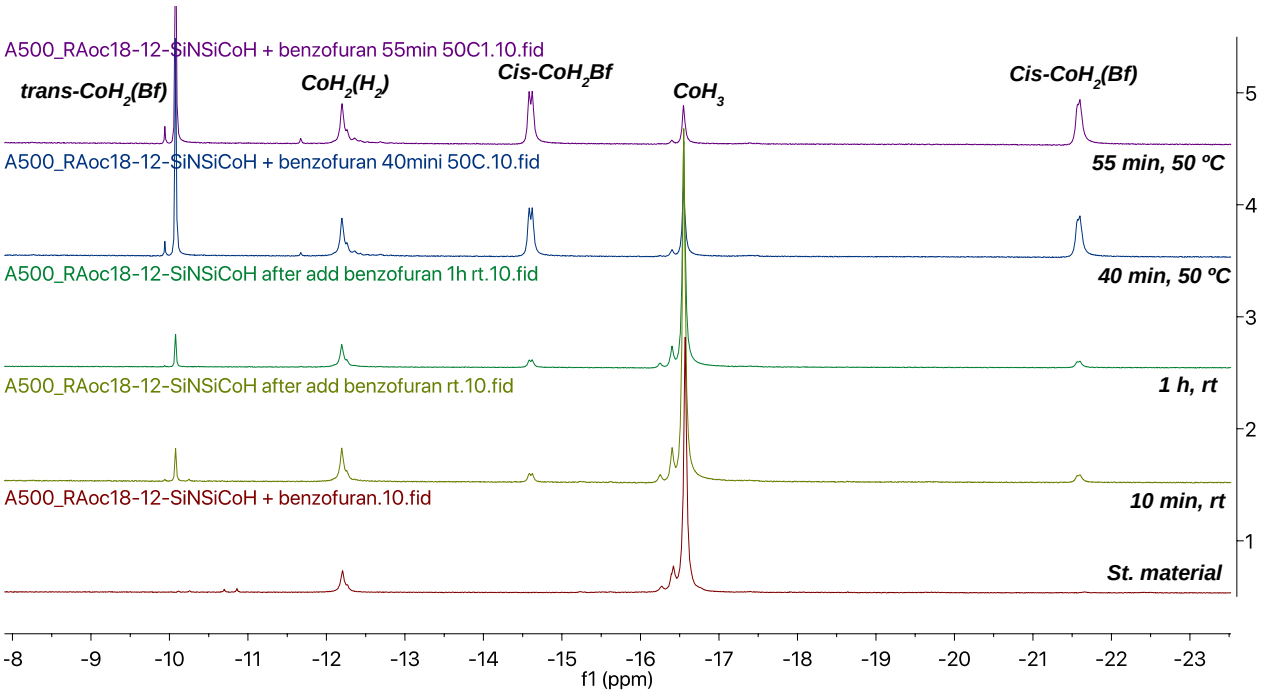

Figure S68. ^{1}H NMR monitoring (until 55 min) of the reaction of **1-H$_3$·NaHBEt$_3$** with 1 equiv of benzofuran in THF-d_8 at room temperature followed by heating up to 50 ºC (hydride region).

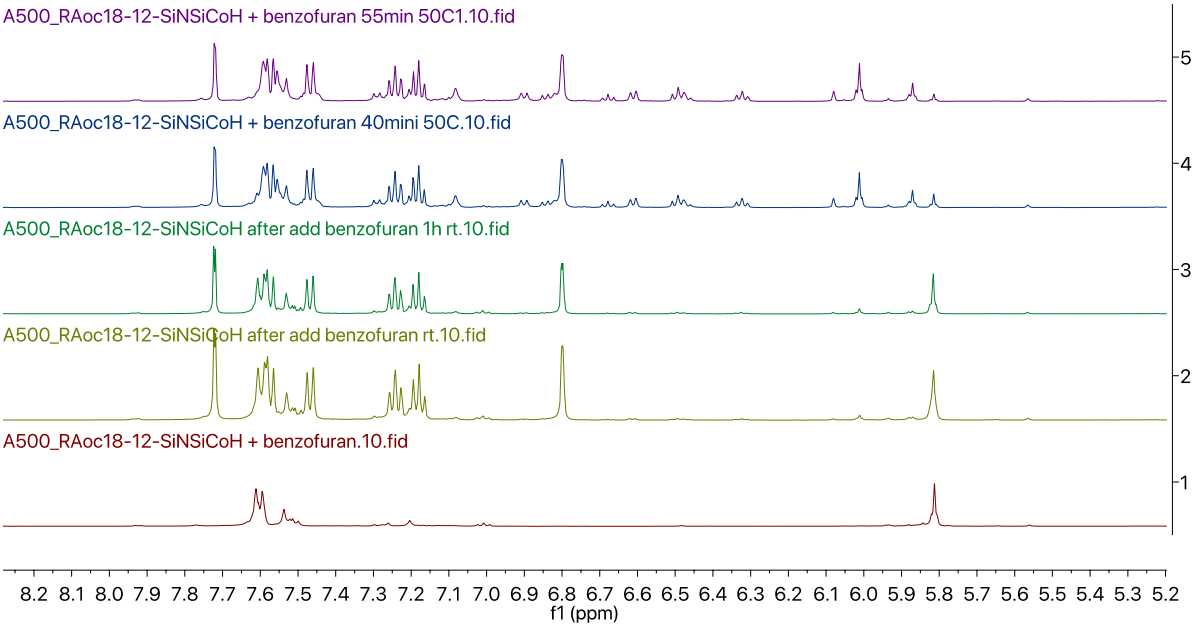

Figure S69. ^{1}H NMR monitoring (until 55 min) of the reaction of **1-H$_3$·NaHBEt$_3$** with 1 equiv of benzofuran in THF-d_8 at room temperature followed by heating up to 50 ºC (aromatic region).

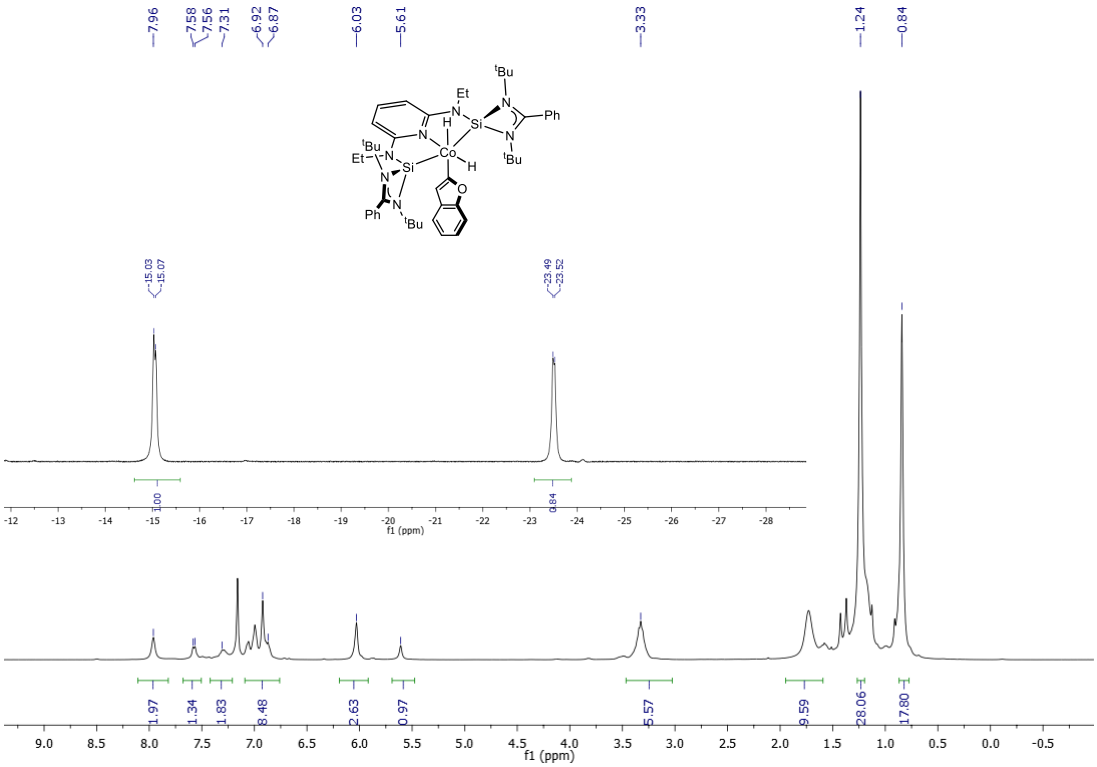

Figure S70. ^{1}H NMR spectrum of *cis*-[(^{Ph}SiNSi)CoH$_2$(Bf)] in C_6D_6 at 300 K. The inset is an expanded view of the hydride region.

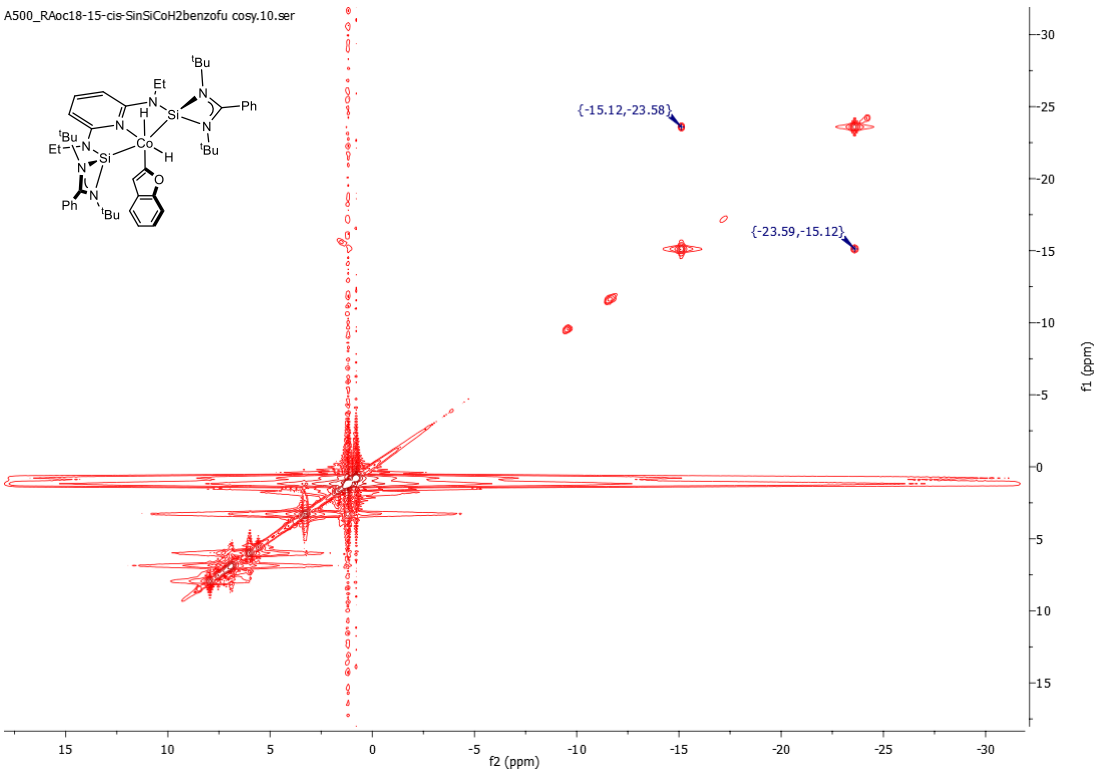

Figure S71. ^{1}H-^{1}H COSY NMR spectrum of *cis*-[(^{Ph}SiNSi)CoH$_2$(Bf)] in C_6D_6 at 300 K.

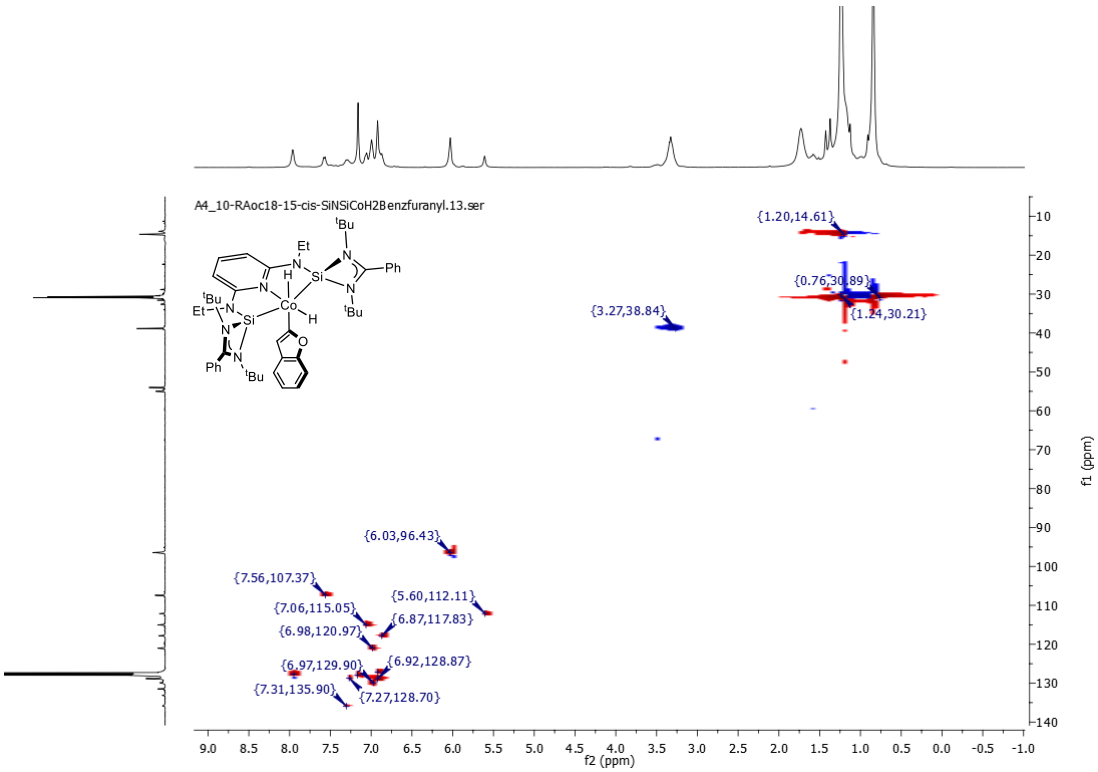

Figure S72. ^{1}H-^{13}C HSQC NMR spectrum of *cis*-[(^{Ph}SiNSi)CoH$_2$(Bf)] in C_6D_6 at 300 K.

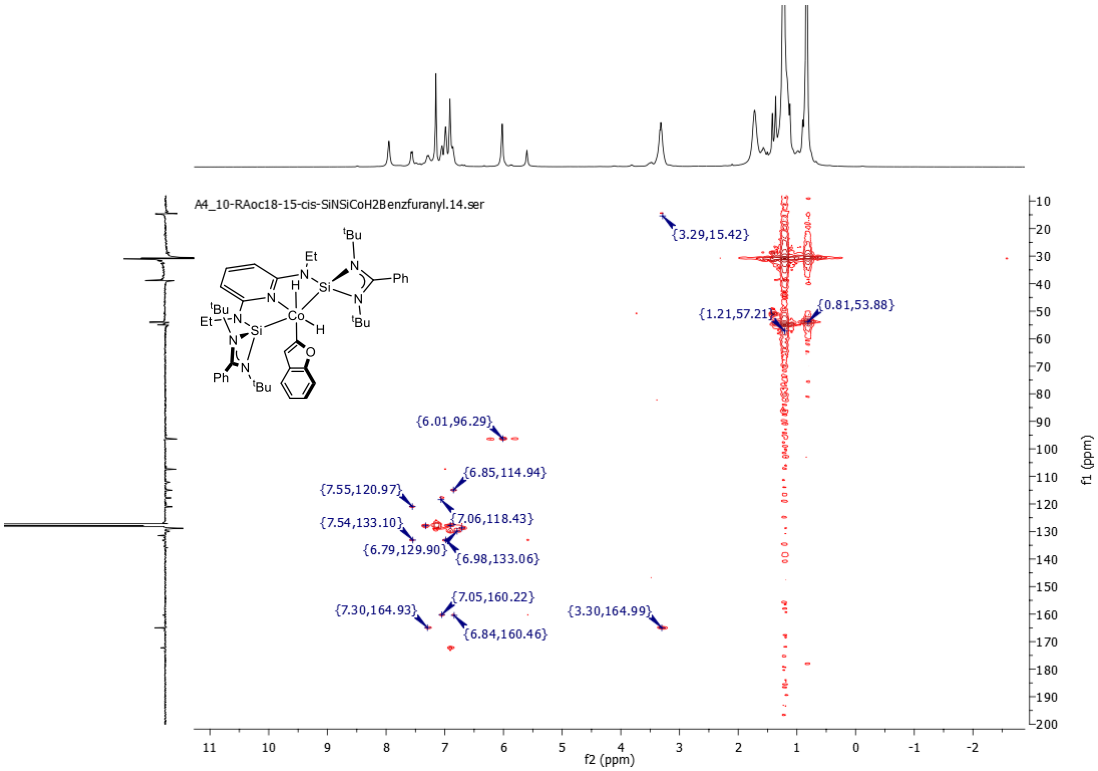

Figure S73. ^{1}H-^{13}C HMBC NMR spectrum of *cis*-[(^{Ph}SiNSi)CoH$_2$(Bf)] in C_6D_6 at 300 K.

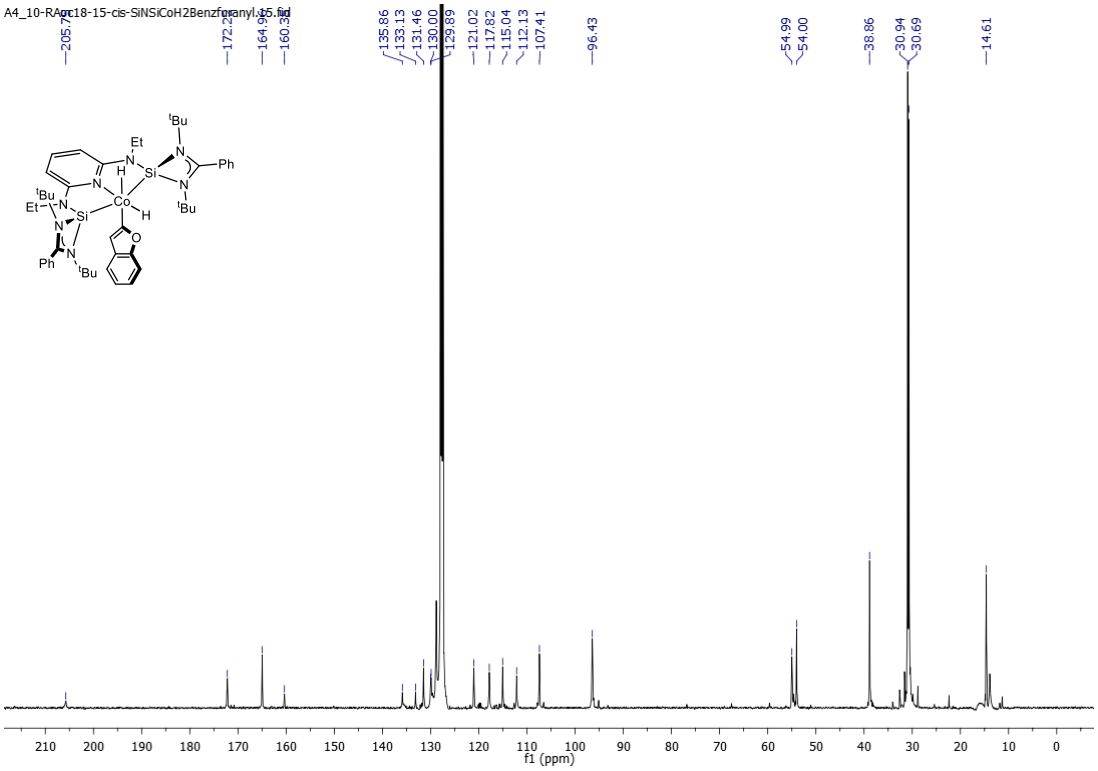

Figure S74. ^{13}C NMR spectrum of *cis*-[(^{Ph}SiNSi)CoH$_2$(Bf)] in C_6D_6 at 300 K.

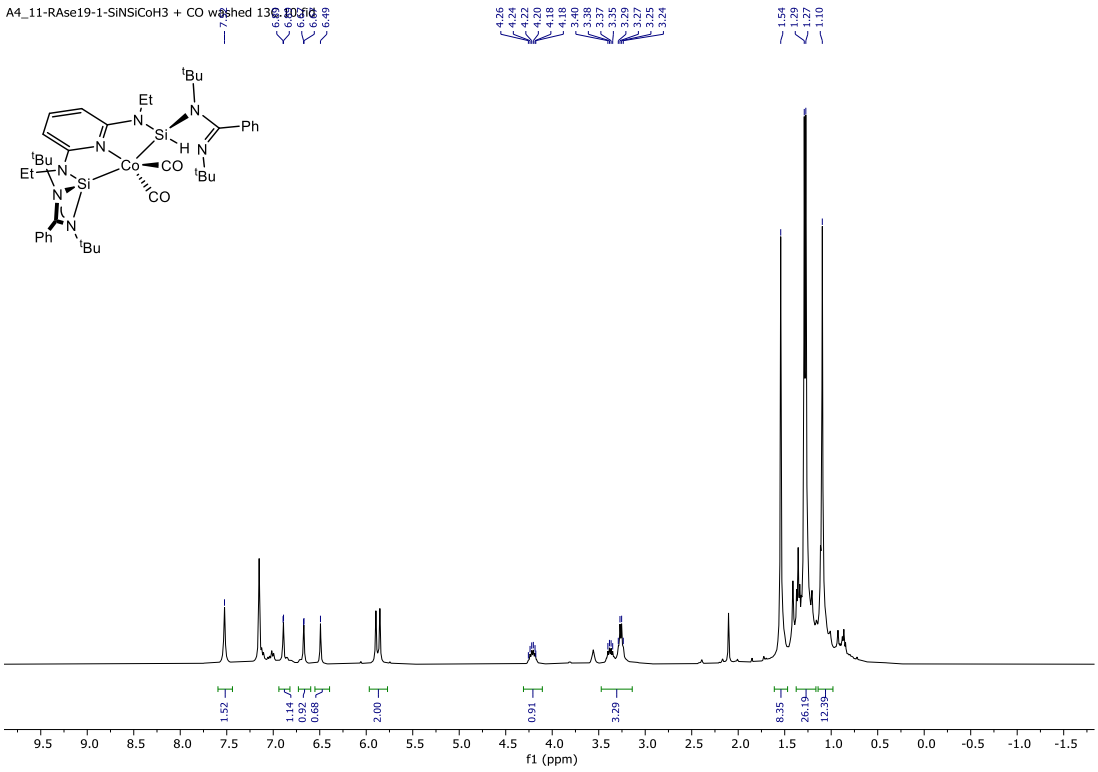

Figure S75. ^{1}H NMR spectrum of **5-(CO)$_2$** in C_6D_6 at 300 K.

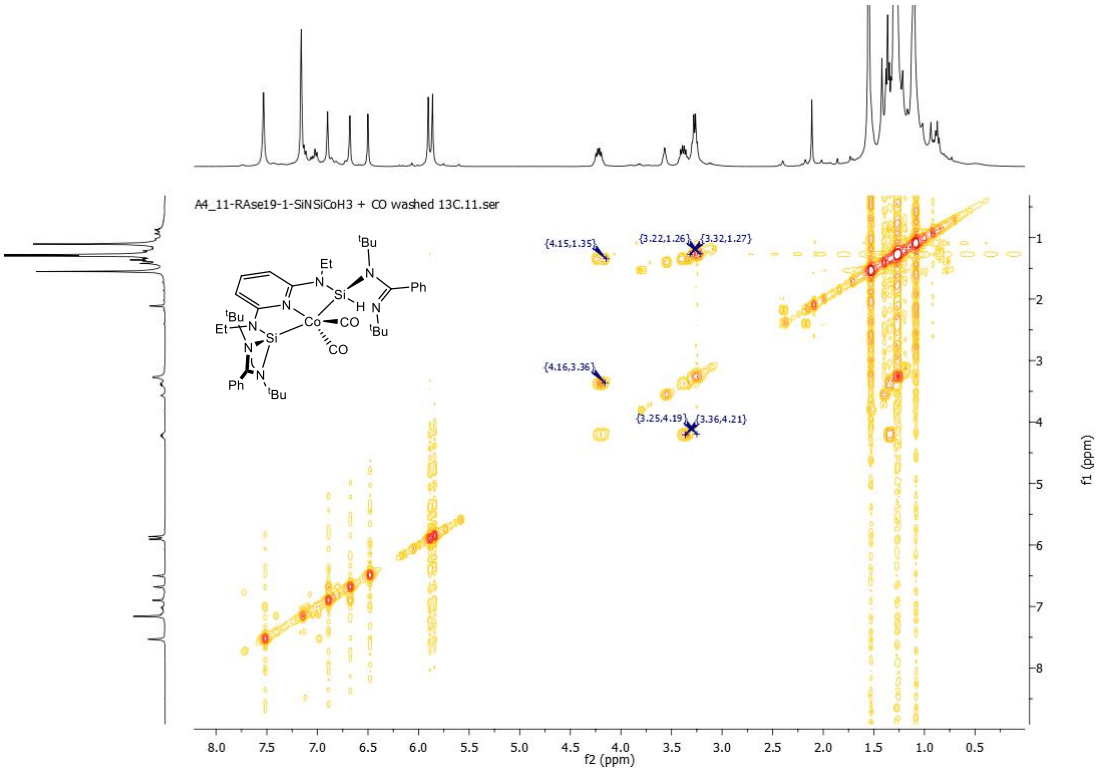

Figure S76. ^{1}H-^{1}H COSY NMR spectrum of **5-(CO)$_2$** in C_6D_6 at 300 K.

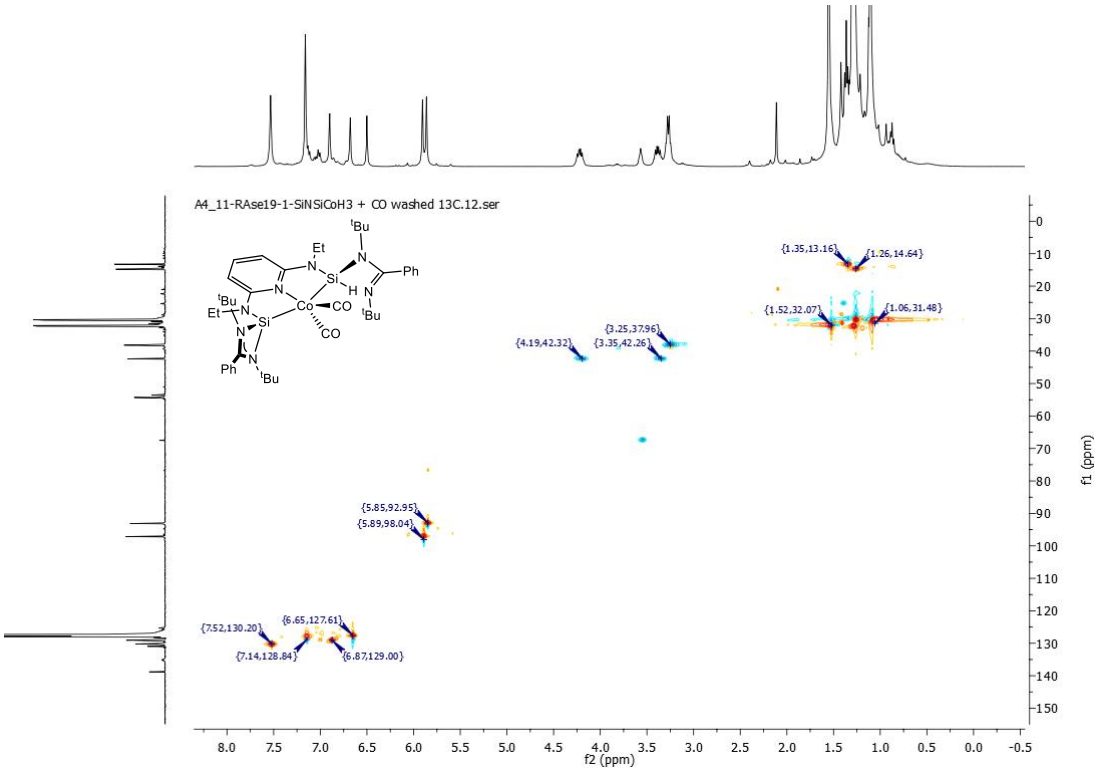

Figure S77. ^{1}H-^{13}C HSQC NMR spectrum of **5-(CO)$_2$** in C_6D_6 at 300 K.

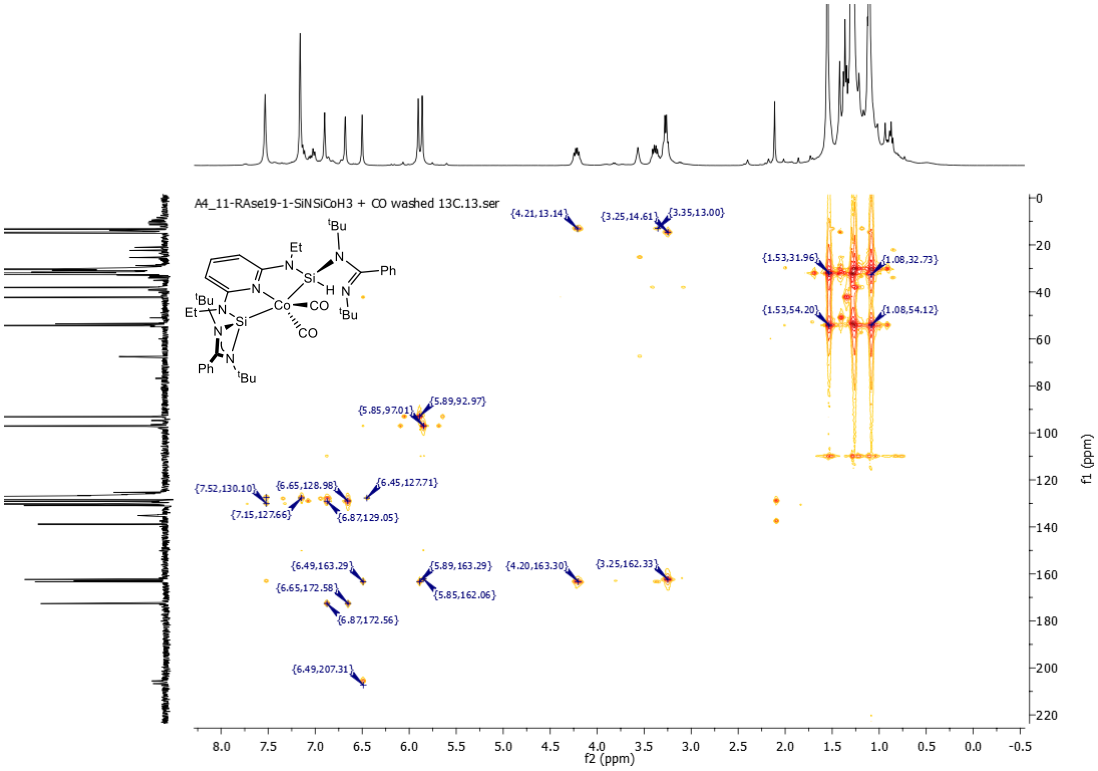

Figure S78. ^{1}H-^{13}C HMBC NMR spectrum of **5-(CO)$_2$** in C_6D_6 at 300 K.

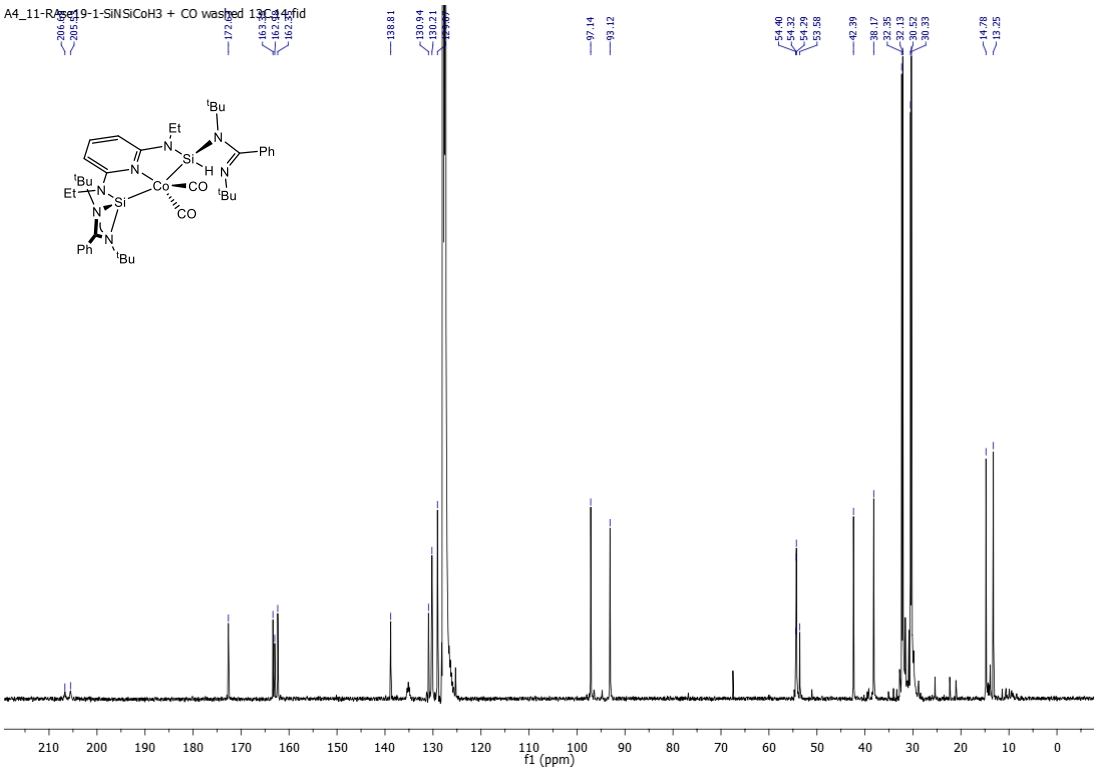

Figure S79. ^{13}C NMR spectrum of **5-(CO)$_2$** in C_6D_6 at 300 K.

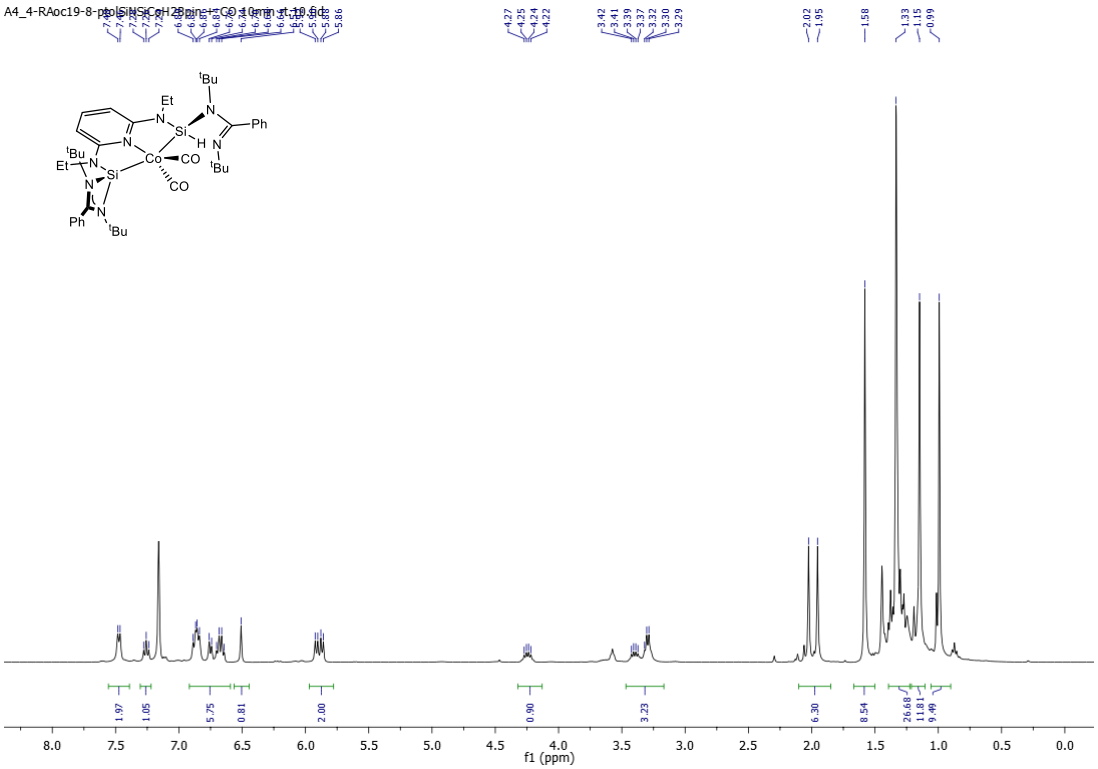

Figure S80. ^{1}H NMR spectrum of **6-(CO)$_2$** in C_6D_6 at 300 K.

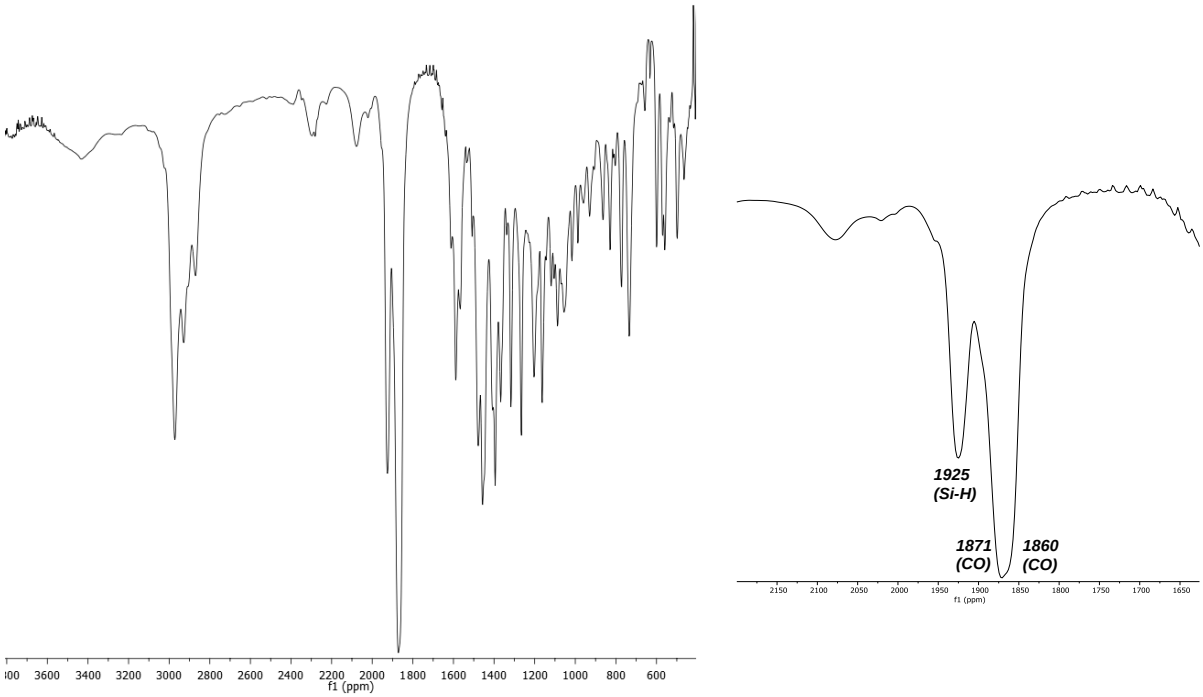

Figure S81. IR spectrum of **6-(CO)$_2$** in KBr. The inset is an expanded view of the νCO (2200-1700 cm^{-1}) region.

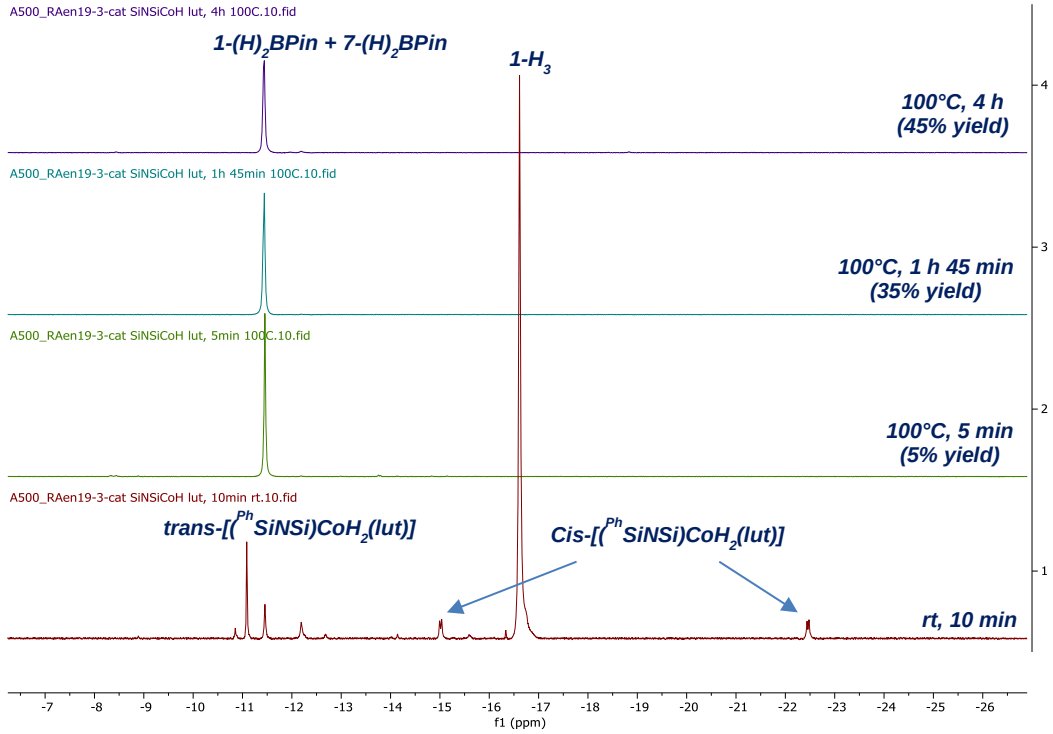

Figure S82. ^{1}H NMR monitoring (5 min – 4 h) of the borylation of 2,6-lutidine with 1 equiv of B_2Pin_2 and 15 mol% of **1-H$_3$·NaHBEt$_3$** at 100 ºC (hydride region).

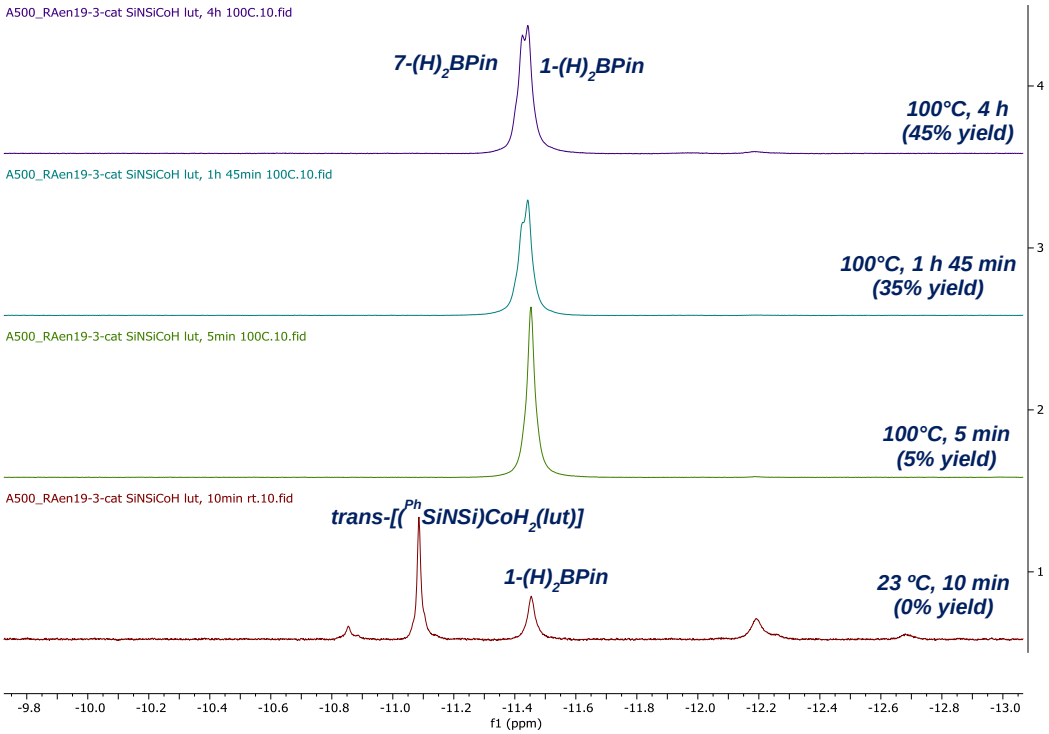

Figure S83. ^{1}H NMR monitoring (5 min – 4 h) of the borylation of 2,6-lutidine with 1 equiv of B_2Pin_2 and 15 mol% of **1-H$_3$·NaHBEt$_3$** at 100 ºC (hydride region).

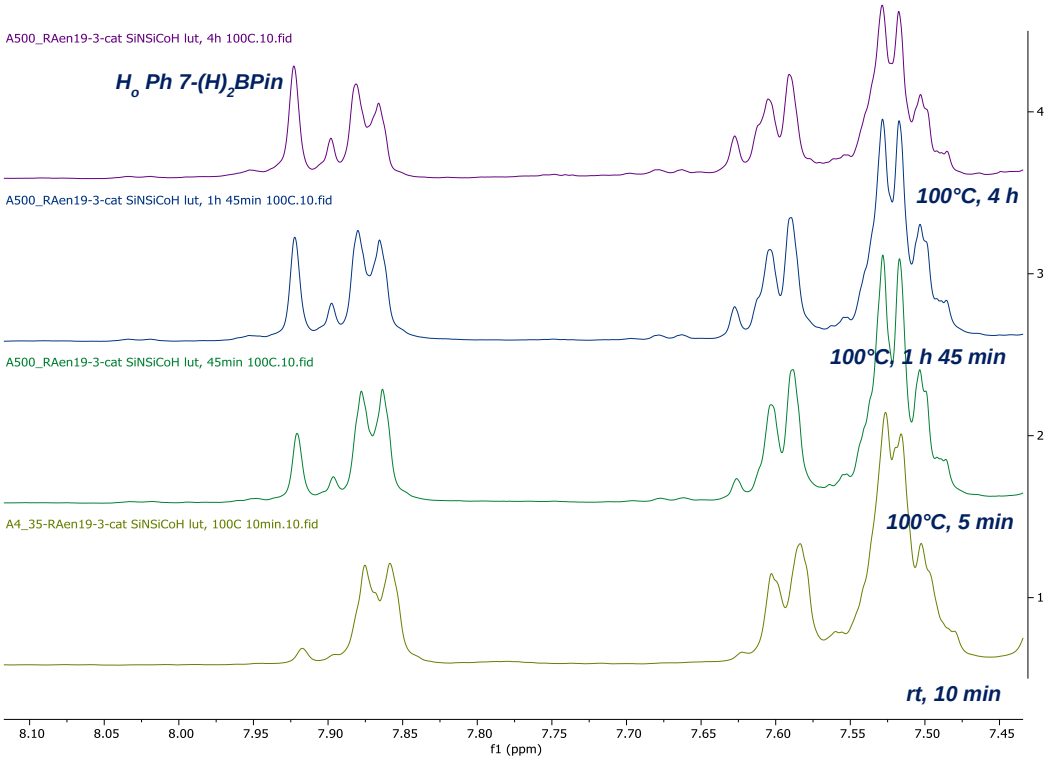

Figure S84. ^{1}H NMR monitoring (5 min – 4 h) of the borylation of 2,6-lutidine with 1 equiv of B_2Pin_2 and 15 mol% of **1-H$_3$·NaHBEt$_3$** at 100 ºC (aromatic region).

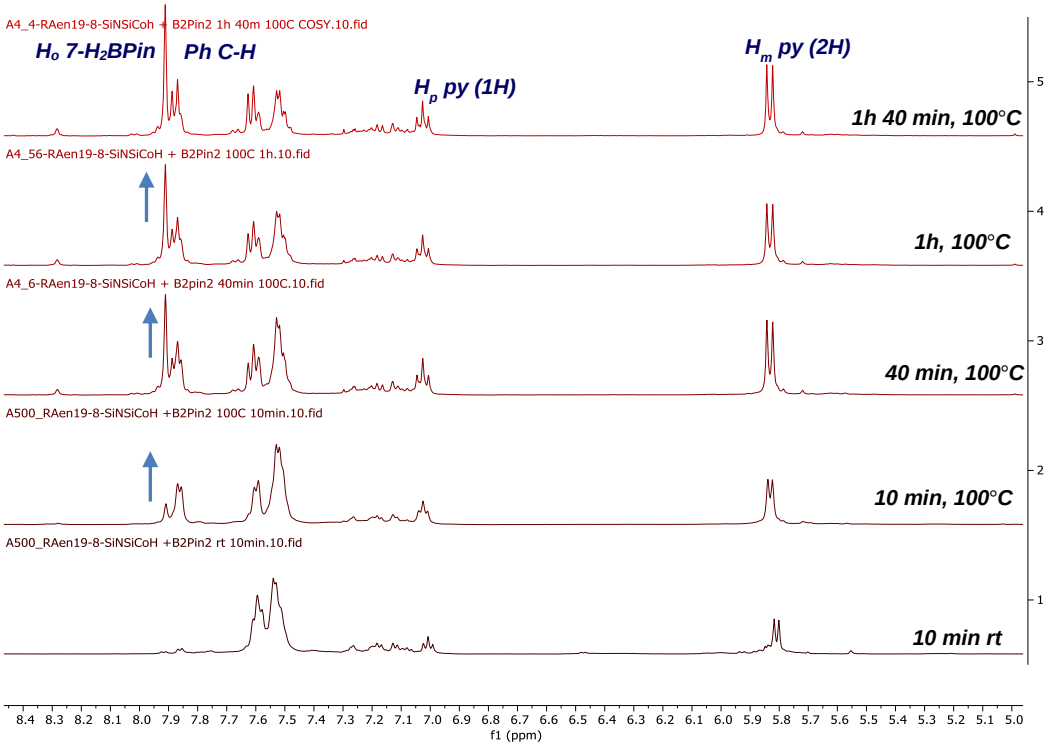

Figure S85. ^{1}H NMR monitoring (10 min – 1 h 40 min) of the reaction of **1-H_3·NaHBEt$_3$** with 10 equiv of B_2Pin_2 in THF-d_8 at 100 ºC (aromatic region).

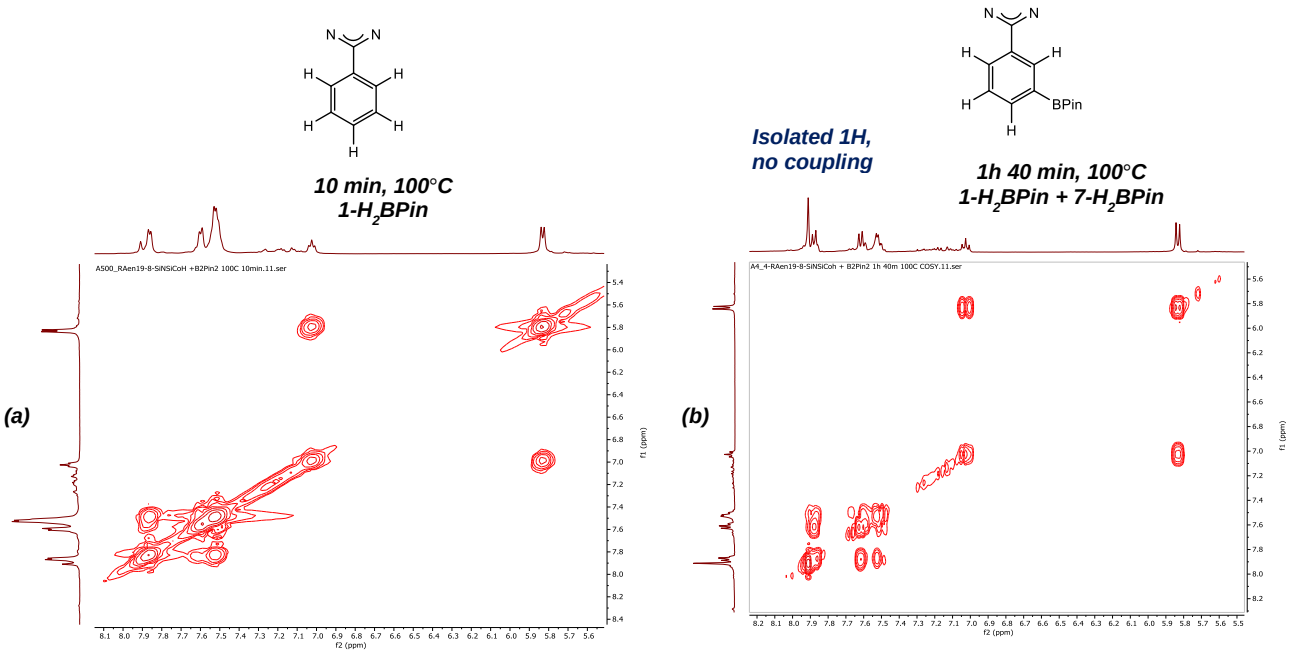

Figure S86. ^{1}H-^{1}H COSY NMR of the reaction of **1-H_3·NaHBEt$_3$** with 10 equiv of B_2Pin_2 in THF-d_8 (aromatic region) at 100 ºC (a) after 10 min, (b) after 1 h 40 min.

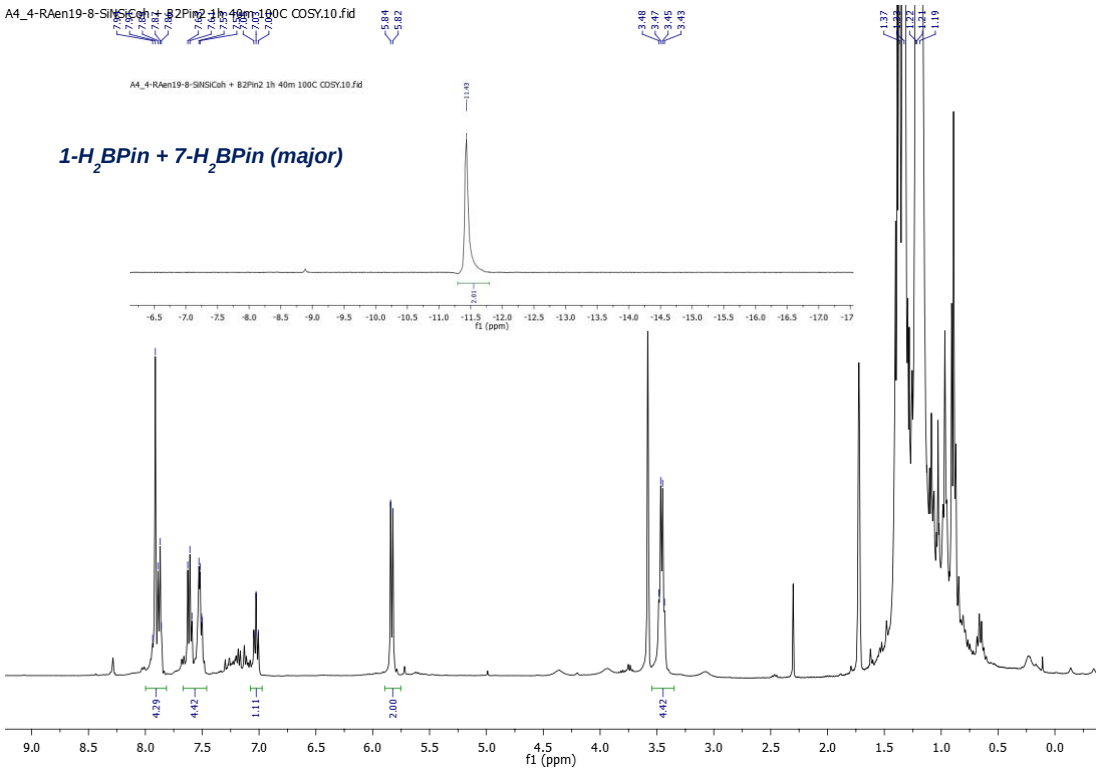

Figure S87. ^{1}H NMR spectrum of the **1-H_2BPin** + **7-H_2BPin** mixture in the presence of B_2Pin_2 in THF-d_8 at 300 K. The inset is an expanded view of the hydride region.

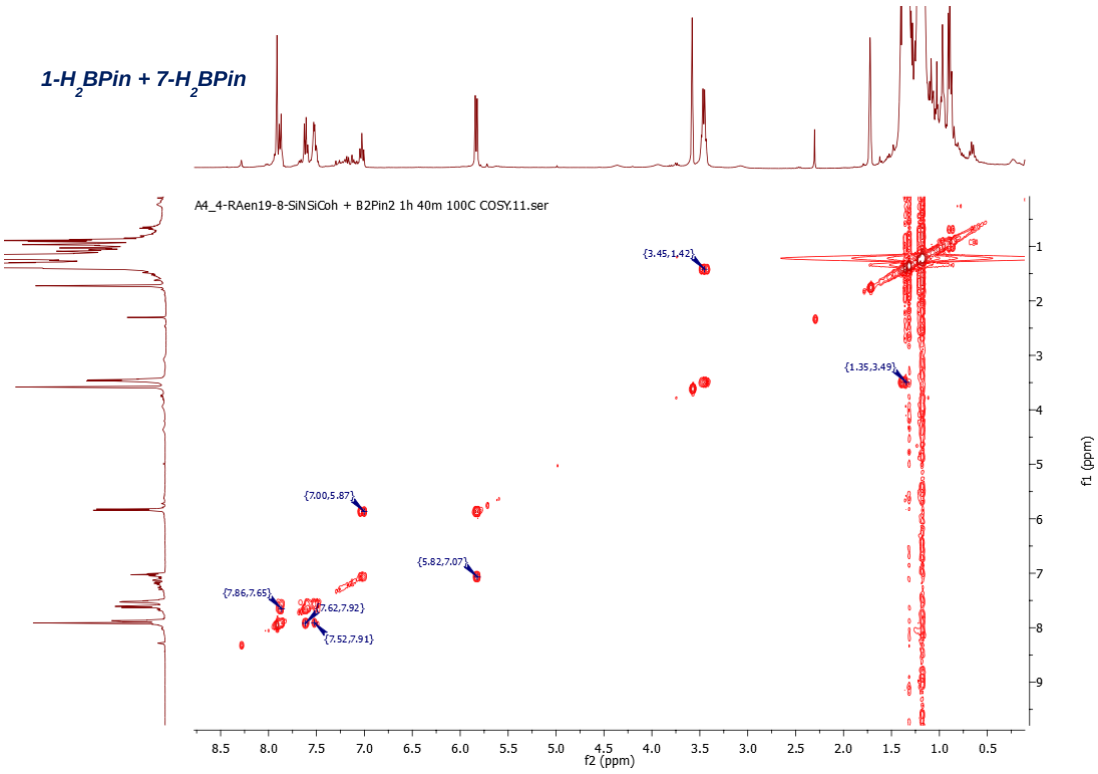

Figure S88. ^{1}H-^{1}H COSY NMR spectrum of the **1-H_2BPin** + **7-H_2BPin** mixture in the presence of B_2Pin_2 in THF-d_8 at 300 K.

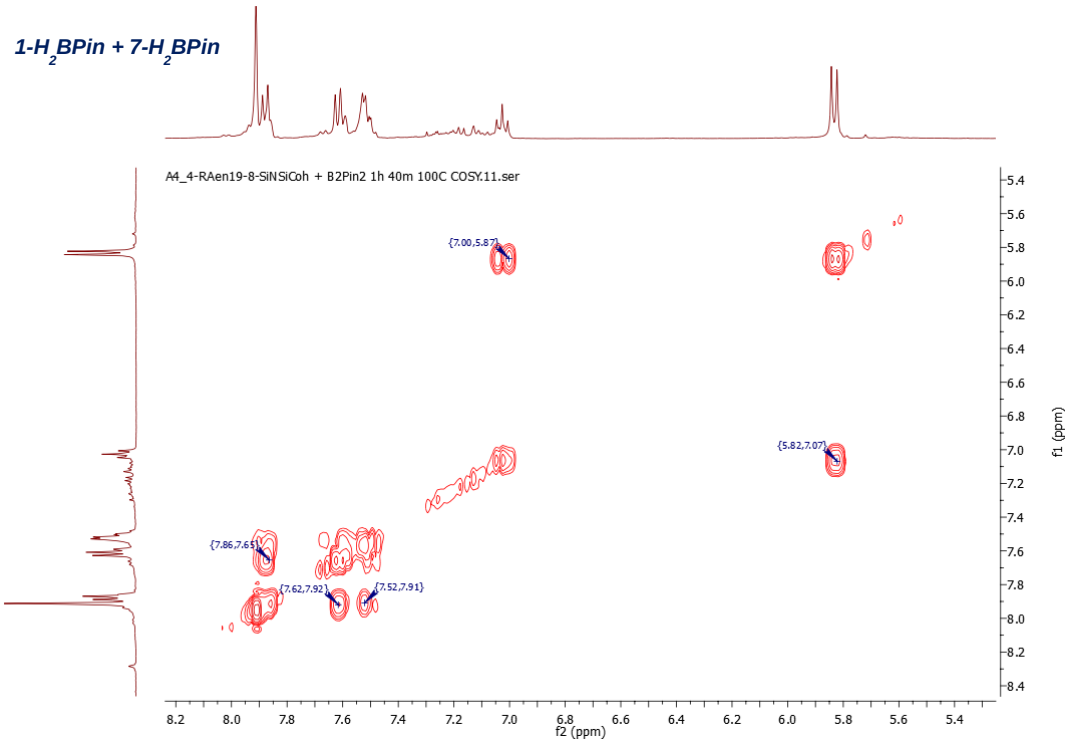

Figure S89. ^{1}H-^{1}H COSY NMR spectrum of the **1-H_2BPin** + **7-H_2BPin** mixture in the presence of B_2Pin_2 in THF-d_8 at 300 K (aromatic region).

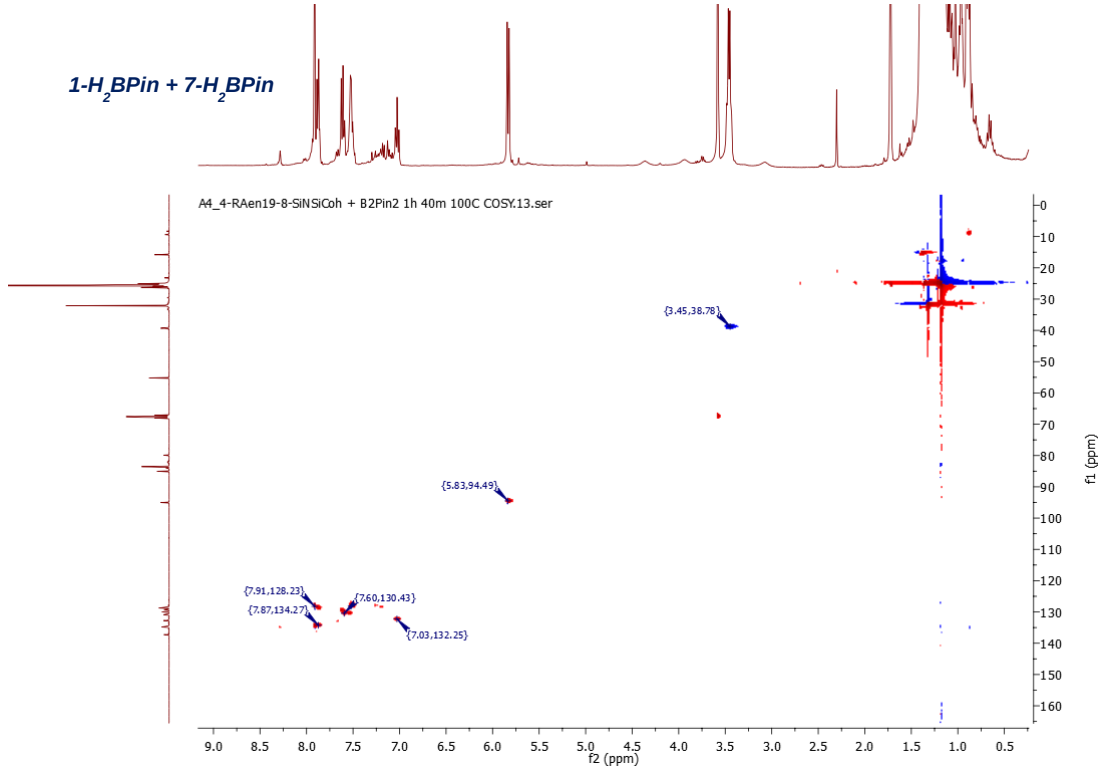

Figure S90. ^{1}H-^{13}C HSQC NMR spectrum of the **1-H_2BPin** + **7-H_2BPin** mixture in the presence of B_2Pin_2 in THF-d_8 at 300 K.

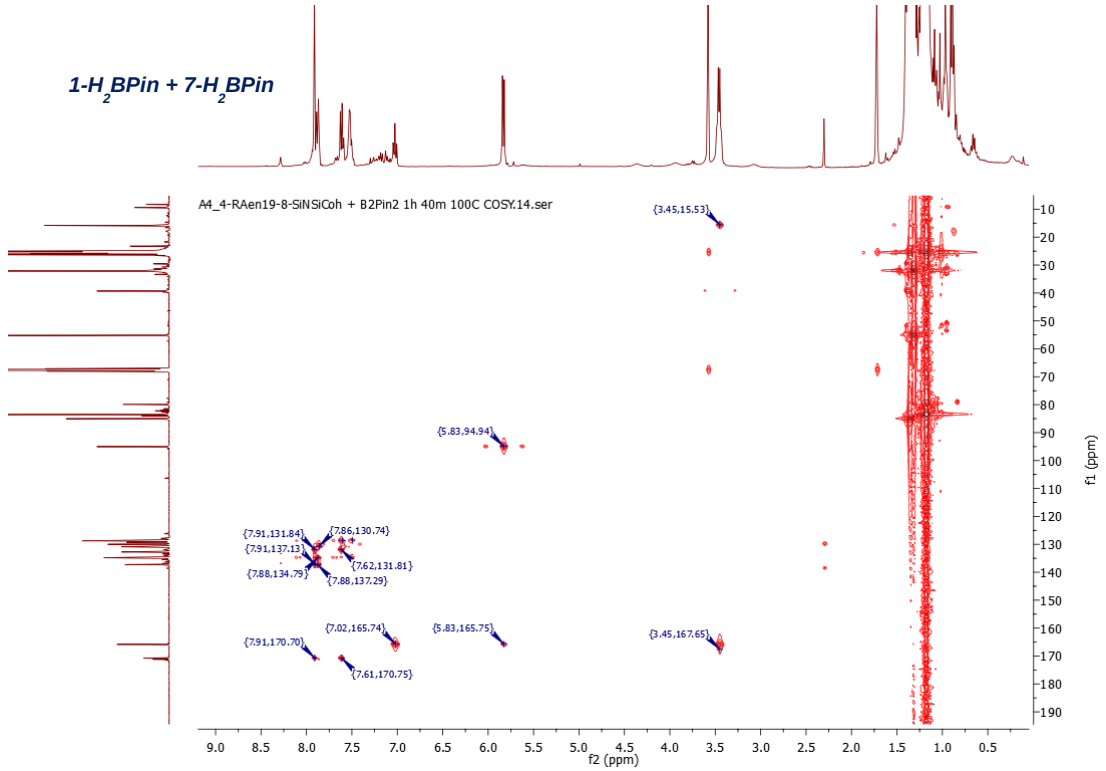

Figure S91. ^{1}H-^{13}C HMBC NMR spectrum of the **1-H_2BPin** + **7-H_2BPin** mixture in the presence of B_2Pin_2 in THF-d_8 at 300 K.

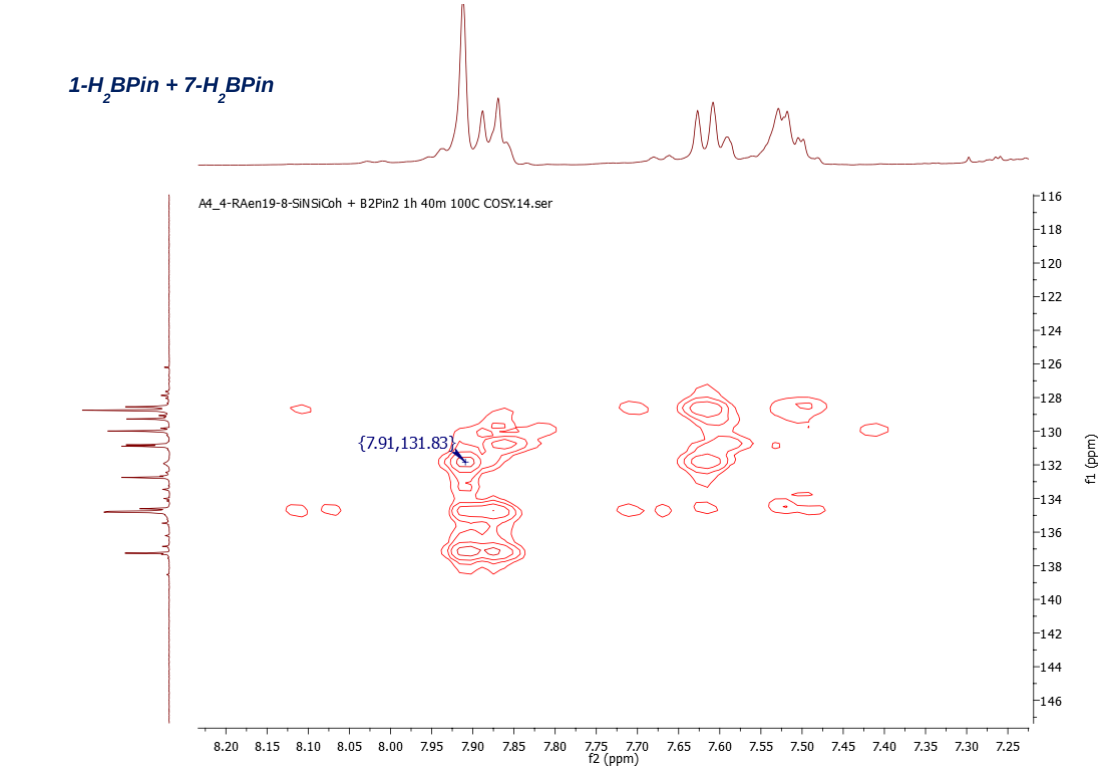

Figure S92. ^{1}H-^{13}C HMBC NMR spectrum of the **1-H_2BPin** + **7-H_2BPin** mixture in the presence of B_2Pin_2 in THF-d_8 at 300 K (aromatic region showing crosspeak between H_o Ph and B-bonded C).

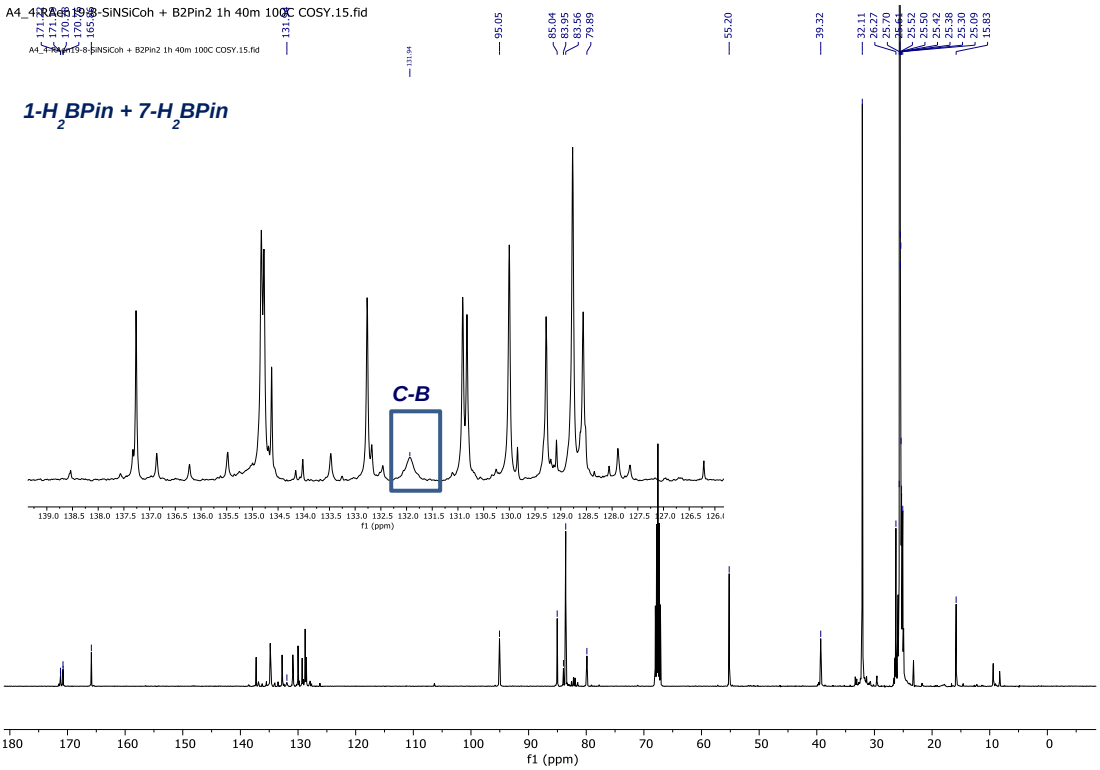

Figure S93. ^{13}C NMR spectrum of the **1-H_2BPin** + **7-H_2BPin** mixture in the presence of B_2Pin_2 in THF-d_8 at 300 K. The inset is an expanded view of the aromatic region.

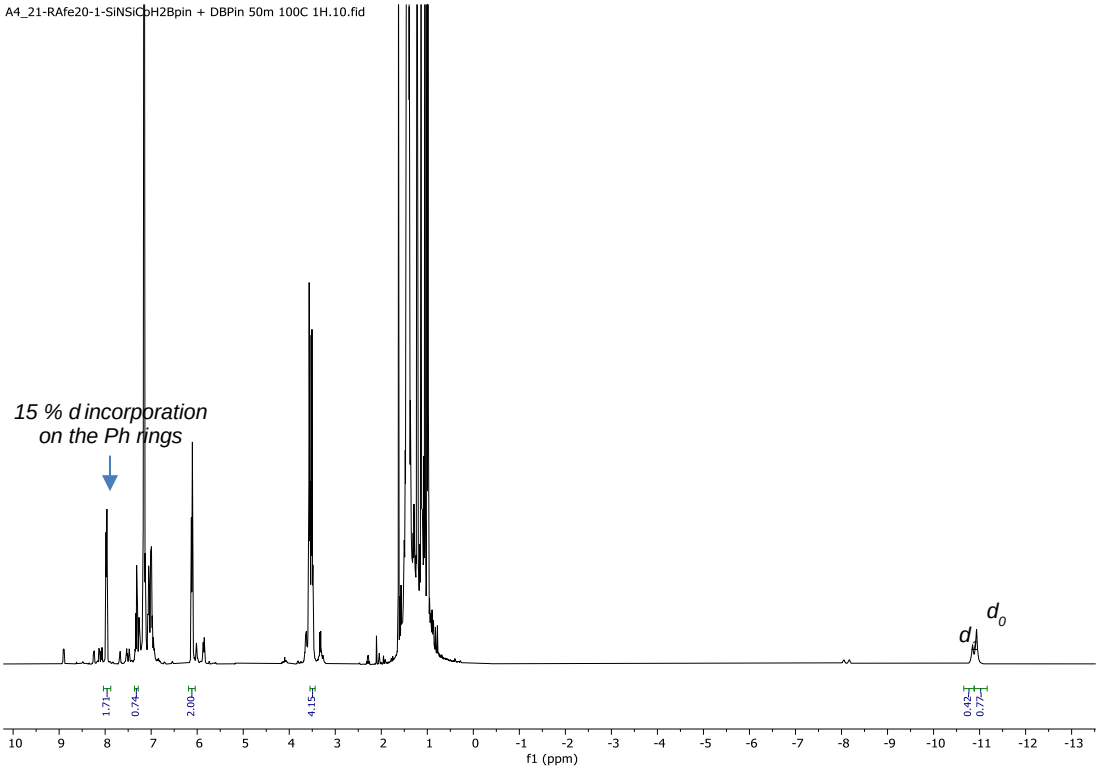

Figure S94. ^{1}H NMR spectrum of the [($^{Ph\text{-}d}$SiNSi)CoD_xH_{2-x}(BPin)] (x = 0, 1, 2) mixture of isotopologues in C_6D_6 at 300 K.

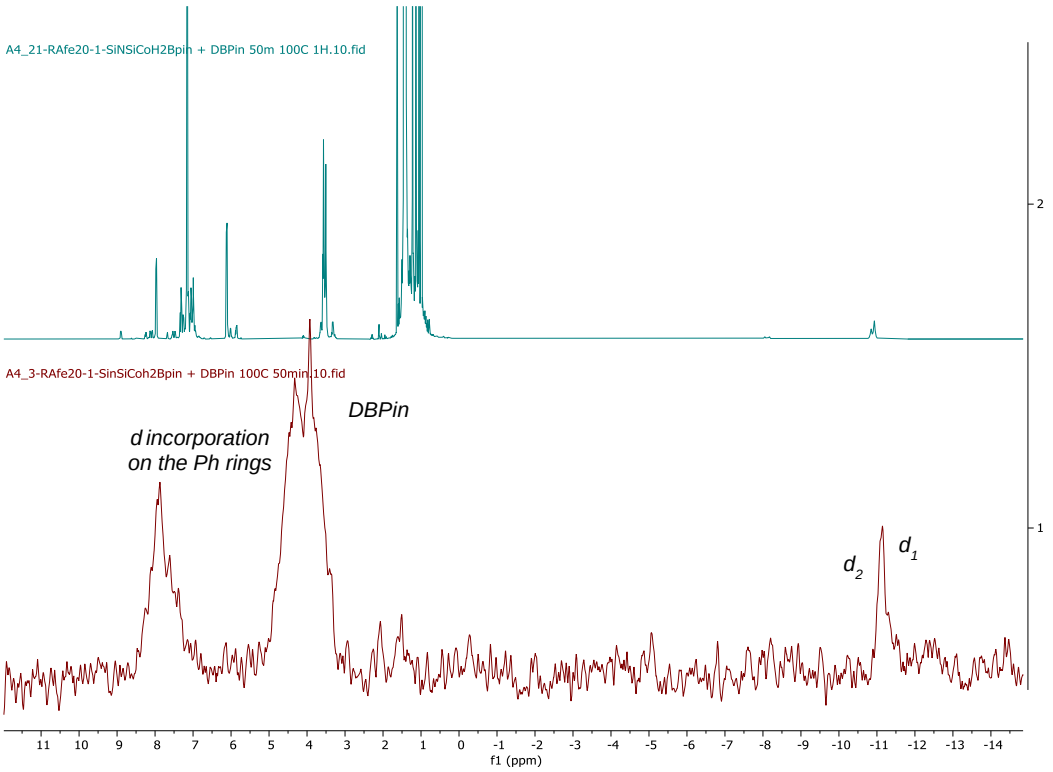

Figure S95. ^{1}H (top) and ^{2}H (bottom) NMR spectra of the [($^{Ph\text{-}d}$SiNSi)CoD$_x$H$_{2-x}$(BPin)] (x = 0, 1, 2) mixture of isotopologues in C_6D_6 and THF respectively at 300 K.

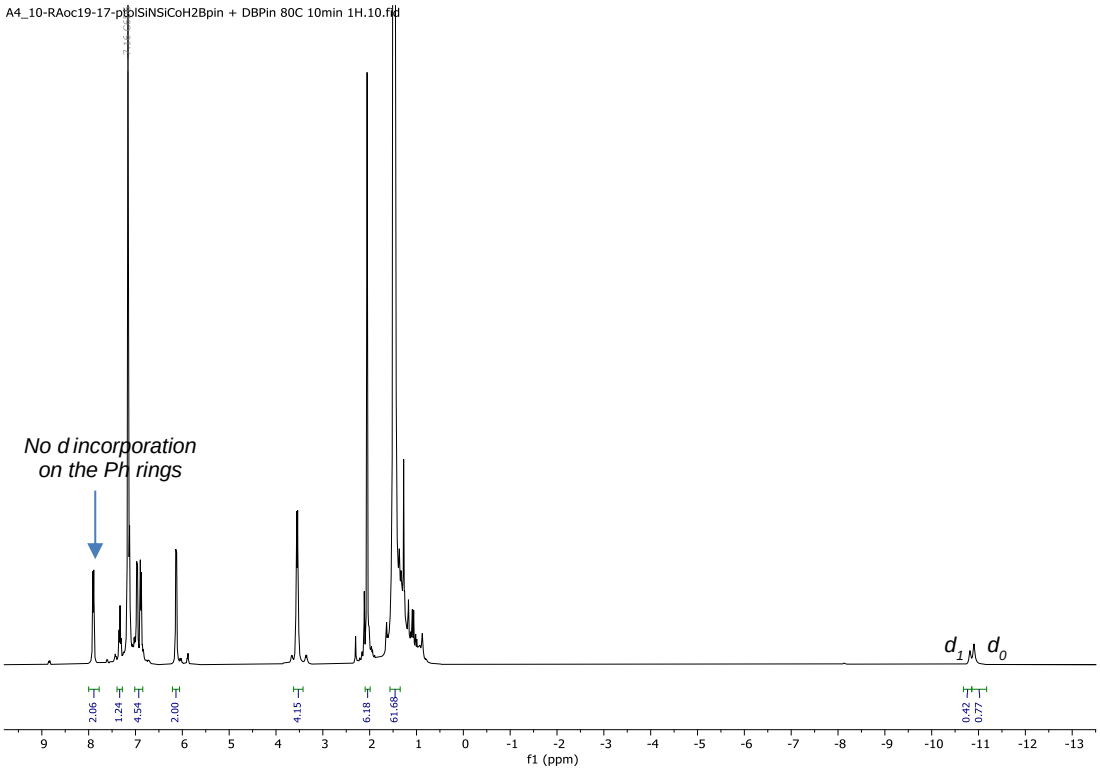

Figure S96. ^{1}H NMR spectrum of the [(^{ptol}SiNSi)CoD$_x$H$_{2-x}$(BPin)] (x = 0, 1, 2) mixture of isotopologues in C_6D_6 at 300 K.

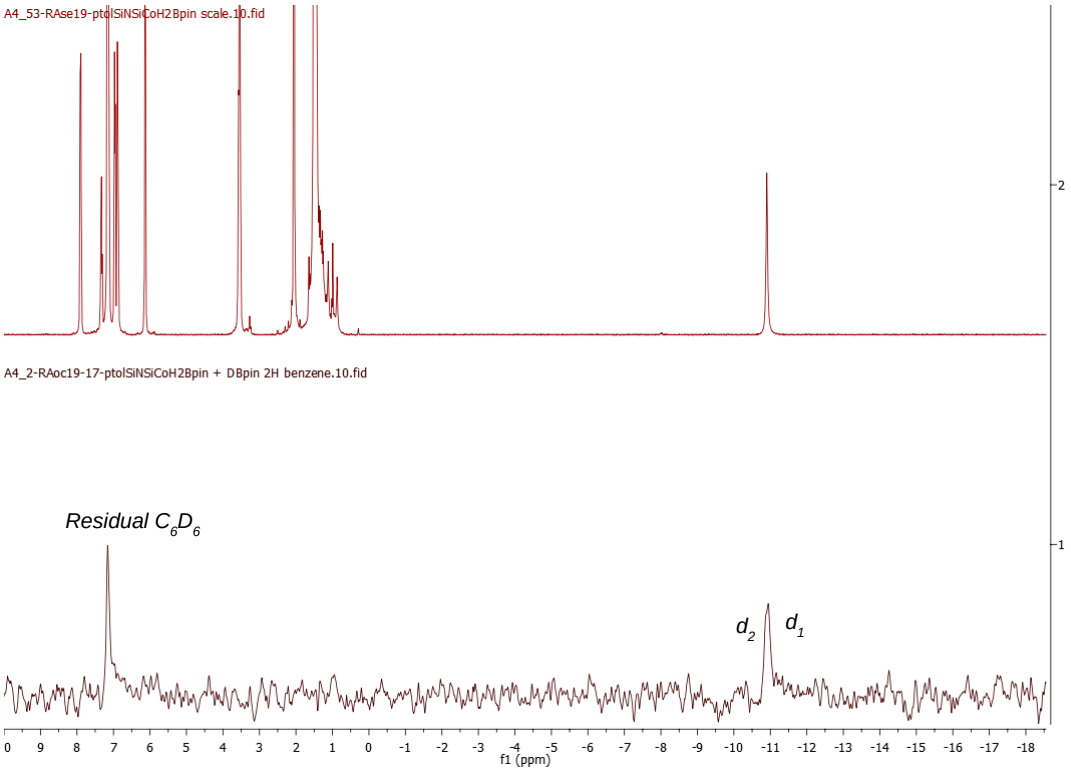

Figure S97. ^{1}H NMR spectrum (top) of **2-(H)$_2$BPin** and ^{2}H NMR spectrum (bottom) of the [(^{ptol}SiNSi)CoD$_x$H$_{2-x}$(BPin)] (x = 0, 1, 2) mixture of isotopologues in C_6D_6 and C_6H_6 respectively at 300 K.

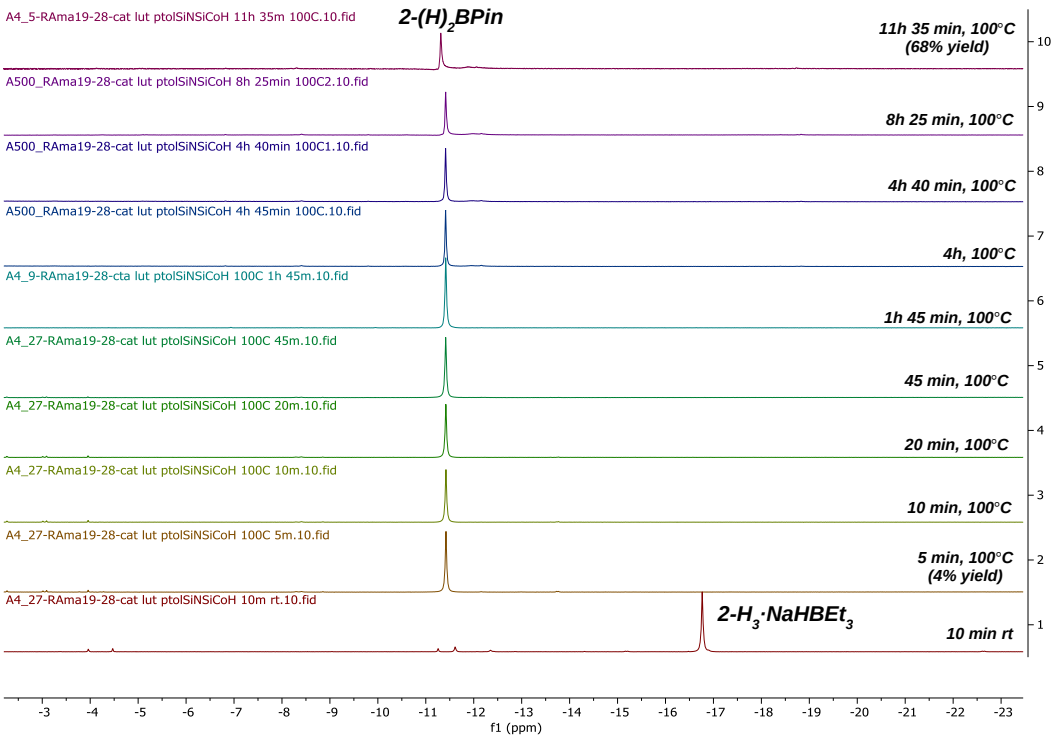

Figure S98. ^{1}H NMR monitoring (5 min – 11 h 35 min) of the borylation of 2,6-lutidine with 1 equiv of B_2Pin_2 and 15 mol% of **2-H$_3$·NaHBEt$_3$** at 100 ºC (hydride region).

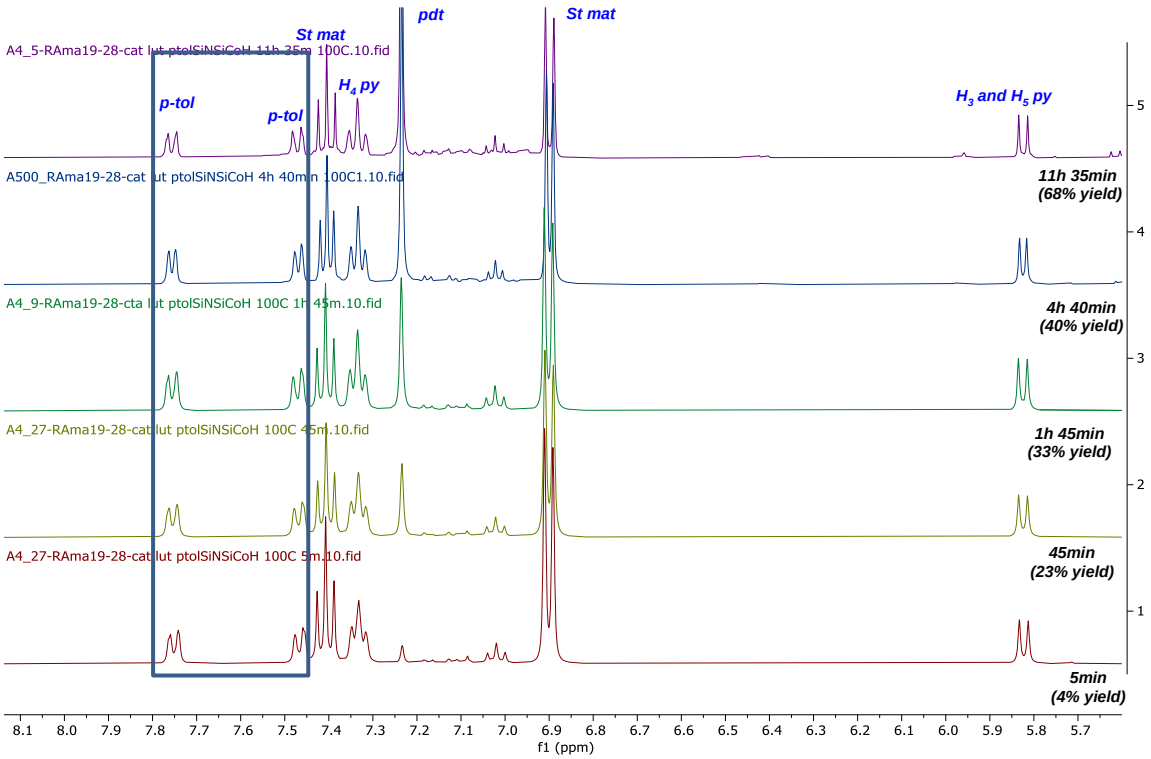

Figure S99. ^{1}H NMR monitoring (5 min – 11 h 35 min) of the borylation of 2,6-lutidine with 1 equiv of B_2Pin_2 and 15 mol% of **2-H$_3$·NaHBEt$_3$** at 100 ºC (aromatic region).

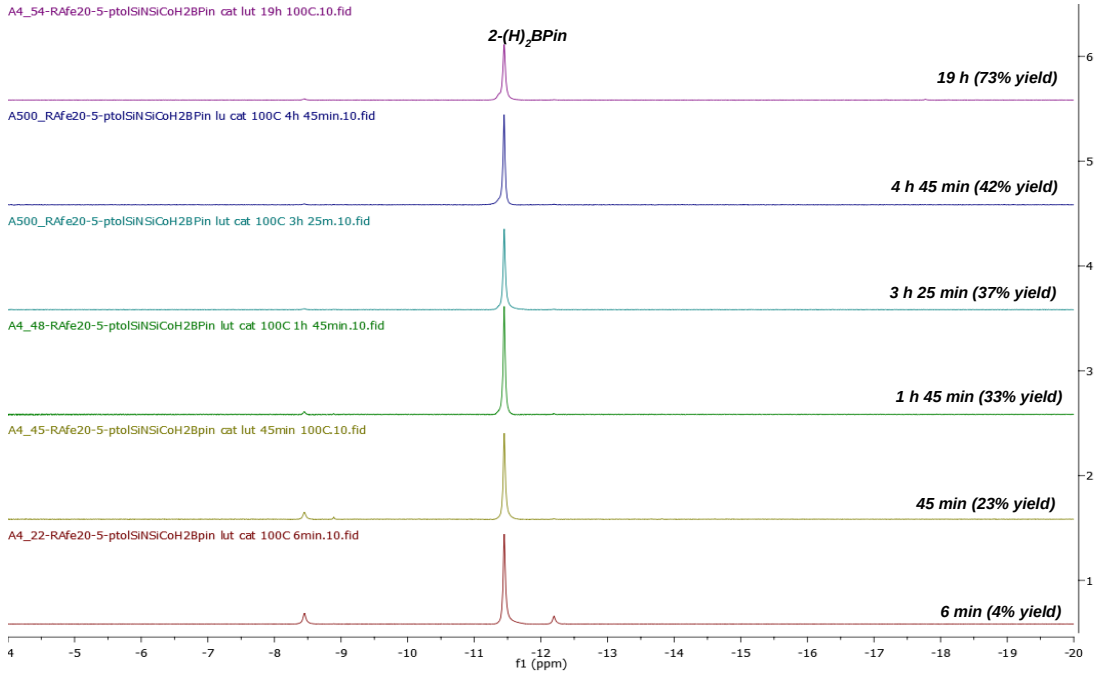

Figure S100. ^{1}H NMR monitoring (5 min – 19 h) of the borylation of 2,6-lutidine with 1 equiv of B_2Pin_2 and 15 mol% of **2-(H)$_2$BPin** at 100 ºC (hydride region).

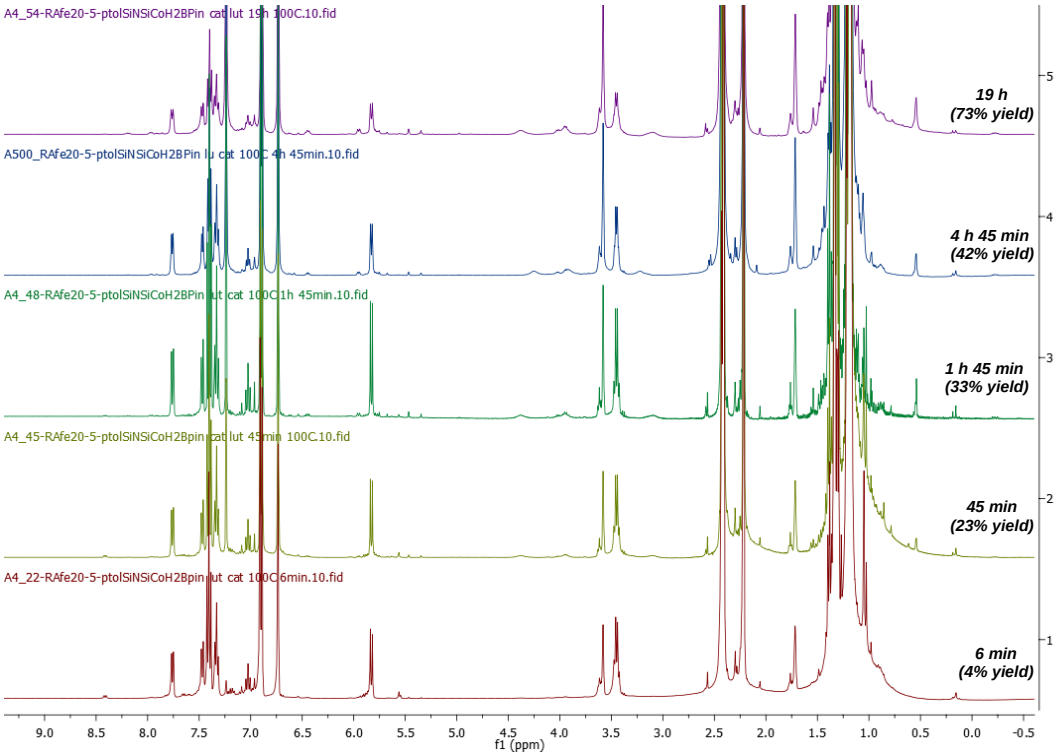

Figure S101. ^{1}H NMR monitoring (5 min – 19 h) of the borylation of 2,6-lutidine with 1 equiv of B_2Pin_2 and 15 mol% of **2-(H)$_2$BPin** at 100 ºC (1 - 10 ppm region).

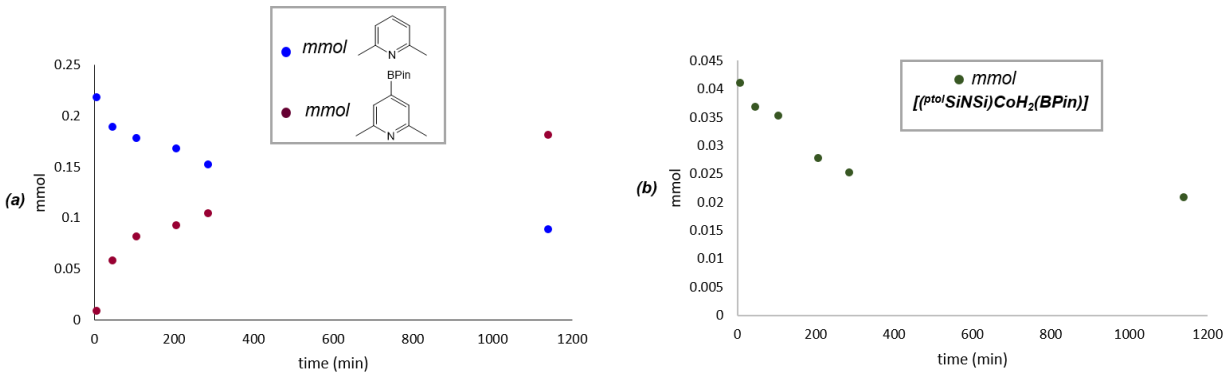

Figure S102. (a) Reaction profile from ^{1}H NMR integration of the borylation of 2,6-lutidine with 1 equiv of B_2Pin_2 and 15 mol% of **2-(H)$_2$BPin** at 100 ºC and (b) catalyst concentration decrease in the borylation reaction from ^{1}H NMR integration of the hydride signal against mesitylene as internal standard.

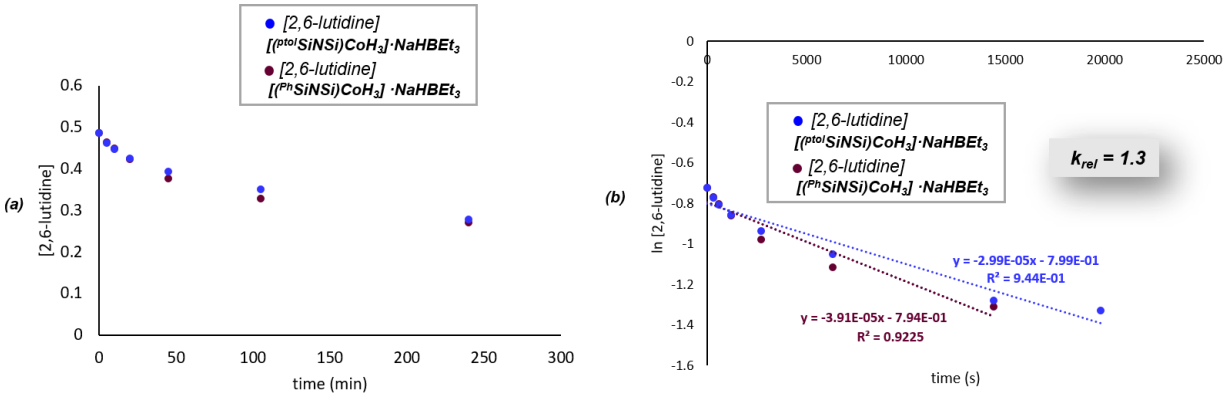

Figure S103. (a) 2,6-lutidine disappearance profile from ^{1}H NMR integration in the borylation of 2,6-lutidine with 1 equiv of B_2Pin_2 and 15 mol% of **1-H$_3$·NaHBEt$_3$** (maroon) or **2-H$_3$·NaHBEt$_3$** (blue) at 100 ºC and (b) linearization to obtain k_{rel}.

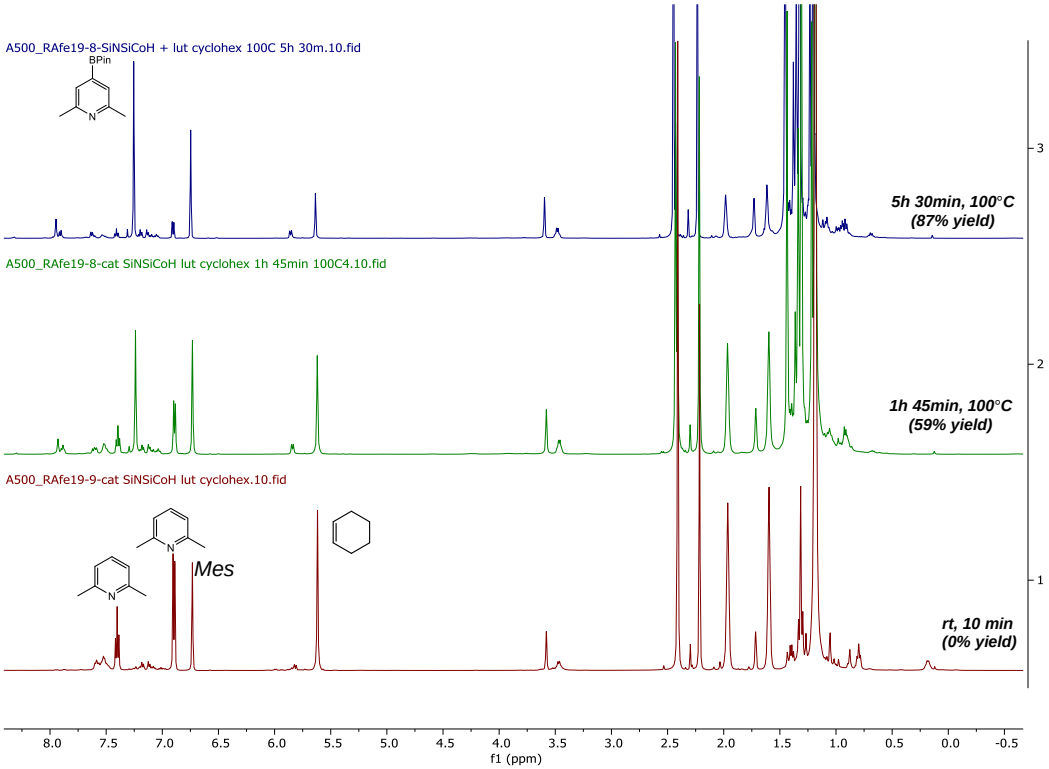

Figure S104. ^{1}H NMR monitoring (1 h 45 min – 5 h 30 min) of the borylation of 2,6-lutidine with 1 equiv of B_2Pin_2 and 15 mol% of **1-(H)$_3$·NaHBEt$_3$** at 100 ºC in the presence of 100 mol% of cyclohexene in THF-d_8 (1 - 10 ppm region). Mes = mesitylene.

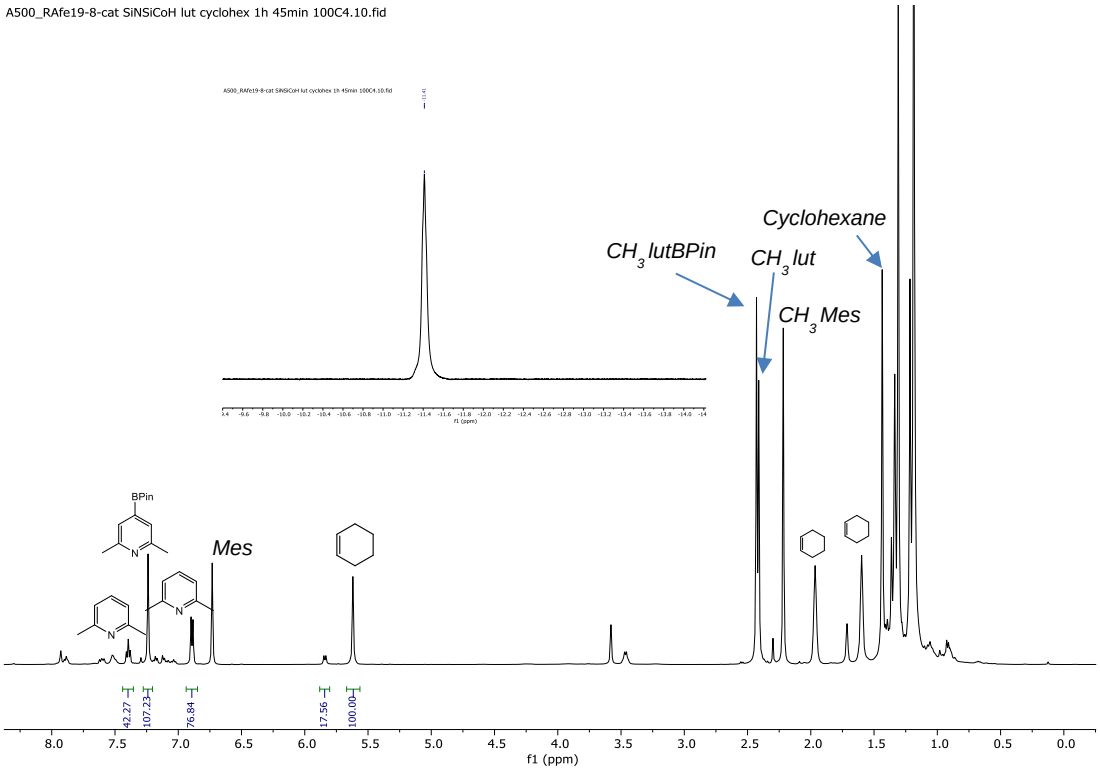

Figure S105. ^{1}H NMR spectrum of the borylation of 2,6-lutidine with 1 equiv of B_2Pin_2 and 15 mol% of **1-(H)$_3$·NaHBEt$_3$** at 100 ºC in the presence of 100 mol% of cyclohexene in THF-d_8 after 1 h 45 min of reaction showing formation of cyclohexane. Mes = mesitylene (internal standard). The inset is an expanded view of the hydride region.

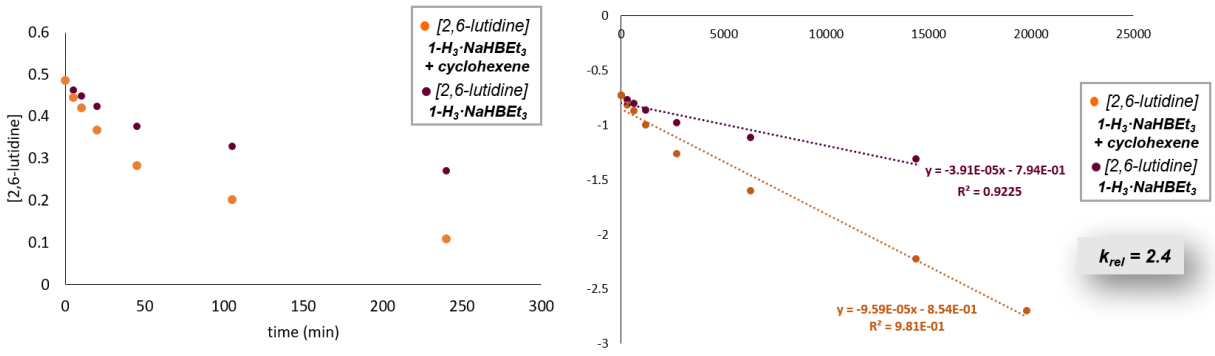

Figure S106. (a) 2,6-lutidine disappearance profile from ^{1}H NMR integration in the borylation of 2,6-lutidine with 1 equiv of B_2Pin_2 and 15 mol% of **1-H$_3$·NaHBEt$_3$** (maroon) or **1-H$_3$·NaHBEt$_3$** in the presence of 100 mol% of cyclohexene (orange) at 100 ºC and (b) linearization to obtain k_{rel}.

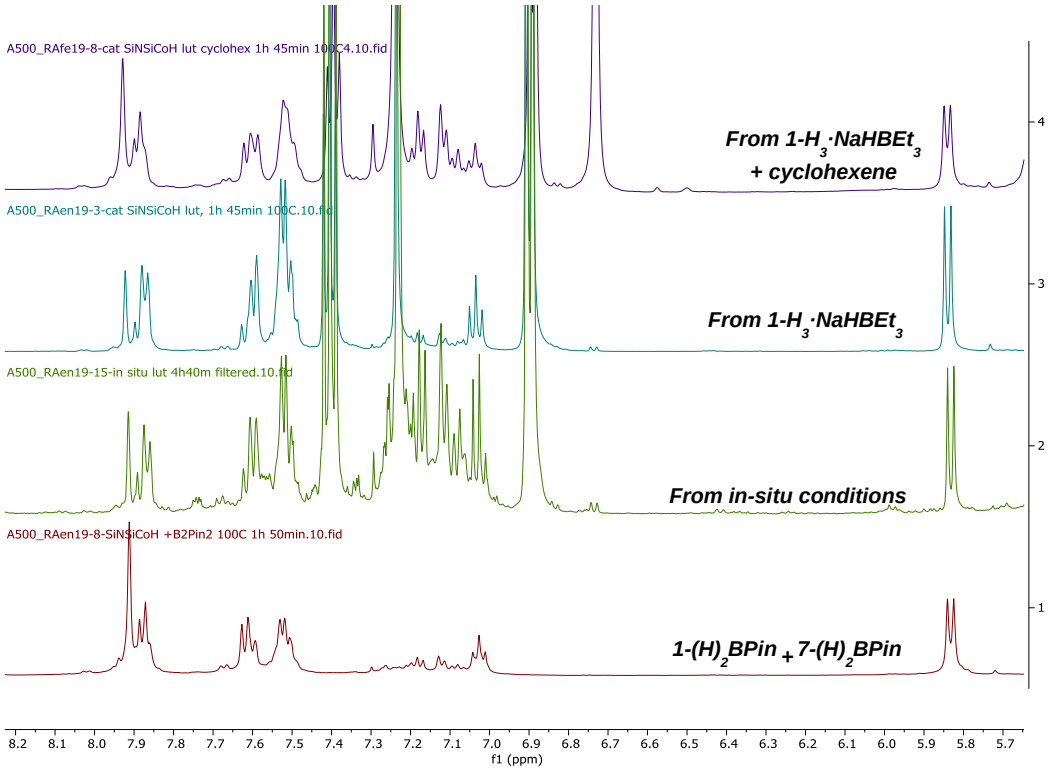

Figure S107. ^{1}H NMR spectra of the borylation of 2,6-lutidine with 1 equiv of B_2Pin_2 at 100 ºC in THF-d_8 employing 2. the in-situ activated precatalyst (15 mol% of [(^{Ph}SiNSi)$CoCl_2$] + 30 mol% $NaHBEt_3$), 3. **1-H_3·NaHBEt_3 or 4. 1-H_3·NaHBEt_3** in the presence of 100 mol% of cyclohexene (aromatic region) all showing borylation of the Ph rings of the catalyst. 1. shows the aromatic region of the ^{1}H NMR spectrum of the independently synthesized **1-H_2BPin** + **7-H_2BPin** mixture.

VI. References

[1] Pangborn, A. B.; Giardello, M. A.; Grubbs, R. H.; Rosen, R. K.; Timmers, F. J. Safe and Convenient Procedure for Solvent Purification. *Organometallics* **1996**, *15*, 1518–1520.

[2] Gallego, D.; Inoue, S.; Blom, B.; Driess, M. Highly electron-rich pincer-type iron complexes bearing innocent bis(metallylene)pyridine ligands: syntheses, structures, and catalytic activity. *Organometallics* **2014**, *33*, 6885-6897 and references therein.

[3] Chen, W.; Ma, L.; Paul, A.; Seidel, D. Direct α-C–H bond functionalization of unprotected cyclic amines. *Nature Chem.* **2018**, *10*, 165-169.

[4] Obligacion, J. V.; Semproni, S. P.; Pappas, I.; Chirik, P. J. Cobalt-Catalyzed C(sp^2)-H Borylation: Mechanistic Insights Inspire Catalyst Design. *J. Am. Chem. Soc.* **2016**, *138*, 10645–10653.

[5] El-Shazly, M. F.; El-Dissowky, A.; Salem, T.; Osman, M. Synthesis and electron spin resonance studies of copper(II) complexes with acid amide derivatives of 2-amino and 2, 6-diaminopyridine. *Inorg. Chim. Acta* **1980**, *40*, 1-6.

[6] Obligacion, J. V.; Chirik, P. J. Bis(imino)pyridine Cobalt-Catalyzed Alkene Isomerization-Hydroboration: A Strategy for Remote Hydrofunctionalization with Terminal Selectivity. *J. Am. Chem. Soc.* **2013**, *135*, 19107-19110.

[7] Ren, H.; Zhou, Y-P.; Bai, Y.; Cui, C.; Driess, M. Cobalt-Catalyzed Regioselective Borylation of Arenes: N-Heterocyclic Silylene as an Electron Donor in the Metal-Mediated Activation of C−H Bonds. *Chem. Eur. J.* **2017**, *23*, 5663-5667.